CHARACTERIZATION OF IMMUNE CELL SUBSETS IN A MODEL DISEASE FOR ENDOCRINE AUTOIMMUNITY BY MASS AND FLOW CYTOMETRY

Master Thesis in Biomedical Sciences

Ifunanya Nwakwuo

This thesis is submitted in partial fulfilment of the requirements for the degree of

Master's in Biomedical Sciences

Department of Biomedicine
Faculty of Medicine and Dentistry
University of Bergen
Bergen, Norway
2022

Table of Contents

ACKNOWLEDGEMENT 7
ABSTRACT 8
1 INTRODUCTION 9
1.1 The Innate immune System 9
1.2 Cells Of The Adaptive Immune System 9
1.2.1 B Cells 10
1.2.2 T Cell Development 11
1.2.3 T Cell Activation 11
1.2.4 T Cell Subsets 13
1.3 Autoimmunity And Immunological Tolerance 16
1.3.1 Immunological Tolerance 16
1.3.2 Autoimmunity 18
1.3.3 The Role of Th17 Cells and Treg Cells in Autoimmunity 18
1.3.4 Biomarkers for Immune Cells. 19
1.4 Autoimmune Polyendocrine Syndrome Type 1 (Aps-1) 19
1.4.1 Diagnosis and Clinical Manifestation of APS-1 19
1.4.2 The Autoimmune Regulator Gene 20
1.4.3 Autoantibodies in APS-1 21
1.5 Hypothesis and Aim 22
1.5.1 Aim of Study 23
2 MATERIALS 24
2.1 List of Antibodies for Mass Cytometry 25
2.2 Kits and Equipment 26
2.3 Instruments 27
2.4 Software 27
3 MATERIALS AND METHODS 28
3.1 Experimental Outline 28
3.2 Sample Materials and Ethical Aspect 28
3.2.1 Patient Samples 28
3.2.2 Healthy Control 29
3.3 Choice Of Methods 29
3.3.1 Mass Cytometry by Time-of-Flight (CyTOF) 29
3.3.2 Flow Cytometry 30
3.3.3 Enzyme-Linked Immunosorbent Assay 31

3.4 Sample Processing for Mass Cytometry……32
3.4.1 Whole Blood Preservation……32
3.4.2 Fixation and Lysis of Erythrocytes……32
3.4.3 Evaluation of Cell Number and Viability……33
3.4.4 Cryopreservation, Thawing and Recovery of Fixed Cells……33
3.5 Maxpar Antibody Conjugation and Titration……33
3.5.1 Antibody Conjugation……33
3.5.2 Antibody Titration of CD66b……35
3.6 Granulocyte Depletion (Negative Selection of Lymphocytes)……35
3.6.1 Magnetic Labelling with CD66abce Microbeads Kit……35
3.6.2 Magnetic Separation with LS Column……36
3.7 Barcoding and Antibody Staining……36
3.7.1 Barcoding……36
3.7.2 Antibody Staining of Barcoded Sample……37
3.8 Cytof Data Acquisition and Analysis……37
3.8.1 Normalization & Concatenation……38
3.8.2 Debarcoding……38
3.8.3 Data analysis……38
3.9 Flow Cytometry……39
3.9.1 Isolation of Peripheral Blood Mononuclear Cells……39
3.9.2 Cryopreservation, Thawing and Recovery of PBMCs……39
3.9.3 Compensation Staining……40
3.9.4 Titration of Fluorescent Conjugated Antibodies……40
3.9.5 Antibody Titration……41
3.10 Differentiation of CD4+ effector T Cells……41
3.10.1 Isolation of Naïve CD4+ T Cells by Magnetic Bead Separation……41
3.10.2 Cell Culture and Differentiation Assay……42
3.10.3 Flow Cytometry Acquisition……43
3.10.4 Fluorochrome Minus One (FMO)……44
3.10.5 Flow Cytometry Analysis……44
3.11 Enzyme linked immunosorbent assays (ELISA)……44
3.12 Statistical Analysis……45
4 RESULTS……46
4.1 Immune Profiling of APS-1 Patients and Healthy Controls……46
4.1.1 Clean up and Gating Strategy for Mass Cytometry……46
4.1.2 Validation of CD66b-Pr141 Titration……47

4.1.3 Panel Validation for CD66b-Pr141 49
4.1.4 Analysis of major immune cell subsets in CyTOF reveals lower frequencies of NKT cells in APS-1 patients compared to healthy controls. 49
4.2 Flow Cytometry 53
4.2.1 Comparison of Flowcytometry Staining Buffer 53
4.2.2 Phenotyping of T cells in unstimulated PBMCs from APS-1 patients and controls and Gating strategy. 54
4.2.3 Altered Eomes expression within effector CD8+ T cells from naïve PBMCs of patients with APS-1 55
4.2.4 There were no differences between CD4+ T cells subsets in undifferentiated PBMCs between APS-1 patients and healthy controls 55
4.2.5 TGF-β Mediates Th17 Differentiation and Induces FOXP3 Expression 56
4.2.6 Th2 Cell Expansion Promotes Proliferation of Gata3 58
4.2.7 Cytokine Production by Th2 and Th17 Differentiated Cells 59
4.2.8 Comparison of T cell population in CyTOF and Flow Cytometry 60
5 DISCUSSION 61
5.1.1 Mass Cytometry allows identification of immune cell population 62
5.1.2 Altered expression of NKT cells in APS-1 patients 63
5.1.3 Optimization of transcription factor panel for flow cytometry 65
5.1.4 Expression of Cells within CD4+ and CD8+ T Cells 66
5.1.5 Comparison of CyTOF and Flow Cytometry Staining on T cell response 67
6 CONCLUSION 69
6.1 Limitations 69
6.2 Future Perspectives 70
REFERENCES 71
APPENDIX 82

Table of Figures

Figure 1.1: Cells of the immune system. 10
Figure 1.2: Overview of T cell activation. 12
Figure 1.3: T cell subset differentiation. 13
Figure 1.4: Mechanism of Tregs suppression. 15
Figure 1.5: Central tolerance and autoimmunity. 17
Figure 1.6: Illustration of the classic components and other minor components of APS-1. 20
Figure 1.7: Schematic representation of the AIRE gene and its functional domain. 21
Figure 3.1: Experimental flow chart. 28
Figure 3.2: CyTOF general workflow. 30
Figure 3.3: A Typical flow cytometry workflow. 31
Figure 4.7: Titration analysis of FOXP3. 41
Figure 4.1: Clean up gating strategy for identifying CD45+ immune cell population. 47
Figure 4.2: Titration analysis of CD66b-Pr141 antibody. 48
Figure 4.3: viSNE representation of cell population. 49
Figure 4.4: Illustration of overlaid FlowSOM clustering data on dimension reduction map categorized into populations by manual gating. 50
Figure 4.5: Heatmap visualisation to marker expression by FlowSOM metacluster: 51
Figure 4.6: Mass cytometry statistical analysis of Six APS-1 patients and six healthy controls. 52
Figure 4.8: Illustration of change in FOXP3 signaling in Th17 cells using the two different buffer conditions. 53
Figure 4.9: Gating strategy for identification of functional markers of undifferentiated cells. ...54
Figure 4.10: Eomes expression in CD8+ T cells. 55
Figure 4.11: Expression of lineage subsets of CD4+ and CD8+ T cells. 56
Figure 4.12: Gating Strategy for Th17 differentiated dells for T cell subsets. 57
Figure 4.13: Frequency of T cell subsets expressed by Th17 polarized cells. 57
Figure 4.14: Gating strategy for Th2 differentiation. 58
Figure 4.15: Comparative analysis of cells expressed in stimulated CD4+ cells. 59
Figure 4.16: Box plot representation of Th2 and Th17 cytokine profile. 60
Figure 4.17: Expression of T cell subsets analysed by CyTOF and flowcytometry. 60

Abbreviations

17α-OH	17α-hydroxylase
21-OH	21-hydroxylase
AAD	Autoimmune Addison's disease
AADC	Aromatic L-amino acid decarboxylase
ACTH	Adrenocorticotropic hormone
AhR	Aryl hydrocarbon receptor
AID	Autoimmune Disease
AIRE	Autoimmune regulator
APECED	Autoimmune polyendocrinopathy-candidiasis-ectodermal dystrophy
APC	Antigen-presenting cell
APC	Allophycocyanin (fluorescent dye)
APS-1	Autoimmune polyendocrine syndrome type 1
AR	Autoimmune retinopathy
B CELL	Bone marrow derived B lymphocyte
BCR	B cell receptor
BSA	Bovine serum albumin
CAS	Cell Acquisition Solution
CD	Cluster of Differentiation
CEA	Carcinoembryonic antigen
CMC	Chronic mucocutaneous candidiasis
CST	Cytometer set up and tracking beads
cTECs	cortical thymic epithelial cells
CTL	Cytotoxic T Lymphocyte
CTLA4	Cytotoxic T-Lymphocyte Antigen 4
CXCR3	(C-X-C Motif Chemokine Receptor 3)
CYTOF	Mass cytometry by time of flight
DC	Dendritic cell
DMSO	Dimethyl sulfoxide
DNA	Deoxyribonucleic acid
DP	Double positive
ELISA	Enzyme-linked immunosorbent assay
EDTA	Ethylene diamine tetra acetic acid
FCS	Flow cytometry standard file
FLOWSOM	Flowcytometry self-organising maps
FMO	Florescence minus one
FOXP3	Fork head box P3
FOXO4	Forkhead Box O4
GATA- 3	GATA-binding protein 3
HLA	Human leukocyte antigen
HP	Hypoparathyroidism
HRP	Horse radish peroxidase
ICP	Inductively coupled argon plasma
Ig	Immunoglobulin
IFN	Interferon
IL	Interleukin
IPEX	Immune dysregulation, polyendocrinopathy, enteropathy X-linked syndrome

LAG3	Lymphocyte activation gene 3 protein
MACS	Magnetic-activated cell sorting
MHC	Major histocompatibility complex
MTEC	Medullary thymic epithelial cells
NCAM	Neural cell adhesion molecule
PAI	Primary adrenocortical insufficiency
PerCP	Peridinin chlorophyll (fluorescent dye)
PBMC	Peripheral blood mononuclear cells
PBS	Phosphate buffered saline
PD-1	Programmed death-1
PGE	Promiscuous gene expression
PMTs	Photomultiplier tubes voltage settings
PTH	Parathyroid hormone
PRR	Pattern recognition receptor
RNA	Ribonucleic acid
ROAS	Norwegian registry of organ-specific autoimmune diseases
RORγt	Retinoic acid receptor-related orphan receptor gamma-T
SLE	Systemic lupus erythematosus
STAT	Signal transducer and activator of transcription
T.BET	T-box transcription factor
T CELL	Thymus-derived lymphocyte
TCR	T-cell receptor
TGF-β	Transforming growth factor-β
TH CELL	T helper cell
TLR	Toll-like receptor
TMB	Tetramethylbenzidine
TNF	Tumour necrosis factor
TOF	Time of flight
Treg	T regulatory cell
tSNE	T-distributed stochastic neighbor embedding maps
TSHR	Thyroid stimulating hormone receptor
T1DM	Type 1 diabetes mellitus
TH	Tyrosine hydroxylase
NALP5	NACHT leucine-reich repeat protein 5
OP	Optical density

ACKNOWLEDGEMENT

First and foremost, I would like to express my gratitude to my supervisor Shahinul Islam for his continuous support, guidance, involvement, and insightful comments.

A dept of gratitude is owed to Anette Bøe Wolff who was a constant source of motivation and inspiration throughout this research project. Your patience, constructive guidance, engagement, and encouragement to take real initiative in solving experimental and analytical problems made this work successful.

I would like to express my thanks to all the members of the research group, led by Eystein Sverre Husebye for supplying most of the materials used in this project and being incredibly helpful by providing training and answering questions about analytical techniques required to carry out the experiments. I acknowledge with special thanks, the many helpful contributions of Bergithe Eikeland Oftedal, Marie Karlsen, Brith Bergum and Jørn Skavland during this project. I am also grateful to Thea Sjøgren for her very useful contributions.

I wish to acknowledge Md Obaidur Rahman, and postdocs Alexander Hellesen and André Sulen and my fellow master's student Abtin Tari; Adrianna Jebrzycka and Emina Majcic for their encouragement and inspiring discussions. Special thanks to Lars Ertesvåg Breivik, the GOD of ELISA, and to Elisabeth Halvorsen, and Hajirah Muneer for their assistance

I am sincerely grateful to my colleagues at the department of immunology and transfusion medicine for their support and valuable conversations.

My heart felt gratitude to my parents and siblings, for their daily prayers and encouragement.

I am deeply grateful and indebted to my soul mate, Chris, who was the solid rock on which I stood throughout this study. Thanking you specially for never letting me quit. Without the huge support, this thesis would not have been possible. Hearty thanks for your patience, constant and unwavering love. To my daily smile and truest love, Kamsi, Kamfe, Kosi and Kobim. You all are the best.

ABSTRACT

The autoimmune polyendocrine syndrome type 1 (APS1) is a complex and rare monogenic form of autoimmunity caused by pathogenic variants of the autoimmune regulator (*AIRE*) gene; a transcription factor primarily expressed in the thymus and crucial for central immune tolerance. As a consequence, these patients display a wide variety of autoimmune manifestations in endocrine organs. The identification of the origin and major immune cell lineages involved in the development and pathogenesis of APS-1, remains an emergent issue due to sparse knowledge.

In this work, a detailed immunological characterization and identification of specific immune subsets using functional lineage markers was performed by mass cytometry (CYTOF, cytometry by time-of-flight) using fixed blood from a cohort of 6 APS-1 patients and corresponding sex- and age-matched healthy controls. The results from this high dimensional CyTOF data showed no large alterations in the positive target populations but revealed a relative reduction in the frequency of CD45+ CD3+ CD14- CD19- CD56+ NKT cells compared to controls (mean APS-1= 4.901%; mean healthy controls= 11.35%, p= 0.00433).

Furthermore, a flow cytometry panel was successfully generated and optimised for T cell transcription factors to phenotypically characterize T cell subpopulations in peripheral blood mononuclear cells (PBMC) from 5 APS-1 patients from our study cohort, as well as healthy controls. High expressions of Eomes were detected in unstimulated PBMCs of APS-1 patients compared to healthy controls. However, expressions from T cell subgroups, CXCR3+, GATA3+, RORgt+, T.BET, FOXP3+ cells did not reach significance. We succeeded in generating Th2- and Th17-polarised cells with their signature cytokines, IL-5, and IL-17 respectively, in a small cohort of APS-I patients. A relative proliferation of RORgt+, GATA3+ and FOXP3+ cells were observed with no major discrepancies compared to healthy controls. In addition, the response of some of the T cell subsets measured by both flow and mass cytometry were comparable and no large variations were detected. This could further indicate that CyTOF analysis with fixed blood and flowcytometry analysis of PBMCs are reliable to reproducibly measure immune subsets in APS-1 patients.

Thus, even though with limited number of patients, our study might enhance and contribute to a better understanding of immune cell responses in AIRE- deficient patients. In depth knowledge about immune cell compositions is important to illuminate disease pathogenesis, predict subsequent diagnosis, improve outcome, and develop new therapies.

1 INTRODUCTION

1.1 THE INNATE IMMUNE SYSTEM

The immune system is the body's primary defence system against disease and infection through elimination of toxic and allergenic substances. It has the capacity to distinguish self from non self; thus, recognises and induces a response to invading pathogenic microbes [1]. The immune system is composed of two lines of defence mechanisms: the innate (natural) immune system and the adaptive (acquired) immune system (*Figure 1.1*).

The innate immune system comprises several components of defensive barriers, including the physical barriers, cellular components, and the complement system. The physical barriers such as the skin, mucous membrane, gastrointestinal and genitourinary tracts are the first line of defence and inhibits entry of pathogens. The cellular components include granulocytes, monocytes, dendritic cells (DCs), natural killer (NK) cells, eosinophils, mast cells, basophils, innate lymphoid cells (ILCs) and phagocytes (macrophages). Macrophages and neutrophils are very crucial early in an immune response [4]. The innate branch is rapid and dependent on pattern recognition receptors (PRRs) on innate immune cells which allows recognition of pathogens with common molecular patterns called pathogen associated molecular patterns (PAMPs) e.g. Toll-like receptors [2, 5]. Cytokines and chemokines, which are critical for recruiting immune cells to inflammation and infection sites, are further essential part of the innate immune system [2].

The complement system plays a role in opsonisation and phagocytosis, as well as in identification of pathogens [2]. In addition, NK cells are the third fundamental part of innate immunity being specific for identification of tumour or viral infected cells [6].

1.2 CELLS OF THE ADAPTIVE IMMUNE SYSTEM

The adaptive immune system, also known as the acquired or specific immune response, is the second line of host defence. It is triggered when pathogens persist after the innate immunity fails to inhibit invading pathogens [7]. Thymus derived T lymphocytes (T cells) and bone marrow derived B lymphocytes (B cells) which both originate from pluripotent lymphoid progenitors are the two core cellular elements that are implicated in adaptive immunity (Figure *1.1*). B cells and T cells have highly specialised antigen specific receptors, the soluble or transmembrane B cell receptor (BCR) and the transmembrane T cell receptor (TCR), respectively, that can recognise a persistent antigen after an encounter [8, 9]. Cross talk between B and T cells with antigen presenting cells (APCs), cells which process and present antigens for recognition by T cells, is

tightly regulated and promotes the elimination of specific pathogens [10]. The adaptive immune response is slow but able to retain immunologic memory in case of reoccurrence of subsequent infection [6].

1.2.1 B Cells

B cells are the key element of humoral immunity. They begin development and complete maturation in the bone marrow [11], undergo various distinct developmental stages and, in the process acquire their specificity to antigen [10]. They migrate further to the peripheral lymphoid tissue and upon activation matures into different B cell subsets [12]. The B cell response is initiated upon antigen interaction with the BCR in the presence of co stimulatory signals provided by T helper (Th) cells. Activated B cells differentiate further into antibody secreting plasma cells or memory B cells through proliferation induced by foreign antigens. Memory B cells are enduring and respond rapidly with any re-infection, whereas plasma cells undergo apoptosis [2]. The major function of B cells is the production of high affinity antibodies against foreign antigens, which provides adequate protection against infectious agents. These antibodies or immunoglobulin (Ig) can be membrane bound or secreted in soluble form [10] and are classified into 5 major isotypes (IgA, IgG, IgM, IgE, and IgD) with distinct functional properties [9] . In addition to production of antibodies, B cells can in some cases act as APCs for T cells. However, unlike T cells, they are independent of APCs as they can identify antigens directly via specialised cell surface antibodies, their BCR [2, 10].

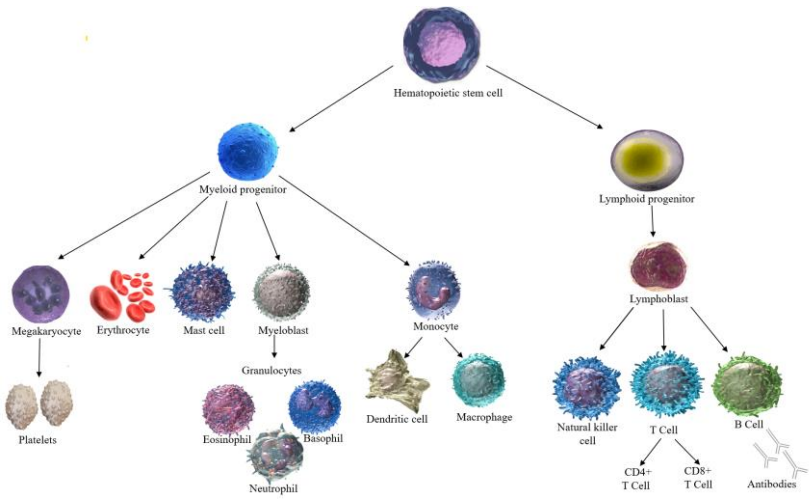

Figure 1.1: Cells of the immune system.

All cellular immune cell components originate from hematopoietic stem cell in the bone marrow. The progenitor is either committed to myeloid or lymphoid lineage and progressively generate different immune cells that work together as part of the innate and adaptive immune system to defend the body against invaders. Modified from Oliveira, C., et al., 2014 [13] using amgen.com images.

1.2.2 T Cell Development

T cells are the key mediators of cellular adaptive immunity and are classified into two major subsets, cluster of differentiation (CD)8- and CD4 T cells. They originate from haematopoietic stem cells within the bone marrow and migrate to a specialised organ called the thymus in a double negative state (CD4-CD8-) for maturation. Producing a functional TCR is a critical step in T cell maturation. The TCR is made up of the alpha and beta (αβ) chains consisting of a constant (C), variable (V), diversity (D), and joining (J) gene segments. The specificity of an antigen for TCR is located in the V segment [14]. TCRs have the ability to recognise antigenic epitopes bound to surface major histocompatibility complex (MHC) molecules of APCs. The TCR also consists of a variation of gamma and delta (γδ) chains. Unlike αβ TCRs, they do not require APCs but binds directly to non-peptide antigens and lack the fine antigen specificity of αβ TCR [15].

Once a functional TCR is produced, the thymocytes now in a double positive state (CD4+CD8+), go through a rigorous selection process in the thymus based on positive and negative selection, where T cells become committed to either CD4+ or CD8+ depending on their ability to bind invariant sites of MHC class I or II molecules (see *1.3.1.1* for more details) and self-reactive thymocytes receive negative signals and are eliminated from the repertoire [16]. The *Autoimmune Regulator (AIRE)* gene is responsible for the clearance of autoreactive T cells through controlled promiscuous expression of tissue specific antigens in medullary thymic epithelial cells (mTECs), as discussed further in section *0*. MHC molecules, also called human leucocyte antigen (HLA) in humans, are grouped into class I or class II, where class I molecules display intracellular peptides and are expressed on all nucleated cells, while the MHC class II molecules display extracellular peptides to T cells. Dendritic cells are excellent professional APCs that are important in these processes as the express high amounts of MHC molecules. Other cell types such as macrophages, epithelial cells, B cells and fibroblasts can also present peptides to T cells in certain environments [4, 10].

1.2.3 T Cell Activation

After thymic selection, thymocytes with appropriate avidity TCR interaction will survive and proceed maturation to naïve T cells. They leave the thymus, and go into circulation through the bloodstream migrating through the lymphoid tissue and peripheral lymphoid tissue until they encounter a specific antigen [17]. In addition, the regulation of immune responses is enhanced through cytokine secretion induced by three signaling cascades [2]. The fate of each surviving thymocyte is dependent on its antigen specificity which is determined by a TCR that recognises

the antigen-MHC complex. Exposure of naïve T cells to antigen orchestrated by these membrane bound molecules on APC lead to clonal expansion and differentiation, and generation of memory and effector T cells [18]. The binding of TCR on both CD4+ and CD8+ cells to its specific antigen-MHC triggers initial activation of T cells.

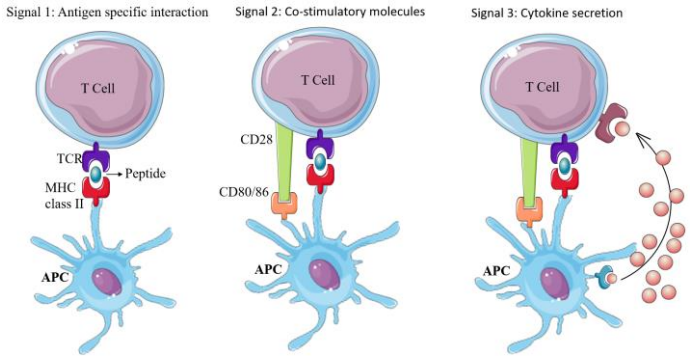

Figure 1.2: Overview of T cell activation.

T cells interacts with dendritic cells through three signals. Signal 1 involves antigen interaction through TCR binding to peptide MHC molecules. Signal 2 is stimulation by co stimulatory molecules to enhance T cell response to antigen. Loss of this signal translates to cell incompetency and deletion. Signal 3 comprises of the release of essential cytokines for T cell expansion and differentiation. Modified from Gutcher 2007 [19].

Besides TCR binding, incorporation of other secondary signals are required for activation and cellular response, such as the binding of CD28 T cell co receptor and the ligands of APC molecules, CD80 (B7-1) or CD86 (B7-2), stimulating cell proliferation in T helper cells. To terminate an immune response, the transmembrane protein CTLA4 (cytotoxic T-lymphocyte antigen-4) on T cells contends with CD28 for B7, and in the process inhibits T cell activation. Cytotoxic T lymphocytes (CTLs) are reliant on signal interaction from CD27/CD70 and 4-1BB (CD137)/4-1BBL co stimulatory molecules for activation. Other signaling molecules and their ligands that can enhance the TCR signaling or provide additional signal for TCR activation and expansion include CD40/CD154 and OX40/OX40L [18].

Upon antigen recognition and reception of the second signal, naïve T cells require signals from specific transcription factors and set of inflammatory cytokines or chemokines to complete its activation process. They undergo functional differentiation processes into distinct effector cells driven by the release of these specific cytokines [20, 21]. The differentiation of CD4+ naïve cells known as T helper (Th) cells is induced depending on what cytokine the cell is exposed to. For instance, Th1 cells are promoted by interferon-γ (IFN-γ) and interleukin (IL)-12, Th2 is dependent on IL-4, and Th17 is promoted by IL-17, IL-6, IL-23 and transforming growth factor-β (TGF-β) [20]. Naïve CD8+ cells upon activation gain effector function and differentiate to CTLs. A small subset of activated CD8+ T cells survive while the majority of the effector cells are phagocytosed

and die by apoptosis. The surviving effector CD8+ T cells are retained and differentiate further to long lived memory cell which plays a critical role upon re-exposure to pathogens [10, 22].

1.2.4 T Cell Subsets

CD8+ CTLs play a role in directly targeting and destroying pathogens including bacteria and viruses mediated through the release of cytolytic granules, containing cytolysin or perforins, otherwise granzymes (Figure *1.3*); or by triggering death receptor ligands, e.g., binding of Fas receptor to Fas ligand (Fas CD95) [21, 23]. CTLs may also kill pathogens through cytokine mediation by the liberation of IFN-γ and tumour necrosis factor (TNF)-α [24].

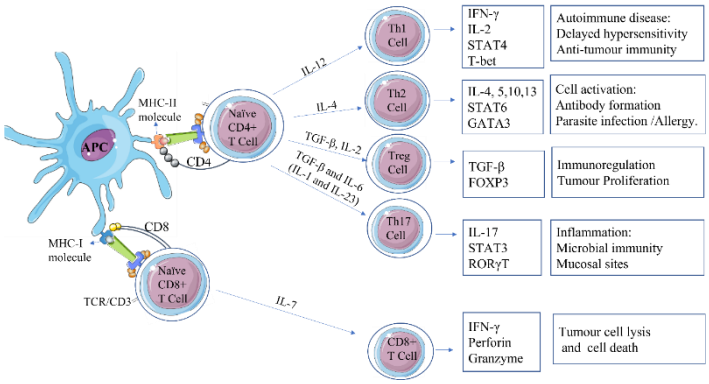

Figure 1.3: T cell subset differentiation.

The TCR and a ubiquitous member of the TCR complex, CD3, are characteristic markers of T cells. CD8+ and CD4+ T cells differentiate further into different subpopulations. Depending on the cytokine environment, CD4+ differentiates mainly into Th1, Th2, Th17 and Tregs. Modified from Joseph A. Bellanti (ed) immunology IV: clinical applications in health and disease [25] using Servier Medical Art.

CD4+ T cells differentiate into any of several subtypes of Th cells and regulatory T cells (Tregs) upon antigen binding and MHC-II activation which includes Th1, Th2, Th17 and Th22. The effector Th cells are critical in the mediation of immune responses to pathogens via the production of cytokines and by stimulating other immune cells to fight infection, such as CTLs and B cells. While the distinct subtypes of Th cells with their characteristic cytokine profile regulate the effective immune response of the innate immune system, the Tregs are crucial for immune tolerance maintenance and able to suppress proinflammatory response through the secretion of effector cytokines such as IL10 and TGF-β [26, 27].

1.2.4.1 Th1 Cells

Th1 cells are one of the major regulators of various central functions within the immune system. They have the ability to recognise and eliminate intracellular pathogens by the activation of macrophages and DCs via the secretion of their signature cytokine IFN-γ [28]. The T-box

transcription factor (T.bet), IL-12 and IFN-γ are central drivers of Th1 cell differentiation [29]. T.bet further downregulates the secretion of the Th2 cytokine, IL-4 [30].

1.2.4.2 Th2 Cells

Th2 cells are crucial in humoral immune responses against parasitic helminth infections and mediate inflammatory responses to allergies and asthma through the secretion of a variety of cytokines such as IL-4, IL-5, IL-9, and IL-13 [31]. IL-4 mediates IgE class switching in B cells [32], induces Th2 cell differentiation from naïve CD4 T cells and is required for the generation of the Th2-derived cytokines. The production of IL-4 is driven by IL-2 which is implicated in Th2 priming and inhibition of Th17 cell development [33]. Th2 cytokines induce mucus secretion and also promote activation and recruitment of the inflammatory cells such as eosinophils, basophils, and mast cells [34]. Th2 differentiation is determined by a network of transcription factors including GATA-binding protein 3 (GATA- 3) and Signal Transducer and Activator of Transcription-6 (STAT6). GATA3 promotes Th2 function and differentiation and inhibits Th1 polarization via downregulation of STAT4 [35].

1.2.4.3 Th17 Cells

Th17 cells are centrally involved in the eradication of extracellular bacterial and fungal infections. This is mediated by neutrophil migration and maturation induced by the secretion of a highly inflammatory cytokine, IL-17 [36]. Beyond the signature Th17 cytokine, IL-17, other effector cytokines such as IL-21, IL-22, IL-6, IL-21, IL-23, and TGF-β participate in Th17 differentiation. The nuclear receptor, retinoic acid receptor-related orphan receptor gamma-T (RORγt) is a key transcription factor for differentiation of Th17 cells from naïve CD4+ T cells in response to IL-1β and IL-6, mimicking the role of T.bet and GATA-3 in Th1 and Th2 differentiation, respectively. RORγt, known for its role in regulating immune homeostasis, induces both IL-17A and IL-17F [37]. IL-21 plays an essential role in RORγt and IL-17 expression while IL-23 together with TGF-β also promotes the expression of IL-17 and RORγt and is critical for Th17 survival and activation [38]. Th17 cells also express the chemokine receptor CCR6 required for the migration of Th17 cells to initiate self-destructive immune reactions [39]. The chemokine receptor CXCR3 is involved in T cell recruitment and trafficking to inflamed tissues and is highly expressed on Th1 cells and implicated in Th17 immune responses [40].

1.2.4.4 Regulatory T Cells (Tregs)

Tregs are specialised CD4+ T cells and negative regulators of other immune cell subset. They are defined by the expression of FoxP3, a classic marker for Tregs and a crucial regulator of Tregs

gene expression. Tregs play major roles in maintenance of immunological tolerance in the periphery [45]. Tregs is characterized by its suppressive function through different mechanisms (Figure 1.4): cytolysis via production of granzymes, secretion of inflammatory cytokines such as IL-10 and TGF-β , association of lymphocyte activation gene 3 protein (LAG3) with MHC class-II molecules, and by downmodulation of DCs [46]. FOXP3 is further involved in regulation of epigenetic modifications by interacting with genes that encode IL-2 and IFN-γ to repress gene expression via deacetylation of histone H3 and also activates the expression of CD25 and CTLA4 by stimulating histone acetylation [47].

AIRE, an essential transcriptional regulator in the central immune system maintains central tolerance by inducing $CD25^{+}CD4^{+}$ Treg production. These attributes portray the key functions of AIRE and Tregs in self-tolerance [48]. Setoguchi and colleagues demonstrated the fundamental role of suppressor T cells and IL-2 in autoimmune disease and maintenance of self-tolerance using mice injected with anti-IL-2 monoclonal antibodies and reported downregulation of CD4+CD25+ Tregs. Neutralisation of IL-2 was also observed to inhibit peripheral $CD25^{+}$ $CD4^{+}$ T cells differentiation. These findings illustrate the importance of IL-2 in the survival and proliferation of Tregs in the periphery. [49].

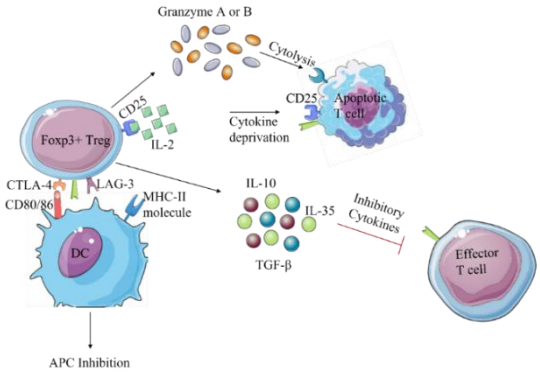

Figure 1.4: Mechanism of Tregs suppression.

Regulatory T cells (Tregs) are critical in the maintenance of immune tolerance and as a regulator of inflammation. FOXP3 Tregs mediates suppression of immune response through different mechanisms which involves either the production of high amount of inhibitory cytokines (IL-10, TGF-β, and IL-35) and cytolytic molecules (granzymes A and B) or the downmodulation of APC through CTLA-4 and LAG-3, and IL-2 deprivation through CD25. Modified from Noval et al 2016 [50].

Alterations in Tregs can predispose to, or cause autoimmunity. Deletion or loss-of-function mutations in the human gene *FOXP3* might lead to severe autoimmunity/immune deficiency (Immune dysregulation, polyendocrinopathy, enteropathy, X-linked (IPEX) syndrome) [51]. Defects in thymic development, *AIRE* mutations and disruption of peripheral tolerance maintenance might be the leading cause of Treg impairment and a significant alteration in the TCR repertoire in APS-1 patients [52, 53]. The suppressive mechanisms of Tregs (Figure 1.4) are not

yet well defined. Further *in vivo* studies are required to elucidate the major targets of Treg suppression.

1.3 AUTOIMMUNITY AND IMMUNOLOGICAL TOLERANCE

1.3.1 Immunological Tolerance

Immunological tolerance is defined as an active regulated lack of response of lymphocytes to self-antigens that have a potential to induce an immune response [54]. Immune tolerance is crucial for the prevention of the development of autoimmune diseases, and it is classified into two operating mechanisms: central and peripheral tolerance.

1.3.1.1 Central Tolerance

Central tolerance takes place in the primary lymphoid organ (bone marrow and thymus) during lymphocyte development when the immature lymphocytes encounter self-antigens and undergo selection processes according to their antigen recognition ability and are clonally eliminated, diverted, or edited [54]. This involves mechanisms of negative and positive selection.

B cell central tolerance occurs in the bone marrow to guarantee the survival of only cells that recognise foreign antigens. Self-reactive BCRs displayed by immature B cells are eliminated by apoptosis.

T cell central tolerance occurs predominantly in medullary and cortex region of the thymus where developing lymphocytes undergo positive (clonal expansion) or negative selection (clonal deletion) based on their TCRs ability to interact with self-peptide MHC molecules [56]. In the outer thymic cortex, thymocytes generate both CD4 and CD8 double positive (DP) cells that express TCRs capable of recognizing antigens in association with MHC molecules presented by cortical thymic epithelial cells (cTECs). For positive selection, thymocytes that survive are committed to either the CD4+ or CD8+ T cell lineage (Figure 1.3) depending on which MHC class that was recognised and by directed migration, relocate into the medulla according to their binding affinity to MHC class I /II molecules on the thymic stromal cells [57, 58]. In the medulla, single positive cells interact with medullary thymic epithelial cells (mTECs), B cells and other APCs through random migration [57].

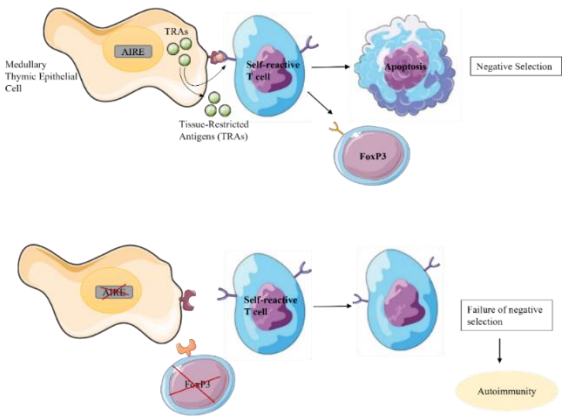

Figure 1.5: Central tolerance and autoimmunity.

AIRE is expressed in the thymic medullary epithelial cells and mediates the expression of tissue specific antigens promoting negative selection of autoreactive thymocytes. It may also regulate immunological tolerance via the induction of regulatory T cells in the thymus. Modified from Husebye et al 2018 [55].

Negative selection is another process of central tolerance where immature lymphocytes with high avidity TCRs for self-peptide + MHC molecules undergo apoptotic cell death [59, 60]. This process ensures the elimination of potential self-reactive lymphocytes, thus prevents the release of potentially dangerous autoimmune cells. [59, 61]. AIRE is a key component in the mechanism of central tolerance in the thymus and mediates the promiscuous expression of tissue restricted antigens (self-antigens) presented on the surface of mTECs via MHC molecules [62, 63]. T cells with medium affinity to antigens in the thymus can become Tregs [80].

1.3.1.2 Peripheral Tolerance

Peripheral tolerance takes place in peripheral tissues (spleen, lymph nodes) and represents a safety net for the elimination of self-reactive immune cells.

Peripheral tolerance operates through at least three main mechanisms; autoreactive T cells are deleted through cell death by apoptosis mediated by the interaction between a cell-surface death receptor, Fas (CD95) and its ligand, FasL (CD178) [60, 64]. The lymphocytes may also become functionally unresponsive to their antigen (clonal anergy). The CTLA-4 and programmed death-1 (PD-1) are fundamental costimulatory molecules in anergy [60, 65]. The binding of CTLA-4 with CD80/86 (B7 ligand) on the APC inhibits T cell signalling. Autoreactive T cells may also differentiate into induced Tregs [66] which can suppress autoimmunity by both cell-contact mediated mechanisms and contact independent mechanisms. Peripheral tolerance mechanisms inhibit or suppress expression of self-reactive lymphocytes that may pose a threat to the immune system.

Peripheral tolerance in B cells occurs in the secondary lymphoid tissues when immature autoreactive B cells escape central tolerance in the bone marrow and migrate into the periphery where they become anergic or are clonally deleted to prevent organ-specific autoimmunity. Anergic B cells become silenced and remain in a state of unresponsiveness upon encounter with self-antigen and are not able to mount antibody response [67, 68].

1.3.2 Autoimmunity

Autoimmunity is defined as the failure of the body to distinguish its own cell and tissues 'self' from foreign and invading bodies 'non-self'; The body then produces antibodies (autoantibodies) and mounts T cell attack on its own cells. It is generally described as the breakdown of immunological tolerance, and affects approximately 5% of the population in Western countries [69]. Genetic and environmental mechanisms are the causative agents of autoimmunity. T cells and self-reactive antibodies are hallmarks of autoimmune disease diagnosis[70].

Failure of tolerance mechanisms is the origin of autoimmune diseases, a life-threatening and chronic condition where the immune system targets and destroys the host organ or tissue [71, 72]. It is categorised into two classes: systemic and organ-specific. In systemic autoimmune disease such as vasculitis, systemic lupus erythematosus (SLE), primary Sjogren's syndrome, rheumatoid arthritis and others, the immune system attacks ubiquitously expressed self-antigens in several organs. Conversely, in organ-specific autoimmune disorder, the immune response is directed preferentially towards self-antigens in a (or several) particular organ(s) or tissue type(s). Examples of organ -specific diseases and their target organs or tissues include type 1 diabetes (the islets of Langerhans are targeted), Hashimoto's thyroiditis (thyroids are targeted), gastritis (gastric parietal cells are targeted), and Addison disease (adrenal cortex is targeted) [70, 73].

1.3.3 The Role of Th17 Cells and Treg Cells in Autoimmunity

Th17 cells are major players in autoimmunity whereas Treg cells block autoimmunity, therefore a balance between Tregs and Th17 provides a better understanding of immune tolerance and autoimmunity [74]. The generation of Tregs and Th17 cells is interlinked through the mediation of TGF-β and IL-2. While IL-2 blocks the generation of Th17 cells, TGF-β deactivates lineage diversion of Th17 cells to Th1 or Th2 cells, and in combination with IL-6 induces Th17 differentiation [75, 76]. Additionally, TGF-β and IL-2 play key roles in Treg cell differentiation. Tregs also acts against Th1 and Th17 responses to evade tissue damage. Its interaction with other

transcription factors such as GATA3 and RORγt in previous studies have provided additional evidence of the role of FOXP3 in regulating gene expression [77, 78].

1.3.4 Biomarkers for Immune Cells.

The immune system is made up of different cell types that are essential in protecting the body against pathogens. Identification and quantification of cellular markers can provide a clearer understanding of the immune system and illuminate a wide variety of T cell functionalities. They are informative and useful tools used to identify a specific immune cell population.

In proteomic analyses, extracellular linage markers with characteristic functional molecules can be combined to identify and assess different immune cell subsets. Particularly, T cell subsets can be distinguished by incorporating analysis of intracellular transcription factors like T.bet, GATA3, RORγt, FOXP3, AHR, and/or Forkhead Box O4 (FOXO4) in functional assays to provide a better discrimination of the various subsets [79]. Some of the potential functions of these transcription factors and cytokines are illustrated in Figure 1.3.

1.4 AUTOIMMUNE POLYENDOCRINE SYNDROME TYPE 1 (APS-1)

Autoimmune polyendocrine syndrome type-1 (APS-1) is a model disease for autoimmunity. It is a rare monogenic disorder involved in multiple organ damage. APS-1, also known as autoimmune polyendocrinopathy-candidiasis-ectodermal dystrophy (APECED, OMIM 240300) is characterized by biallelic mutations in the autoimmune regulator (*AIRE*) gene localised on chromosome 21q22 which impairs the development of immune tolerance causing autoimmunity. [80, 81]. It is an autosomal recessive inherited disease, although some cases of heterozygous dominant negative variants have been reported [82, 83].Numerous cases of this rare disorder have been reported worldwide, with the highest prevalence reported among the Iranian Jewish population as 1:9000, Sardinians (1:14 000) and Finns (1:25 000) [84]. In Norway, the prevalence is estimated to about 1:90 000 [85].

1.4.1 Diagnosis and Clinical Manifestation of APS-1

APS-1 usually manifests in childhood or in adolescence, although other manifestations may appear over time in life [86, 87]. The prevalence of APS-1 components increases with age and affects both male and female equally [88]. This disorder is characterized by a classic triad of chronic mucocutaneous candidiasis (CMC), hypoparathyroidism, and primary adrenal insufficiency or Addison's disease (illustrated in Figure *1.6*). For diagnosis, patients must fulfil at least two of the

classic triad components [89, 90]. Most APS-1 patients develop other endocrine and non-endocrine disorders over time, such as alopecia, nail dystrophy, vitiligo, gonadal failure, type 1 diabetes, chronic hepatitis, etc [84, 88, 89, 91]. The clinical phenotype of APS-1 is highly variable even seen among siblings. Many APS-1 subjects present up to seven different manifestations of this disorder. [88, 89]. Hence, they require close follow-up in the clinic.

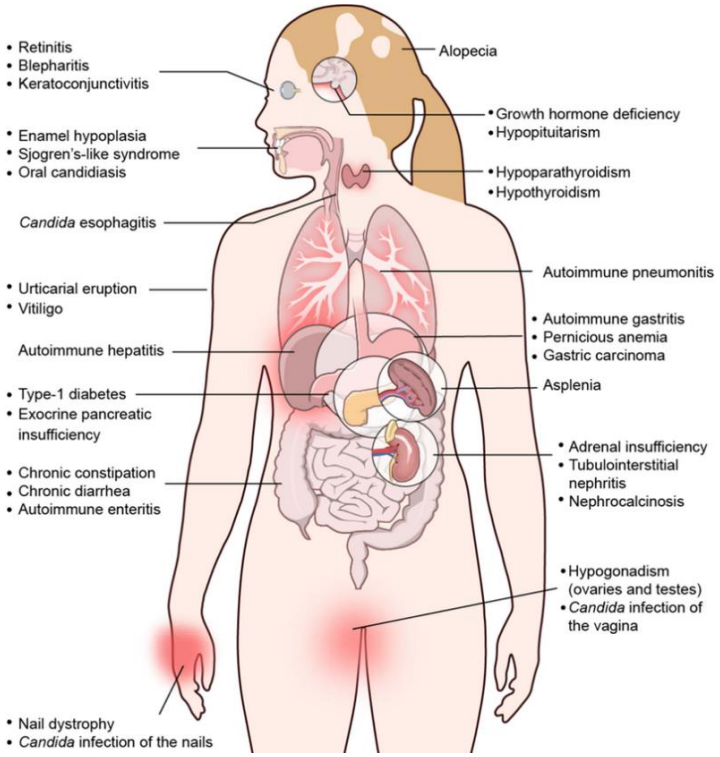

Figure 1.6: Illustration of the classic components and other minor components of APS-1.

The rare monogenic disorder APS-1 is characterized by the presence of 2 of the major components, Addison's disease, hypoparathyroidism, and chronic candidiasis. Patients also acquire several other manifestations. Figure adapted from Constantine et al 2019 [92].

1.4.2 The Autoimmune Regulator Gene

The transcription factor autoimmune regulator (AIRE) is a key component in the mechanism of central tolerance in the thymus. Mutations in the *AIRE* gene is the essential core cause of APS-1 [81]. AIRE is located in the cell nucleus and majorly expressed in the thymic medullary epithelial cells (Figure 1.5); however, it has also been reported to be relatively expressed in some atypical and rare cells in hematopoietic lymph node populations, and in spleen and fetal liver [98, 99], although these data are controversial.

The *AIRE* gene consists of 14 exons coding for a 545 amino acid protein that functions as transcription regulator with a predicted molecular mass of 58kDa. AIRE regulates the expression

of some peripheral auto-antigens in the thymus, such as preproinsulin, and plays a critical role in generating immune tolerance to self-antigens by facilitating negative selection in the thymus through apoptosis or induction of specialised regulatory T cells [100, 101]. The AIRE protein is further composed of several specific functional domains which includes, nuclear localisation sequences (NLS), the caspase recruitment domain/homogeneously staining (CARD/HSR) region, a DNA binding domain named SAND (SP100, AIRE, Nuc p41/75, DEAF), four LXXLL motifs and two plant homeodomain (PHD) zinc finger motifs signifying its regulatory effect in transcription [80, 101] (Figure 1.7).

The loss of function mutations of the *AIRE* gene causes failure to mediate clonal deletion of autoreactive T cells in the thymus causing the rise of APS-1 disorder. These dangerous T cells are then released to the blood stream with potential to target and destroy endocrine and other epithelial tissues [103, 104], reflected by findings of autoreactive T cells and organ-specific antibodies in APS-I patients.

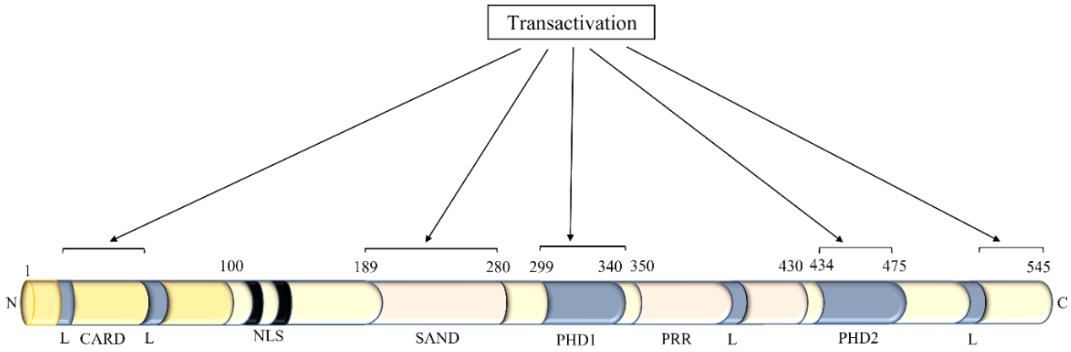

Figure 1.7: Schematic representation of the AIRE gene and its functional domain.

The AIRE protein is composed of the CARD/HSR domain; crucial for the dimerization of the polypeptides, a SAND domain that has a function in DNA binding, AIRE transactivation capacity and subcellular localization, a PRR region and four LXXLL motifs associated with transcription regulation and two PHD domain that plays a role in protein–protein interactions. Modified from Peterson et al, Nature Reviews Immunology 2008 [102].

1.4.3 Autoantibodies in APS-1

Due to the rarity and non-specific clinical appearance of APS-1, the presence of autoantibodies has improved the identification of APS-1 development. APS-1 patients produce autoantibodies that target tissue-specific antigens or against cytokines of the immune system. The early appearance and high specificity of these autoantibodies are a hallmark and characteristic features of APS-1. They can elucidate disease pathogenesis and serve as biomarkers which can aid in the prediction, clinical diagnosis and follow-up of APS-1 [103, 105, 106].

Common organ-specific autoantibodies displayed by APS-1 patients with their associated disease components include 21-hydroxylase (21-OH) associated with Addison's disease, Aromatic L-amino acid decarboxylase (AADC) associated with hepatitis and vitiligo, Tyrosine hydroxylase (TH) associated with alopecia and NACHT leucine-reich repeat protein 5 (NALP5) associated with hypoparathyroidism [107]. APS-1 patients also have autoantibodies against type 1 interferon (IFN) and TH17 related cytokines [108, 109].

Taken together, the defective function of AIRE activity disrupts central immunological tolerance which causes severe autoimmunity and immune deficiency. This illustrates the fundamental role of an intact tolerance machinery in avoiding autoimmune disease [86, 110-112]. The rarity of the APS-1 syndrome, long time between the onset of different disease components and unawareness of disease among practitioners have contributed to misdiagnosis, delayed diagnosis and treatment and mortality [86]. More research work is required for improved and effective management and treatment of APS-1 disease.

1.5 HYPOTHESIS AND AIM

The human immune cell composition is very complex with diverse localisations, as well as biological and chemical functions. Therefore, an adequate comprehensive assessment using different methodologies is imperative. Identifying aberrated frequencies of major immune cell lineages or the absence of an immune subset can unravel deeper explanation and understanding of rare autoimmune diseases like APS-1. There are very few studies conducted on the characterization of immune subsets at the site of the autoimmune reaction (the adrenal and other endocrine organs) in APS-1 due to restricted access to the organs in patients in addition to the rarity of the disease. Hence, knowledge about the mechanisms and development of the immune cells is insubstantial and limited. Blood is easier to obtain and can be a valuable substitute in order to investigate immune cell subsets that are involved in disease specific processes.

We hypothesize that by using high dimensional, high throughput immune monitoring technologies like mass and flow cytometry, we can identify distinct functional biomarkers and potential therapeutic targets in APS-1. Furthermore, it may provide a deeper understanding of the pathogenesis and function of AIRE; In addition, our approach offer further insights on general immunological mechanisms.

1.5.1 Aim of Study

The overall purpose of this project is to characterize immune cell subsets in APS-1 patients with specific focus on T cells.

The specific aims are:

I. To characterize a wide specter of immune cell subsets in APS-1 patients compared to healthy controls using fixed whole blood by an existing mass cytometry (CYTOF) panel.
II. To investigate the T cell subsets of APS-I patients more in depth by generating and optimizing a flow cytometry panel for transcription factors.
III. Compare the T cell subpopulations identified by CYTOF with the optimized flow cytometry panel.

2 MATERIALS

Chemicals	Producer	Cat. Number
Cytodelic Stabiliser (100mL)	Cytodelics	hWBCS002-100
Cryo#20	Cytodelics	CR020-100
4x Lysis Buffer (1000mL)	Cytodelics	hC002-1000-L01
5x Wash Buffer (900mL)	Cytodelics	hC002-1000-W01
Fix-Diluent (500 mL)	Cytodelics	hC002-1000-F01
Fix-Concentrate (500 mL)	Cytodelics	hC002-1000-D01
Anti-CD3, BV510, Clone UCHT1	BioLegend	300448
Anti-CD4, Alexa Fluor 700, Clone: RPA-T4	BD BioSciences	557922
Anti-CD8, PerCP-Cy5.5, Clone:SK1	BD BioSciences	565310
LIVE/DEAD Fixable Yellow Dead Cell Stain Kit	Invitrogen	L34959
CXCR3-PE-GO25H7	Biolegend	353706
EOMES- APC-eFluor780-WD1928	Invitrogen eBioscience	47-4877-42
GATA-3 -eFluor 450 (Pacific Blue)-TWAJ	Invitrogen eBioscience	48-9966-42
T.BET- Alexa Fluor 488 EBio4B10 (4B10)	Invitrogen eBioscience	53-5825-82
Anti- FOXP3-PE-TR-ECD-236A/E7	BD BioScience	563955
RORGT-APC-AFKJS-9	Invitrogen	17-6988-82
Human BD Fc Block	BD BioScience	564220
Heparin	Sigma Aldrich	H3393
Dimethyl Sulfoxide (DMSO)	Sigma Aldrich	D2650
Dulbecco's Phosphate Buffered Saline (PBS)	Sigma Aldrich	D8537
AB Serum	Sigma Life Science	H4522
Ficoll-Paque PLUS	Cytiva	GE17-1440-02
AutoMACS Rinsing Solution 99,5%	Miltenyi Biotec	130-091-222
MACS BSA Stock Solution	Miltenyi Biotec	130-091-376
Penicillin-Streptomycin	Lonza	17-602E
MACs Cell Acquisition Buffer	Fluidigm	SKU 201244
16% Para Formaldehyde	ThermoFisher Scientific	28906
Maxpar Water	Fluidigm	SKU-201069
Iridium Intercalator	Fluidigm	201192
TexMACS medium	Miltenyi	130-097-196
PBS Tablets	Merck	524650-1EA
Trypan Blue Solution 0.4%	ThermoFisher Scientific	15250-061
Ultra-Comp eBeads	ThermoFisher Scientific	01-3333-41
Nuclease Free Water	VWR chemicals	4311814

2.1 LIST OF ANTIBODIES FOR MASS CYTOMETRY

	Antibody	Metal	Clone		Company
1	CD10	156Gd	HI10a	1:800	Fluidigm
2	CD103	151Eu	Ber-ACT8	1:100	Fluidigm
3	CD11b	167Er	ICRF44	1:200	Fluidigm
4	CD11c	147Sm	Bu15	1:400	Fluidigm
5	CD123 (IL3R)	143Nd	6H6	1:400	Fluidigm
6	CD127 (IL7Ra)	149Sm	A019D5	1:100	Fluidigm
7	CD15/SSEA-1	172Yb	W6D3	1:50	Fluidigm
8	CD152 (CTLA-4)	161Dy	14D3	1:100	Fluidigm
9	CD16	209Bi	3G8	1:800	Fluidigm
10	CD161	164Dy	HP-3G10	1:100	Fluidigm
11	CD20	116Cd	2H7	1:200	*Conjugated in house*
12	CD25 (IL2R)	169Tm	2A3	1:200	Fluidigm
13	CD27	158Gd	L128	1:400	Fluidigm
14	CD274 (PD-L1)	159Tb	29E.2A3	1:100	Fluidigm
15	CD278 (ICOS)	148Nd	C398.4A	1:100	Fluidigm
16	CD279 (PD-1)	155Gd	EH12.2H7	1:800	Fluidigm
17	CD28	160Gd	CD28.2	1:400	Fluidigm
18	CD31/ PECAM1	144Nd	WM59	1:200	Fluidigm
19	CD4	145Nd	RPA-T4	1:400	Fluidigm
20	CD45RA	153Eu	HI100	1:800	Fluidigm
21	CD45RO	165Ho	UCHL1	1:400	Fluidigm
22	CD5	166Er	UCHT2	1:1600	*Conjugated in house*
23	CD57	176Yb	HCD57	1:100	Fluidigm
24	CD66b	141Pr	G10F5	1:100	*Conjugated in house*
25	CD69	162Dy	FN50	1:100	Fluidigm
26	CD8a	168Er	SK1	1:1600	Fluidigm
27	HLA-DR	174Yb	L243	1:800	Fluidigm
28	IgD	146Nd	IA6-2	1:200	Fluidigm
29	CD134	150Nd	ACT35	1:50	Fluidigm
30	TCRγδ	152Sm	11F2	1:50	Fluidigm
31	Tigit	154Sm	MBSA43	1:200	Fluidigm
Backbone Panel					
33	CD45	89Y	HI30	1:800	Fluidigm
34	CD3	170Er	UCHT1	1:800	Fluidigm
35	CD14	112Cd	MEM15	1:200	*Conjugated in house*
36	CD56	163Dy	NCAM16.2	1:800	Fluidigm
37	CD19	142Nd	HIB19	1:400	Fluidigm

2.2 KITS AND EQUIPMENT

Product Name	Producer	Cat. Number
Cell-ID™ 20-Plex Pd Barcoding Kit	Fluidigm	SKU: 201060
CD66abce Microbead	Miltenyi Biotec	130-092-393
Maxpar® X8 Antibody Labelling Kit, 141Pr-40 Rxn	Fluidigm	Fluidigm
C-Chip disposable hemacytometer Burker B	NanoEntek	DHC-B01
CoolCell freezing container	Corning	432001
Cryotubes 1,2 mL	VWR	479-1254
Cryogenic vials 1.5ml	Nalgene	5000-1020
CellXVivo Human Th2 Cell Differentiation Kit	R&D Systems	CDK002
CD4+ T Cell Isolation Kit	Miltenyi	#130-091-155
Dynabeads Human T-Activator CD3/CD28	Thermo Fisher Scientific	11132D
Dynal Magnet	Dynal Biotech	MPC-S 120.20
T Cell Activation/Expansion Kit	Miltenyi	130-091-441
Human IL-17 DuoSet ELISA	R&D Systems	DY317-05
Human IL-5 DuoSet ELISA	R&D Systems	DY205-05
DuoSet Ancillary Reagent kit 2	R&D Systems	DY008
Disposable Glass Pasteur pipettes 150mm	VWR	612-1701
Culture plates - 96-well round-bottom plate - 48- plate	 -Applied Biosystems -Corning	 N8010560 35484
Centrifuge Filter Unit: 3kDa Amicon Ultra 500 µL V bottom	Millipore	UFC500396
Centrifuge Filter Unit: 50kDa Amicon Ultra 500 µL V bottom	Millipore	UFC505096
eBioscience FOXP transcription factor Fixation/Permeabilization Kit	Invitrogen	00-5521-00
Finnpipette F1 Variable Volume Single-Channel Pipette - 0.2-2 µL - 0.5-5 µL - 1-10 µL - 2-20 µL - 10-100 µL - 20-200 µL - 100-1000 µL	Thermo Fisher Scientific	 4641020N 4641010N 4641030N 4641050N 4641070N 4641080N 4641100N
Falcon serological pipettes - 10 mL - 25 mL	Corning	357551 P8250
Falcon tube - 15 mL - 50 mL	VWR	 525-1085 525-1109
Eppendorf tubes DNA LoBind Tube 1,5 mL	Eppendorf	022431021
Nitrile Medication Examination Gloves		
LS column	Miltenyi Biotec	130-042-401
MiniMACS Separator	Miltenyi Biotec	130-042-102
Microtube 2 mL	Sarstedt	72.694.006
MS column	Miltenyi Biotec	130-042-201

Product Name	Producer	Cat. Number
OctoMACS Separator	Miltenyi Biotec	130-042-109
Pasteur pipette	VWR	1612-1613
Pipetboy acu 2 Controller	Integra Biosciences	
Pre-separation Filters	Miltenyi Biotec	130-041-407
Finn pipette F1 Multichannel Pipette 3-300µL 8 Channels	Thermo Fisher Scientific	
QuadroMACS Separator	Miltenyi Biotec	130-098-308
Scepter Sensors 40 uM	Merck (Millipore)	PHCC40050
Vacuette K3 EDTA tubes 9 mL	Greiner bio-one	455036
Vacuette Lithium Heparin tubes 10 mL	Greiner bio-one	455084

2.3 INSTRUMENTS

Instrument Name	Producer
BD LSR Fortessa	BD Biosciences
CYTOF Helios	Fluidigm
Centrifuge 5810	Eppendorf AG
CO2 incubator	Sanyo
Incubator 1000	Heidolph
Multifuge 3SR+ Centrifuge	Thermo Scientific
Nanodrop ND-1000 Spectrophotometer	BD
Olympus CKX53 microscope	Olympus
Scepter handheld automated cell counter	Merck (Millipore)
Shaker Unimax 1010	Heidolph
Test tube rotator	Labinco
Milli-Q-IQ 7003/05/15 Water purification system	Merck
Vacusafe inspiration system	Integra Biosciences
Vortex 1 S000	Ika

2.4 SOFTWARE

Software Name	Developer
BD FACS Diva	BD Biosciences
Flow Jo 10.8.1	FlowJo LLC
Graphpad Prism 9.0	GraphPad
Thermo Fisher connect	Thermo Fisher Scientific
Cytobank	Beckman Coulter (Life Science)
CYTOF software (7.0.8493.0)	Fluidigm

3 MATERIALS AND METHODS

3.1 EXPERIMENTAL OUTLINE

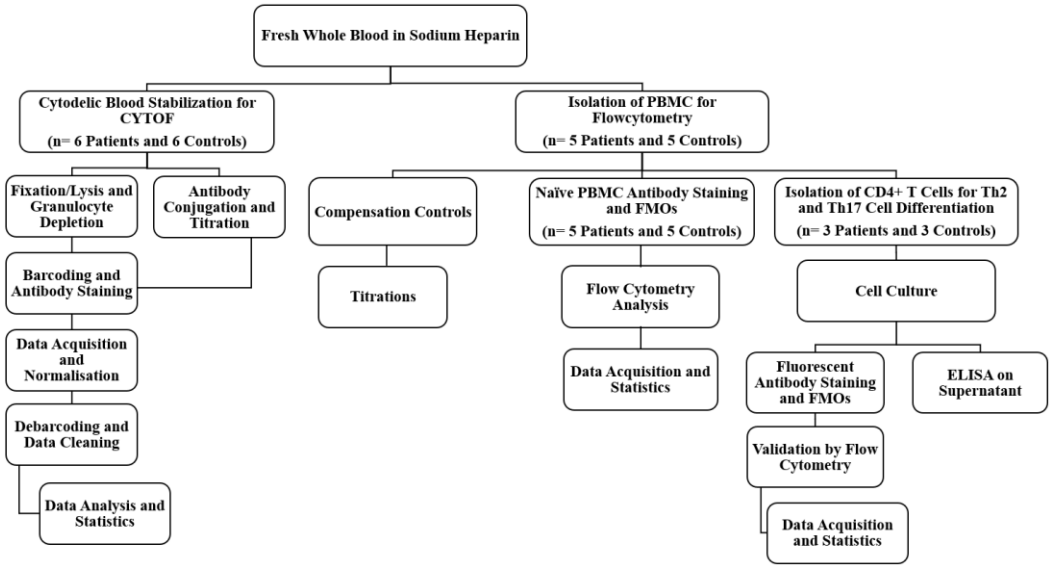

Figure 3.1: Experimental flow chart.

Stabilised fixed whole blood samples were processed to generate cell suspension which were depleted of granulocytes by magnetic separation. Agranulocytes were barcoded with unique IDs, pooled as one sample, and stained with metal conjugated antibody before further mass cytometry analysis. For flow cytometry analysis, CD4+ T cells were furthermore separated from peripheral blood mononuclear cells (PBMC) using density gradient centrifugation in positive selection by magnetic bead separations. The CD4+ T cells were stimulated by cytokines to drive differentiation into Th2 and Th17 cells, followed by cell culture and collection of supernatant to determine cytokine expression using ELISA. Flow cytometry was performed on naïve CD4+ T cells and the expanded Th2 and Th17 polarising cells to assess and phenotype immune cells in patients and controls.

3.2 SAMPLE MATERIALS AND ETHICAL ASPECT

3.2.1 Patient Samples

Six APS-1 patients with confirmed *AIRE* mutations were recruited from the Norwegian Registry for Organ Specific Autoimmune Diseases (ROAS/FOAS), Haukeland University Hospital, Norway (REK biobank 2013/1504), the world's largest biobank and registry with clinical information of patient with APS-1 and Addison's disease. We included four males and two female, (mean age: 47 years, range age: 31-62 years). ROAS was established in 1996 and its biobank contains whole blood, peripheral blood mononuclear cells (PBMCs) and other biological materials from relevant patients. All the patients included in this study fulfilled the criteria for clinical diagnosis of APS-1 and signed informed written consent for participation in compliance with the Declaration of Helsinki Ethical Principles and Good Clinical Practices. This project was approved

by the Regional Ethical Committee of Western Norway (approval number 2018/1417 and 2009/2555).

3.2.2 Healthy Control

Fresh whole blood was collected by venepuncture from six gender- and age- matched anonymous healthy blood donors using BD vacutainer sodium heparin tubes (four males and two female, (mean age: 48 years, range age: 30-65 years) were obtained from Haukeland University Hospital blood bank, Bergen, Norway.

3.3 CHOICE OF METHODS

The two major technological platforms used in this project are mass cytometry (CyTOF) and flow cytometry. Cell culture and enzyme-linked immunosorbent assay (ELISA) were also performed. The figure below gives an overview of the experimental outline of this study.

3.3.1 *Mass Cytometry by Time-of-Flight (CyTOF)*

Mass Cytometry, a high dimensional proteomic single cell analysis technology, is one of the major techniques employed in this project to identify distinct immune cell subsets that distinguish APS-1 patients from healthy donors. Mass cytometry allows the simultaneous detection of up to 50 parameters at a single cell resolution. In CyTOF, antibodies are labelled with rare heavy metal isotopes from the lanthanide series that are non-existent in biological products. This reduces spectral overlap between channels, with very low background noise and requires minimal compensation [113-115].

Labelled cell suspensions are nebulised and aerosolised into droplets containing single cells. The droplets are subsequently passed through an inductively coupled argon plasma (ICP) to generate ion clouds, which is also referred to as a push. The ICP burns at a temperature of approximately 7000 kelvin (K), hence all molecules in the suspension are vapourised and atomized. The metal ions are therefore converted to cloud of charged ions [116]. The ion cloud shrinks into a focused beam of ions which are filtered by the deflector and quadrupole to remove impurities, thereby enhancing the heavy metal ions and separates them by their mass-to-charge ratio in a time-of-flight (TOF) mass spectrometer [114].

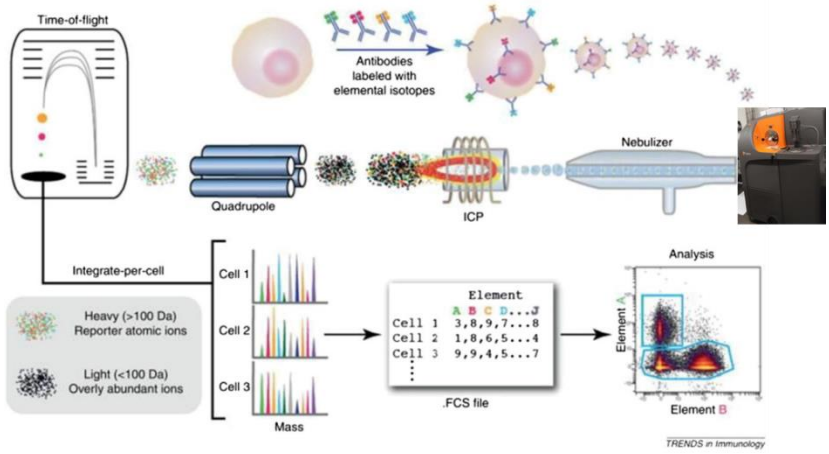

Figure 3.2: CyTOF general workflow.

Cells tagged with metal conjugated antibodies are introduced through a nebuliser in single cell containing droplets and injected into an argon plasma where it is ionised and atomised into ion clouds and measured in a time-of-flight (TOF) chamber. Adapted from Bendall et al., Trends Immunol 2012 ***33:****325* [117].

The TOF is measured as the time it takes an ion cloud to hit the detector at a specified distance [113].The focused ion beams enter the TOF chamber by voltage pulses and hit the detector in the sequence of increasing ion mass. Since all the ion probes have the same charge, they are therefore exclusively separated by their atomic mass. So, lighter ions with high velocity travel faster and hit the detector, while the heavier ions with longer TOF arrive at the detector later [118]. The ions exit the TOF chamber in the same sequence and are detected by a discrete dynode electron multiplier. When ions are detected in high concentrations, there is an overlap in the generated pulse signals. However, they tend to have a low signal overlap, when detected in lower concentrations. The intensity values and pulse counts are recorded over time as dual data for each channel, saved as an FCS formatted file and analysed using flow cytometry software [117].

3.3.2 Flow Cytometry

Flow cytometry is another major technique that was exploited in this project to characterize and phenotype immune cells from peripheral blood. It is a laser-based technology that has emerged as a fundamental tool for profiling of the immune system. Flow cytometry enables single cell analysis through quantitative and qualitative measurement of fluorescent antibodies bound to antigens of interest [119]. Similar to CyTOF, the antigens used in flow cytometry are lineage markers or cluster of differentiation (CD) markers, including different functional markers, such as transcription factors, cytokines, or proliferation markers that help to define certain immune cell populations and activation level. However, antibodies are conjugated to fluorochromes in flowcytometry as opposed to metal tagged antibodies used in CyTOF. One of the limitations for

flowcytometry is the reduced number of parameters that can be analysed at a time because of spectral overlap between the tags.

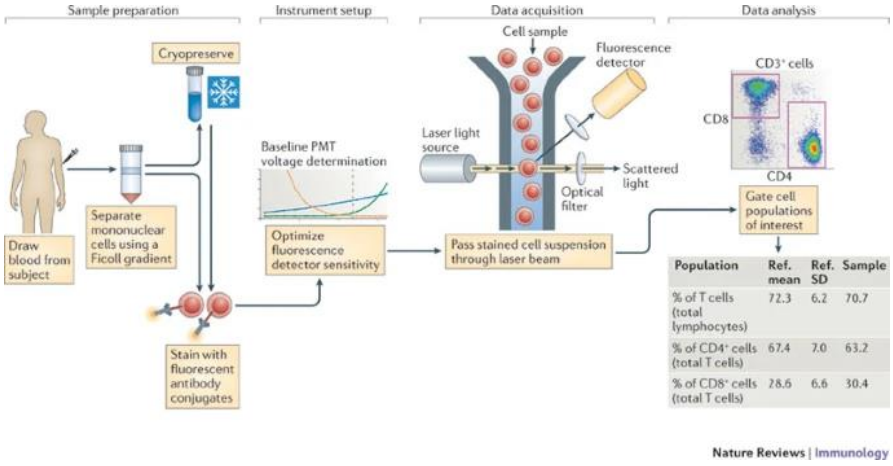

Figure 3.3: A Typical flow cytometry workflow.

PBMCs are prepared by Ficoll gradient centrifugation and cryopreserved prior to staining with fluorescent antibody conjugates. Cells in suspension are passed through a focused light source to measure the amount of scattered light, which is detected as side scatter (SS), or forward scatter (FS), which correlates to cell granularity or complexity and size respectively. Figure adapted from Maecker et al., 2012 [120].

In this study, PBMCs isolated from APS-1 patients and healthy controls were incubated with fluorescently labelled antibodies specific for cell surface or intracellular proteins of interest. The fluorochrome is excited at a specific wavelength and light is emitted at a specific lower wavelength which is subsequently detected by the flow cytometer [121]. The varying wavelengths of the emitted lights causes spectral overlap which must be compensated mathematically. Consequently, this limits the number of fluorochromes which can be used simultaneously, because the greater number of fluorophores used could lead to exaggerated spill overs and false signals in neighbouring channels. Flow cytometry measures light scatter in two different directions, the forward (FS) and side scatter (SSC) indicating cell size and granularity or complexity respectively.

3.3.3 Enzyme-Linked Immunosorbent Assay

A solid phase sandwich Enzyme linked immunosorbent assay (ELISA) was performed to quantify the production of IL-5 and IL-17 in supernatants from Th2 and Th17 cell culture, respectively. Sandwich ELISA is a highly specific and sensitive immunoassay used for the qualitative detection of antibodies in a complex mixture. This method requires the use of two antibodies: a capture antibody and a detection antibody specific to the cytokine or protein of interest [122]. By principle, the plate is coated with the capture antibody to bind the protein of interest, while the detection antibody that is linked to an enzyme named Horse radish peroxidase (HRP) is added to provide detection of the bound protein. The substrate Tetramethylbenzidine (TMB) is added to HRP which

forms an enzyme-substrate complex resulting to a coloured reaction. The intensity of the colour is directly proportional to the concentration of the protein of interest. The presence and quantity of the protein is determined by measuring the absorbance via optical density (OD) in a spectrophotometer [123].

3.4 SAMPLE PROCESSING FOR MASS CYTOMETRY

The experiments were performed on separate days, therefore samples were processed appropriately and preserved at cryogenic temperature for long term storage as well as to preserve the fine structures of cells and maintain the biological sample in a way to suspend their normal metabolic activity [124]. When cells are preserved properly, the optimal viability of recovered cells are retained, at the same time the sterility and reproducibility is ensured [125].

3.4.1 Whole Blood Preservation

Fresh whole blood was processed immediately after collection with Cytodelic blood stabiliser (Cytodelics AB, Stockholm). Cytodelic blood stabiliser was aliquoted in cryogenic vials and allowed to equilibrate for 10 mins at room temperature. Whole blood was transferred in equal ratio into the cryogenic vial and mixed by inverting up and down 10-15 times before being incubated for 10 min at room temperature.

The stabilised blood samples were thereafter placed in a CoolCell freezing container and stored at -80 °C until further analysis by mass cytometry. At the time of experimentation, frozen stabilised whole blood samples were thawed as described in section *3.4.4*.

3.4.2 Fixation and Lysis of Erythrocytes

For each patient and control donor, four 1.5 mL frozen cytodelic stabilised whole blood were processed. Each sample was thawed by hand and treated with fix-buffer (Cytodelics; 1:1 dilution of 2x Fix Concentrate in Fix Diluent), incubated at room temperature for 15 min while vortexing occasionally. Following incubation, erythrocytes were lysed by adding 30 ml lysis buffer (Cytodelic) 1:3 dilution of lysis buffer in milli-Q water and incubated at room temperature for 20 min. Lysed cells were then centrifuged at 400 x *g* for 5 mins, and the supernatant was aspirated. Cells were resuspended twice in 30 ml 1x wash buffer (Cytodelics; 1:4 dilution of wash buffer concentrated in milli-Q water) and centrifuged at 400 x *g* for 5 mins. The supernatant was carefully removed by aspiration and the four tubes for each patient containing the cell suspension were merged into one sample. The cells were resuspended in 3 ml sterile Phosphate Buffered Saline

(PBS) solution and the number of viable cells present in the cell suspension was determined using trypan blue dye exclusion method.

3.4.3 Evaluation of Cell Number and Viability

Cell concentration of fixed cells was also visually determined through a microscope and manual counting using a hemacytometer (Bio Rad) in conjunction with trypan blue cell exclusion dye. Trypan blue selectively differentiates between the healthy viable cells and dead cells. Dead (non-viable) cells with damaged cell membrane absorb the dye, while live (viable) cells with intact cell membrane are not penetrated by the dye [126] . To assess cell viability, 1 part of 0.4% trypan blue (Life Technologies Co) was mixed with 1 part cell suspension and 10 µL of the mix was loaded in the counting chamber of a disposable hemacytometer (C-chip) for counting. The viable cells in the three large squares above were counted and for each square, cells were counted from the top and the left boundaries. Concentration of cells/ml was calculated using the following formula.

Concentration of cells/ml = average number of cells x dilution factor x volume of cell in suspension x volume factor.

3.4.4 Cryopreservation, Thawing and Recovery of Fixed Cells

CRYO#20 (Cytodelics) is the cryoprotective agent used for freezing cells in CyTOF analysis. After the determination of cell concentration, cell suspensions were centrifuged at 400 x g for 5 mins, the supernatant was removed by aspiration, leaving a residual volume of 100 µL to dissolve pellets. Thereafter, 500 µL of Cryo#20 (Cytodelics) was added to the suspended pellets and transferred to -80°C for storage. For further procedures, frozen fixed cells were retrieved from -80°C and rapidly thawed by hand to room temperature and gently inverted 3-5 times. The cells were immediately transferred to a sterile 5 mL flow tube containing PBS to remove freezing medium. The supernatant was aspirated after centrifugation at 400 x *g* for 5 mins at RT, and the pellets were resuspended in PBS for viability check.

3.5 MAXPAR ANTIBODY CONJUGATION AND TITRATION

3.5.1 *Antibody Conjugation*

Antibody conjugation was performed using Maxpar X8 Antibody Labelling Kit (Fluidigm), TCEP and Antibody stabiliser (supplemented with 0.05% (w/v) sodium azide), according to manufacturer's protocol for Ln metals. The kit contains polymers, loading buffer (L-buffer), reduction buffer (R-buffer), conjugation buffer (C-buffer), and wash buffer (W-buffer). The

Maxpar X8 polymer retrieved from -80°C was thawed to room temperature (RT) and resuspended in 95 µL L-buffer. 5 µL of 50 mM Ln metal solution was subsequently added, mixed thoroughly by pipetting and the solution was incubated at 37 °C for 40 min in a water bath. The target antibody was centrifuged at 12,000 × *g* for 5 min to sediment antibody aggregates, and the concentration was verified by NanoDrop spectrophotometer (Thermo Scientific). An equivalent of 100 µg antibody was transferred to a 50 kDa filter and volume adjusted to 400 µL with R-buffer. The solution was spun down at 12,000 × *g* for 10 mins at RT and the flow through was discarded by aspiration. For the partial reduction of antibody, the antibody was resuspended in 100 µL TCEP solution (4 mM) containing 8 µL of 0.5M TCEP and 992 µL R-buffer and incubated in a water bath at 37 °C for 30 mins.

After 40 mins incubation of the lanthanide polymer, approximately 100 µL was transferred to a 3 kDa filter and 200 µL L-buffer was added for washing. The L-Buffer-metal-loaded polymer solution was centrifuged at 12 000 × *g* for 25 min at RT. Flow-through from this centrifugation was discarded by aspiration and the polymer was washed again in 400 µL C-buffer and centrifuged at 12 000 x *g* for 30 min at RT. Following the 30 mins antibody reduction, the 50 kDa filter containing the partially reduced antibody was washed twice with 300 µL and 400 µL C- buffer, respectively. For each wash, the solution was gently mixed by pipetting before centrifugating at 12,000 x *g* for 10 min at RT and flow-through discarded by aspiration.

The flow through from the 3 kDa filter containing the purified Ln polymer after the 30 mins centrifugation was discarded, leaving an approximate residual volume of 20 µL Ln loaded polymer, which was further resuspended in 60 µL C-buffer to make a total volume of 80 µL. The 80 µL resuspended Ln polymer was transferred to the 50 kDa filter containing the partially reduced antibody. The 50 kDa filter now containing both the polymer and the antibody (conjugate) was gently mixed by pipetting and incubated at 37 °C for 90 mins in a water bath. The 50 kDa filter was subsequently washed with 200 µL W-buffer after incubation, before being centrifuged at 12,000 x *g* for 10 min. Flow-through was discarded by aspiration and the conjugate was washed three times with 400 µL W-buffer, centrifuged at 12,000 x *g* for 10 mins and flow-through aspirated after each wash. Following the last wash, the conjugate was resuspended in 80 µL W-buffer, mixed gently and the conjugated antibody concentration was measured using the Nanodrop spectrophotometer. The 50 kDa filter was centrifuged at 12 000 x g for 10 min at RT and the W-buffer was discarded. The measured concentration was used to calculate the volume of antibody Stabilization buffer supplemented with 0.05% sodium azide and this was added to the 50 kDa filter to get a final concentration of 0.5 mg/ml antibody conjugate. The filter was then transferred to a

clean collection tube in an inverted position and centrifuged at 1000 x *g* for 2 mins at RT to collect the conjugated antibody. The conjugated antibody was further transferred into a LoBind tube and stored at 4 °C until further processing.

3.5.2 *Antibody Titration of CD66b*

Antibody titration is used to determine optimal concentrations of target antibodies. Most of the antibodies in the panel were already titrated and the optimal concentration of the antibodies were available prior to this project. However, conjugation of anti-CD66b and the subsequent titration was done in this project.

About 5 million cells were washed with Maxpar Cell staining buffer twice. The cells were pre-incubated with Fc-block and heparin (10 U) (Sigma, H3393 in stock 10,000 U / ml) for 10 mins. CD66b was serially diluted in the concentrations of 1:50, 1:100, 1:200, 1:400, 1:800 and 1:1600. 3 µL master mix containing CD45-89Y, CD3-170Er, CD14-112Cd, Cd56-163Dy, CD19-142Nd and CD8-Er168 (collectively referred to as "the backbone"), was added to each concentration and transferred into six FACs tubes containing at least 900 000 cells for staining. The stained samples were incubated for 30 minutes at RT and afterwards washed in Maxpar cell staining buffer (Fluidigm), centrifuged at 400 x *g* for 5 mins and supernatant removed by careful aspiration. Cell-ID intercalator-Iridium-191/193 (Fluidigm) diluted in Maxpar PBS containing 16% PFA and saponin was subsequently added and left overnight at 4°C. Immediately before sample acquisition, cells were washed in Maxpar cell staining buffer and PBS. Data was analysed in Cytobank, and the best signal to noise ratio or stain index was obtained. The stain index is derived by using the difference between the positive and negative population of the titrated antibody, divided by the standard deviation of the negative population multiplied by two. A good antibody concentration is indicated by higher staining index with low background noise.

$$stain\ index\ (\Delta) = \frac{MFIpos - MFIneg}{2\ x\ SD}$$

3.6 GRANULOCYTE DEPLETION (NEGATIVE SELECTION OF LYMPHOCYTES)

3.6.1 *Magnetic Labelling with CD66abce Microbeads Kit*

Granulocyte depletion was achieved by magnetic activated cells sorting separation (MACS) (Miltenyi Biotec) of CD66abce MACS microbeads (Miltenyi Biotec) using an LS column. Fixed-lysed cells in 3 ml PBS suspension were passed through a 30 µm nylon mesh (Pre-Separation Filters) to remove cell clumps which may clog the column. The cell suspension was subsequently

centrifuged at 300×g for 10 minutes and supernatant aspirated completely. Then the cell pellet was resuspended in 40 µL of separation buffer solution containing PBS (pH7.2). 0.5% BSA and mM EDTA, prepared by diluting MACS BSA stock solution and auto MACSTM rinsing solution in 1:20 ratio dilution. The rinsing solution was degassed before use to avoid clogging by air bubbles. The resuspended cells were incubated with 10 µL of CD66abce-Biotin per 10^7 total cells for 10 minutes at 4°C. Following incubation, 30 µL of buffer per 10^7 total cell and 20 µL of Anti-Biotin Microbeads were added, mixed properly, and incubated for 15 minutes at 4°C. After incubation, cells were washed with 2 mL of buffer per 10^7 cells and centrifuged at 300×g for 10 minutes, supernatant was aspirated, and the pellets were resuspended in 500 µL of separation buffer.

3.6.2 *Magnetic Separation with LS Column*

The LS column was placed in the magnetic field of a MACS Separator (Miltenyi Biotec) and prepared by rinsing the filter with 3 mL separation buffer solution. CD66abce magnetically labelled cell suspension was applied onto the column and unlabelled cells that passed through the column was collected in a clean 15 mL falcon tube. Following this, the column was washed three times with 3 mL separation buffer, with new buffer for each wash added only when the column reservoir was empty. The total effluent which is the unlabelled cell fraction, containing lymphocytes and monocytes flow-through was collected in negative selection; this cell fraction is thus depleted of CD66 abce cells. The labelled cells (granulocytes) retained in the magnetic field were recovered in positive selection by removing the column from the magnetic separator and placed on a clean 15 mL falcon tube. A total of 5 mL separation buffer was added onto the column and the magnetically labelled cells were eluted by firmly pushing the plunger into the column. The granulocytes and agranulocytes were centrifuged at 300 x *g* for 10 mins and the supernatant was removed by aspiration and pellets resuspended in PBS to a final volume of 3 mL. Cells were counted and viability measured by trypan blue exclusion.

3.7 BARCODING AND ANTIBODY STAINING

3.7.1 Barcoding

Barcoding analysis was performed using 20-Plex Palladium (Pd) Barcoding Kit (Fluidigm). The patients and control samples were analysed in two groups, comprising of three APS-1 patients and three corresponding healthy control donors, including a standard control, making a total of 14 samples. At least 1 x 10^6 cells from each sample were rapidly thawed and resuspended in Maxpar cell staining buffer (Fluidigm) in a new 5 mL tube. The samples were centrifuged at 400 x *g* for 5

mins, the supernatants were carefully aspirated, and cells were subsequently resuspended in 1 mL 1x Fix-buffer (1-part (5x) Maxpar Fix-buffer + 4 parts Maxpar PBS) and then incubated for 10 mins at room temperature. Immediately after incubation, the samples were centrifuged at 800 x *g* for 5 mins and supernatant removed. They were gently vortexed and washed twice with 1 mL of 1x barcode perm buffer (Fluidigm) containing 1-part Maxpar 10x Barcode perm buffer and 9 parts Maxpar PBS.

Following the last wash, cells were resuspended in 800 µL 1x barcode perm buffer and 100 µL 1x barcode perm buffer was added to the barcode solution. Both resuspensions were mixed by pipetting and incubated for 30 mins at room temperature. The cells were tapped to mix after 15 mins of incubation. Samples were centrifuged at 800 x *g* for 5 mins after incubation and supernatant was carefully aspirated before being washed twice with 2 mL Maxpar cell staining buffer. Each sample was resuspended in 100 µL Maxpar cell staining buffer. All barcoded samples were pooled together in a 5 ml tube, and subsequently centrifuged and aspirated supernatant.

3.7.2 Antibody Staining of Barcoded Sample

About 7 x 10^6 cryopreserved barcoded samples (7 samples in each barcode) were washed in 3 mL PBS and supernatant aspirated, leaving a residual at a minimal volume of least 100 µL and volume was adjusted to 225 µL with PBS. Before antibody staining, the cells were incubated with 3 µL Fc blocking reagent (Miltenyi) followed by 3 µL heparin (10U) (sigma, H3393 in stock 10000U/µL) for 10 mins at room temperature. Already prepared frozen antibody master mix was rapidly thawed by hand and mixed properly. The cells were stained with 75 µL master mix of metal conjugated surface antibodies. The cell mixture was quickly vortexed and incubated for 30 mins RT. The cells were washed twice with 2 mL Maxpar cell staining buffer (Fluidigm), centrifuged at 400 x *g* for 5 mins and supernatant removed by careful aspiration. The stained cells were incubated over night at 4°C in the presence of 1 mL 191/193 iridium DNA intercalator containing 700 µL PBS, 250 µL (fresh vial) 16% PFA, 100 µL 10X saponin and 0.25 µL (125nM/million) 500 µM Iridium. Intercalar. The next day, the cells were washed twice with 2 mL Maxpar cell staining buffer (Fluidigm) and 1 mL PBS respectively, centrifuged at 500 x *g* for 5 mins RT and supernatant discarded. Pelleted cells were stored at -80°C until ready to run on CyTOF.

3.8 CYTOF DATA ACQUISITION AND ANALYSIS

Prior to acquisition, cells were immediately washed with Maxpar cell staining buffer (Fluidigm), and then with subsequent washes in Cell Acquisition Solution (CAS) (Fluidigm), to remove buffer salts. The cells were resuspended in Maxpar water supplemented with a 1:10 dilution of the EQ™

Four Element calibration beads (Fluidigm) and then filtered through mesh strainer capped tubes. Samples were acquired on a Helios XT CyTOF Mass Cytometer (Fluidigm) equipped with a Super Sampler (Victorian Airship & Scientific Apparatus) at an event rate 400 events per second to limit the number of acquired doublets. Prior to sample acquisition, the instruments were prepared by tuning and cleaning according to the manufacturer's recommendation using tuning and cleaning solutions (Fluidigm).

3.8.1 Normalization & Concatenation

After acquisition, the raw fcs files from the mass cytometry analysis were normalized using the bead-based Normalizer and concatenated before further analysis. Normalisation controls for any decline in instrument sensitivity during acquisition. Calibration bead 140Ce was used to detect and correct fluctuations in signal intensity and as a reference for normalising signals. It was also processed for noise reduction by removing cell debris, doublets, beads, or any undesired events [116].

3.8.2 Debarcoding

The barcoded samples were debarcoded to extract individual samples using the Fluidigm debarcoding software (7.0.8493.0) with a 20-plex-debarcoding key (Fluidigm). Debarcoding in principle is performed by separating each events using the intensity of the barcoding isotopes to identify the largest separation. After all the events are completed, the Mahalanobis distance was applied to remove outliers.

3.8.3 Data analysis

Debarcoded data files were exported and analysed using the Cytobank platform (Cytobank, Inc) to manually gate different populations using biaxial plots. Initial gating was performed according the four Gaussian parameters: centre, width, offset, and residual [127]. Visualisation of *t*-distributed stochastic neighbor embedding (viSNE) maps were plotted to analyse the expression pattern of the antibody markers in high dimensions. This was performed using equal sampling per comparison. FlowSOM clustering algorithm was used for grouping and detection of immune cell populations based on marker expression. Statistical analyses (box plots and heat maps) were performed using Mann Whitney unpaired non-parametric tests. Significant differences were represented as $p<0.05$, (Astrolabe service).

3.9 FLOW CYTOMETRY

3.9.1 Isolation of Peripheral Blood Mononuclear Cells

PBMCs were isolated by performing Ficoll-paque density gradient centrifugation using whole blood collected in a heparinised BD vacutainer tube and inverted multiple times to ensure homogenization of the sodium heparin anti-coagulant and blood. About 18 mL of heparinized blood was aliquoted into 50 mL conical tubes (BD Falcon, Franklin Lakes, NJ) and diluted in equal volume of phosphate buffered saline (PBS). The blood sample was carefully layered over 12 mL Ficoll–Paque PLUS (GE Healthcare) and centrifuged at 400 × *g* for 30 min at room temperature in a swinging-bucket rotor with the brake applied. The PBMC layer was collected by pipetting and transferred into a 50 mL falcon tubes. The pellets were washed with PBS, followed by centrifugation at 400 x *g* for 10 min at room temperature. Supernatant was removed by decanting and PBMC pellets were transferred into a 15 mL falcon tube and resuspended in 10 mL PBS for counting. To determine cell concentration, an aliquot of freshly isolated PBMCs was mixed with PBS and counted using a Millipore automated cell counter with 40µM chip to determine the cell number and viability. Live cells were gated on 5µm while the upper gate was set at 10-11µm to include all cells. The value on the cell counter was multiplied by the dilution factor to determine the number of cells/ml, and multiplied by volume of cells suspension to determine the absolute cell count.

3.9.2 Cryopreservation, Thawing and Recovery of PBMCs

For PBMC preservation, PBMCs in PBS were subsequently centrifuged at 400 x g for 5 min at room temperature. Following centrifugation, the supernatant was carefully aspirated using vacusafe and the pellets were dissolved in 500µL human AB serum (Sigma-Aldrich). About 250 µL of cells were aliquoted in a cryo vial containing 250µL freezing medium composed of human AB serum and 20% cryoprotectant; Sigma-Aldrich) in 1:4 ratio. The cells were allowed to rest in room temperature for 10 min, before being placed in a CoolCell® freezing chamber (consistent and reproducible -1°C/min cell freezing rate) [125] and stored at -80°C for two days to allow gradual and even cooling, before being moved to -150°C for long-term storage until required for downstream analyses. Preserving cells in DMSO and freezing in a controlled temperature inhibits formation of ice crystals and minimises cell damage [128].

To achieve good cell recovery, the cryovials containing frozen PBMCs were taken from -150°C ROAS freezer storage and quickly thawed by hand. The thawed cells were transferred from the vial to a 15 mL falcon tube containing 37°C pre-warmed flow staining buffer composed of PBS with 0.5% bovine serum albumin (BSA). The cell suspension was centrifuged at 350 x *g* for 10 min

at RT. Supernatant was carefully aspirated, cell pellet was resuspended in 1 mL PBS and cell suspension was filtered through a cell strainer (45 µM, BD Falcon®) nylon mesh to remove debris.

3.9.3 *Compensation Staining*

The occurrence of spectral overlap is evident in flow cytometry when using several fluorochromes. Therefore, these overlapping signals must be compensated. For this purpose, a single stained compensation was performed for each fluorochrome to mathematically correct fluorescence spill over between detectors. To generate single colour compensation controls, one drop of UltraComp eBeads (Invitrogen by Thermo Fisher Scientific) was loaded in a well of a v-bottom 96 well plate and stained individually with 1 µL of the corresponding fluorochrome-labelled surface and intracellular antibodies.

3.9.4 Titration of Fluorescent Conjugated Antibodies

Antibodies for flow cytometry were titrated under the same staining conditions as the regular protocol to determine the optimal concentration and staining performance of each antibody to give the best separation of cell populations in each cell sample.

Table 3.1: Flow cytometry panel for extracellular antibodies.

Target	Fluorochrome	Clone	Optimal dilution Factor
CD3	BV510	UCHT1	1:50
CD4	Alexa Fluor 700	RPA-T4	1:100
CD8	PerCP-Cy5.5	SK1	1:400
CXCR3	PE	GO25H7	1:100

Table 3.2: Flow Cytometry panel for intracellular antibodies.

Target	Fluorochrome	Clone	Optimal dilution Factor
EOMES	APC eFluor780 (APC-Cy7)	WD1928	1:50
GATA3	eFluor 450 (Pacific Blue)	TWAJ	1:50
T.BET	FITC (Alexa Fluor 488)	EBio4B10 (4B10)	1:50
FOXP3	PE-TR-ECD	236A/E7	1:50
RORGT	APC	AFKJS-9	1:50
Dead cell stain	Qdot.585		1:50

3.9.5 Antibody Titration

Cells were stained in serial dilutions of 1/50, 1/100, 1/200, 1/400 and 1/800 for surface (table 3.1)) and intracellular antibodies (table 3.2). The data was analysed to determine the best optimal concentration and staining quality for each antibody using FlowJo software 10.6.2. Live and single cell were gated before defining the negative and positive populations and the staining index was calculated. Live cells from each dilution were concatenated to visualise data.

Separation index = Median Positive-Median Negative/ (84% Negative-Median Negative)/0.995

The optimal titers were defined by choosing the best separation between positive and negative signal with minimal signal to noise ratio. The titration of FOXP3 is shown below as an example (Figure 3.4).

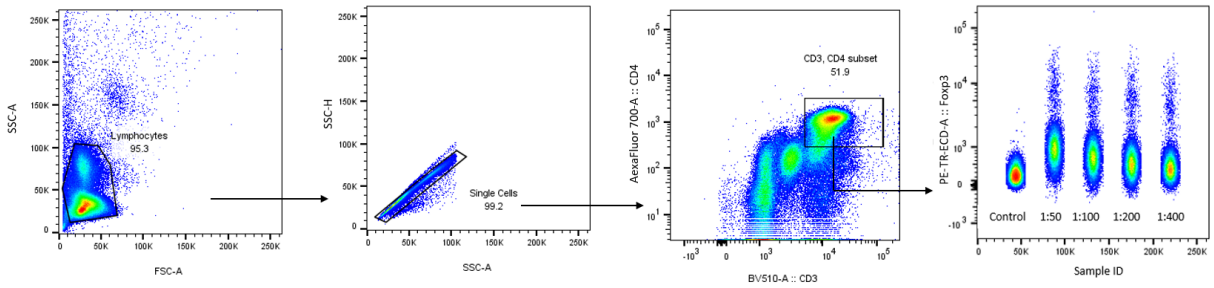

Figure 3.4: Titration analysis of FOXP3.

Concatenated data of antibody concentrations for PE-TR_ECD-A-FOXP3 stained at different concentrations and obtained fluorescence visualized as a function of titer. The optimal antibody concentration used in the study was 1:50. The gating strategy is shown in the first three panels, and the FOXP3 staining for the different concentrations to the right.

3.10 Differentiation of CD4+ effector T Cells

Effector CD4+ T cells were differentiated into Th2 and Th17 lineages in the presence of cytokines to generate more polarizing cells using the CellXVivo™ Human Th2 Cell Differentiation Kit and the T Cell Activation/ Expansion Kit, human (Miltenyi Biotec) with added specific cytokines for the respective T helper cell types. For this purpose, naïve CD4+ T cells were first isolated from PBMCs from five APS-1 patients (same patients although another time of sampling as for the CyTOF experiment) and five healthy controls as described in the following section.

3.10.1 Isolation of Naïve CD4+ T Cells by Magnetic Bead Separation

CD4+ T cells were isolated from PBMCs in positive selection by magnetic activated cells sorting separation (MACS) (Miltenyi Biotec) using CD4 MACS beads (Miltenyi). PBMCs were isolated

as described in section 3.9.1 and centrifuged at 300 x *g* for 10 minutes. The supernatant was completely removed, and pellets were resuspended in 80 µL of flow buffer (PBS with 0.5% BSA) per 10^7 total cells and 20 µL of CD4 MicroBeads was added per 10^7 total cells and mixed well. The sample was incubated for 15 minutes at 4 °C and cells washed with by 2 mL flow buffer (PBS with 0.5% BSA) per 10^7 cells and centrifuged at 300×*g* for 10 minutes.

Up to 10^6 cells were resuspended in 500 µL of buffer and placed in MS-column in the magnetic field of a miniMACS-column. The column was prepared by rinsing with 500 µL flow buffer (PBS with 0.5% BSA) before the cell suspension was applied onto the column and unlabelled cells were allowed to flow through. The column was washed thrice with the 500 µL flow buffer (PBS with 0.5% BSA) and the total effluent; (unlabelled cell fraction: non-CD4 cells) was collected in negative selection and discarded. To elute CD4+ cells, the column was removed from the magnet and placed it on a sterile collection tube. 1 mL of flow buffer (PBS with 0.5% BSA) was added onto the column and the magnetically labelled cells CD4+ cells was immediately flushed out by firmly pushing the plunger into the column. Cells were counted using trypan blue exclusion assay (*3.4.3)*.

3.10.2 Cell Culture and Differentiation Assay

3.10.2.1 Th2 Differentiation

A 96-well plate was coated with 1x Mouse Anti-Human CD3 (0.2 ml/well) and incubated overnight at 4 ℃ (CellXVivo Human Th2 Cell Differentiation Kit). In brief, approximately 2 x 10^5 cells/ml of naïve CD4+ cells were resuspended in Human Th2 Differentiation Media, (TECSMACS medium) supplemented with penicillin (100 IU/mL) and streptomycin (100 IU/mL) and primed in the presence of IL-2 (25 U/mL). The cells were rested for 24 hours in a 37 °C, 5% CO2 humidified incubator. The next day, the plate containing anti-CD3 was washed twice in 1x buffer containing 1x wash buffer prior to adding cells. The cells were then transferred into the wells of the anti-human CD3 antibody-coated plate and incubated in a 37 °C, 5% CO2 humidified incubator for 13 days. The Human Th2 Differentiation Media was refreshed every 3-.4 days by removing 180 µL of the media from each well of a 96-well plate and replenishing with the same volume of fresh Human Th2 Differentiation Media. The supernatant was collected from each replenishing event. Th2 differentiation was verified after 13 days by flowcytometry.

3.10.2.2 Th17 Differentiation

Purified naïve CD4+ T cells were stimulated with Dynabeads human T-activator CD3/CD28 for T cell expansion and activation (Miltenyi Biotec) in a bead to cell ratio of 1:2. Before stimulation, 100 µL Dynabeads were washed by resuspending them in equal volume of flow buffer (PBS with 0.5 % BSA) in an Eppendorf tube and mixing well. The tube was placed on a Dynal magnet (Dynal Biotech) for 1 min and the supernatant was discarded completely before the tube was removed from the magnet. The washed Dynabeads was resuspended in 100 µL TECSMEX medium. Purified naïve CD4+ T cells in 100 µL TECSMEX culture medium were seeded in a 96-well plate (1 x 10^5 per well) and treated with 1.5 µL pre-washed Dynabeads suspension (anti-CD3/anti-CD28) per 100 µL cells in the presence of the following Th17 polarising cytokines: IL-1β (20 ng/mL), IL-6 (30 ng/mL), TGF-β (2.5 ng/mL) and IL-23 (30 ng/mL); (eBioScience). To inhibit unwanted deviation to Th1 or Th2 subsets, 1 µg/mL anti-IFN-γ and 2.5 µg/mL anti-IL-4 (eBioScience) per well were added. The cells were cultured for 7 days at 37 °C and 5% CO2 with no media exchange. After 7 days, the cultured cells were washed, and their viability was checked by trypan blue exclusion before they were stained with fluorescent antibodies for verification. The supernatant was collected.

3.10.3 Flow Cytometry Acquisition

T cell subsets within the naïve PBMCs were first analysed on day 0 using two different buffer conditions according to the protocols outlined below. Following differentiation of Th17 cells (after 7 days) and Th2 cells (after 13 days), was verification via flow cytometer. Flow staining buffer containing PBS with 0.5% BSA was used unless otherwise stated. In all experiments, a 10% excess of antibody cocktail was prepared to account for loss during pipetting. Cells with no antibody were also used in each experiment to check for variations and background fluorescence between experiments. Dead cell exclusion was used for viability for each sample. The same instrument settings were used for all experiments.

For the cell culture samples, the cells were counted and washed with TECSMEX medium once and then resuspended in 1 mL PBS on the harvesting day (day 7 for Th17 and day 13 for Th2). The cells were incubated in the dark for 20 mins at room temperature with 1 µL dead cell stain. The cells were thereafter washed with 1mL flow buffer after incubation, centrifuged at 300 x *g* for 10 mins at 4°C. The supernatants were discarded, and pellets resuspended in 100 µL flow buffer in preparation for staining. The cells were stained with a master-mix of monoclonal surface antibody cocktail (table 3.1) and incubated for 30 mins at 4 °C. After incubation, they were washed

twice in flow staining buffer by centrifuging at 300 x *g* for 10 mins at 4 °C and resuspended in 100 µL flow staining buffer. Next, the cells were divided in two batches prior to fixation and permeabilization with eBioscience™ FOXP3 / Transcription Factor Staining Buffer Set and BD Cytofix/Cytoperm™ following the manufacture´s protocols. For intracellular staining, the cells were fixed and permeabilised by incubation with their respective fix/perm buffers for 1hr at 4°C, followed by overnight incubation with intracellular antibody cocktail at 4°C. Following incubation, the cells were washed twice by centrifugation at 600 x g for 7 mins at RT with eBioscience™ FOXP3 / Transcription Factor Staining Buffer Set and BD Cytofix/Cytoperm™ and kept on ice until ready for acquisition by flow cytometry using the BD LSR Fortessa, at the Flow Cytometry Core Facility, Department of Clinical Science, University of Bergen. To analyse the results FlowJo software 10.6.2 was used.

3.10.4 Fluorochrome Minus One (FMO)

To systematically identify cell populations, and make sure that gating is set appropriately, FMO controls were prepared for each marker except CD3, CD4 and CD8. Generation of FMOs enables a better definition of positive cell population when compared to unstained cells. The FMO for each fluorescent antibody was stained with all the conjugated antibodies used in the experiment except the fluorescent marker of interest to determine which threshold the specific antibody shows a positive signal and to differentiate background autofluorescence.

3.10.5 Flow Cytometry Analysis

Analysis was performed using BD LSR Fortessa, at the Flow Cytometry Core Facility, Department of Clinical Science, University of Bergen. The BD cytometer set up and tracking (CST) beads were used to identify the optimal baseline photomultiplier tubes (PMTs) voltage settings for each fluorescent channel. Overall, up to 200,000 events were recorded for each sample and the FCS data were collected using the BD FACSDiva software by using FlowJo 10.6.2.

3.11 ENZYME LINKED IMMUNOSORBENT ASSAYS (ELISA)

Cytokine level in differentiated Th2 and Th17 cell culture supernatant was determined using IL-5 and IL-17 using Human Duo Set IL-5 ELISA (Bio-Techne, R&D Systems) respectively, according to manufacturer's instruction. Standard curves were generated by preparing a six-fold serial dilution of IL-5 and IL-17 standard with starting concentration of 0.3 ng/ml in reagent diluent.

First, a 96 well microplate for each cytokine was coated with 100 dilution of IL-5 and IL-17 standard from 0.3 ng/ml in reagent diluent of respective capture antibody diluted to working

concentration (4μg/ml) in PBS. The plate was sealed and incubated overnight at room temperature. The next day, the coated plate was washed 3x with 400 μL wash buffer, followed by blotting against clean paper towel after each wash for complete removal of remaining wash buffer, a critical step for good performance. The plates were subsequently blocked with 300 μL 10X reagent diluent, sealed and incubated for 1hr at RT. The plates were washed after incubation as described previously. Samples were diluted in 1:2 and 1:5 in reagent diluent for Th2 and Th17 supernatant, and a 100 μL standard and samples were added in duplicates, the plates were sealed and incubated for 2 hours at RT. After incubation, the plates were washed 3x before an addition of IL-5 (125ng/ml) and IL-17 (20ng/ml) detection antibody diluted in reagent diluent and incubated for 2 hours at room temperature. Following washing after incubation was an addition of 100 μL working dilution of streptavidin HRP (1:40) with reagent buffer to each well, with plates covered and a subsequent 20 mins incubation at room temperature under dark conditions. The plates were washed after incubation and 100 μL TMB substrate solution was added to each well and incubated for another 20 mins protected from light. This was followed by 50 μL stop solution added to each well. The blue color changed to yellow, and the plate was read at 450nm wavelength using Spectramax plus. The cytokine concentration and standard curves for each sample were determined using the SoftMax Pro software.

3.12 STATISTICAL ANALYSIS

The graphical representation and statistical tests for flow cytometry and ELISA were done using Graph pad Prism version 9. The statistical significance between patients and healthy controls were estimated using an unpaired, non-parametric t-test two tailed Mann-Whitney test and a p-value of <0.05 was considered statistically equivalent in flow cytometry results. Figures and statistics for mass cytometry was performed using Cytobank.

4 RESULTS

4.1 IMMUNE PROFILING OF APS-1 PATIENTS AND HEALTHY CONTROLS

We used an in-house optimised mass cytometry panel of antibodies to phenotypically characterize immune cells in fixed whole blood samples from six patients with APS-1 and six healthy controls with focus on eleven major lineage markers: CD3+, CD4+, CD8+ T cells, CD56+ NK T cells, γδ T cells, CD19+ CD20+ B cells, CD14+ monocytes, CD56+ NK cells, CD66b granulocytes, CD11c+ HLADR+ dendritic cells and CD45+ cells.

Table 4.1: Phenotyping of immune cell subsets.

Cell Subsets	Markers for Subset Definition
CD3+ T cells	CD45+ CD3+ CD14- CD19- CD56-
γδ T cell	CD45+ CD3+ CD14- CD19- CD56- TCRγδ+
CD8+ T cell	CD45+ CD3+ CD14- CD19- CD56- CD4- CD8+
CD4+ T cell	CD3+ CD14- CD19- CD56- CD4+ CD8-
NK cells	CD45+ CD3- CD14- CD19- CD56+
NK T cells	CD45+ CD3+ CD14- CD19- CD56+
B cells	CD45+ CD3+ CD14- CD19+ CD56-
Monocytes	CD45+ CD3- CD14+ CD19-
Granulocytes	CD45+ CD3- CD66b+
Dendritic cells	CD45+ CD3- CD14- CD19- CD56- CD11c+ HLADR+
Tregs	CD3+ CD14- CD19- CD56- CD4+ CD8- TCRγδ- CD25+ CD127-

4.1.1 Clean up and Gating Strategy for Mass Cytometry

Preliminary gating of Cytof data to define populations of interest for downstream analysis was performed manually using the gaussian parameters in Cytobank https://cellmass.cytobank.org. For the clean-up strategy, each parameter was plotted against time as depicted in Figure 4.1 to remove debris, dead cells, normalisation beads (140Ce) and doublets. Debris and doublets were excluded by biaxial plotting of the iridium intercalator containing both 191Ir and 193Ir isotopes.

A.

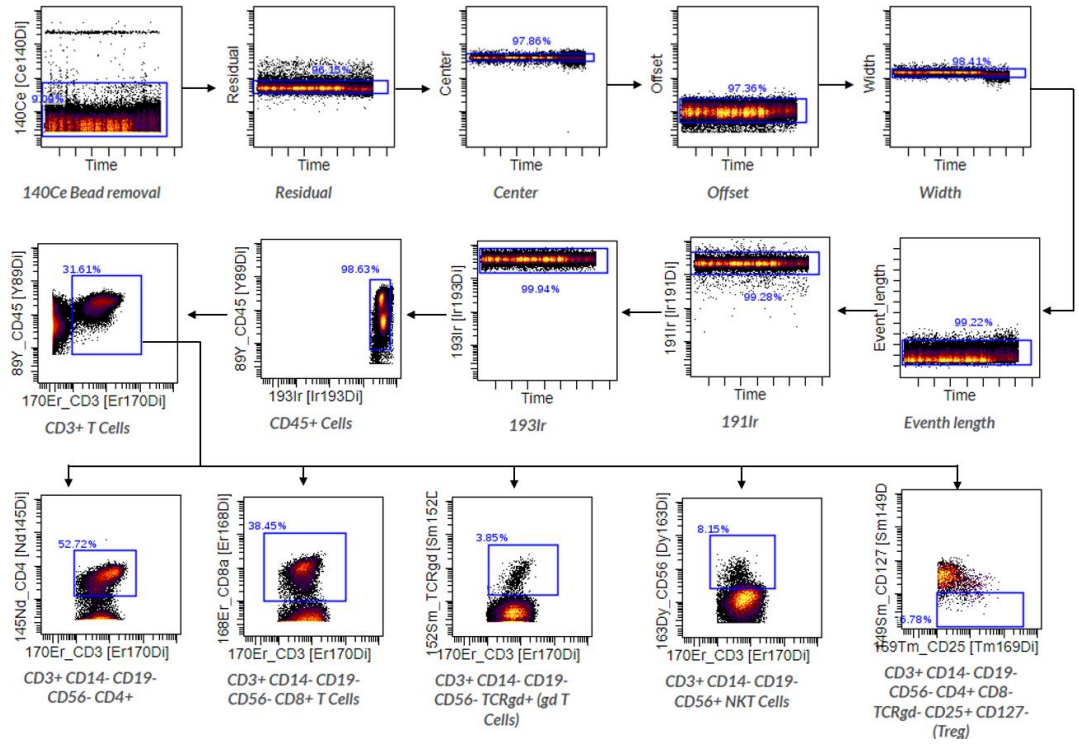

B.

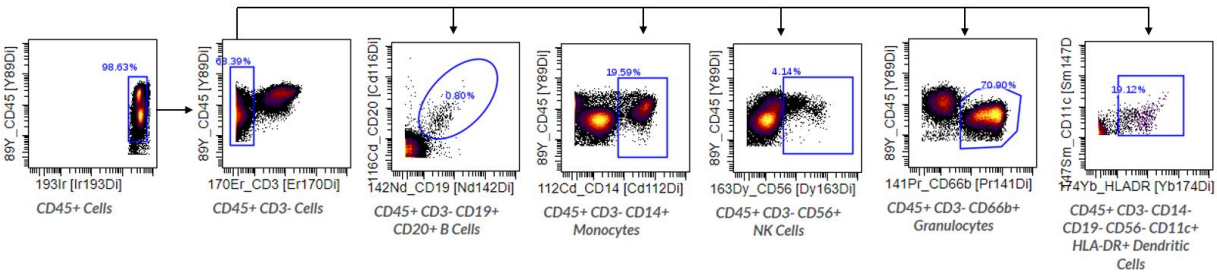

Figure 4.1: Clean up gating strategy for identifying CD45+ immune cell population.

Manual gating to identify the main leukocyte parent population (CD45+ cells) used for defining each immune cell subgroup in the established panel. ***A)*** *CD3+ cells are gated from CD45+ cells and other T cell subgroups were subsequently identified from CD3+ cell population.* ***B)*** *Other subgroups covering the major population of the immune system were gated out from CD45+ CD3- cell population.*

4.1.2 Validation of CD66b-Pr141 Titration

Following the panel design, unlabeled CD66b was conjugated to the metal isotope, Pr141 with initial concentration of 0.97mg/ml. For quantification, the absorbance was measured at 280nm to ensure that the volume of antibody solution corresponded to the intended quality within a tolerance of +/-10%. The expected recovery of conjugated antibody is ≥60%. The final concentration after conjugation was 0.55mg/ml with recovery rate of 56.7% indicating adequate quantity.

CD66b-Pr141 was titrated and stained together with the backbone panel, CD45-89Y, CD3-170Er, CD14-112Cd, Cd56-163Dy, CD19-142Nd and CD8-Er168. The fcs files for CD66b-Pr141

titration were concatenated to identify the positive and negative populations. The median counts of positive (orange) and negative (green) controls across the range of 1:100-1:1600 were summarized using dot plots represented in Figure 4.2A. Signal generated from CD66b-Pr141 is represented in a histogram Figure 4.2B and a concatenated scatter plot (Figure 4.2: Titration analysis of CD66b-Pr141 antibody.

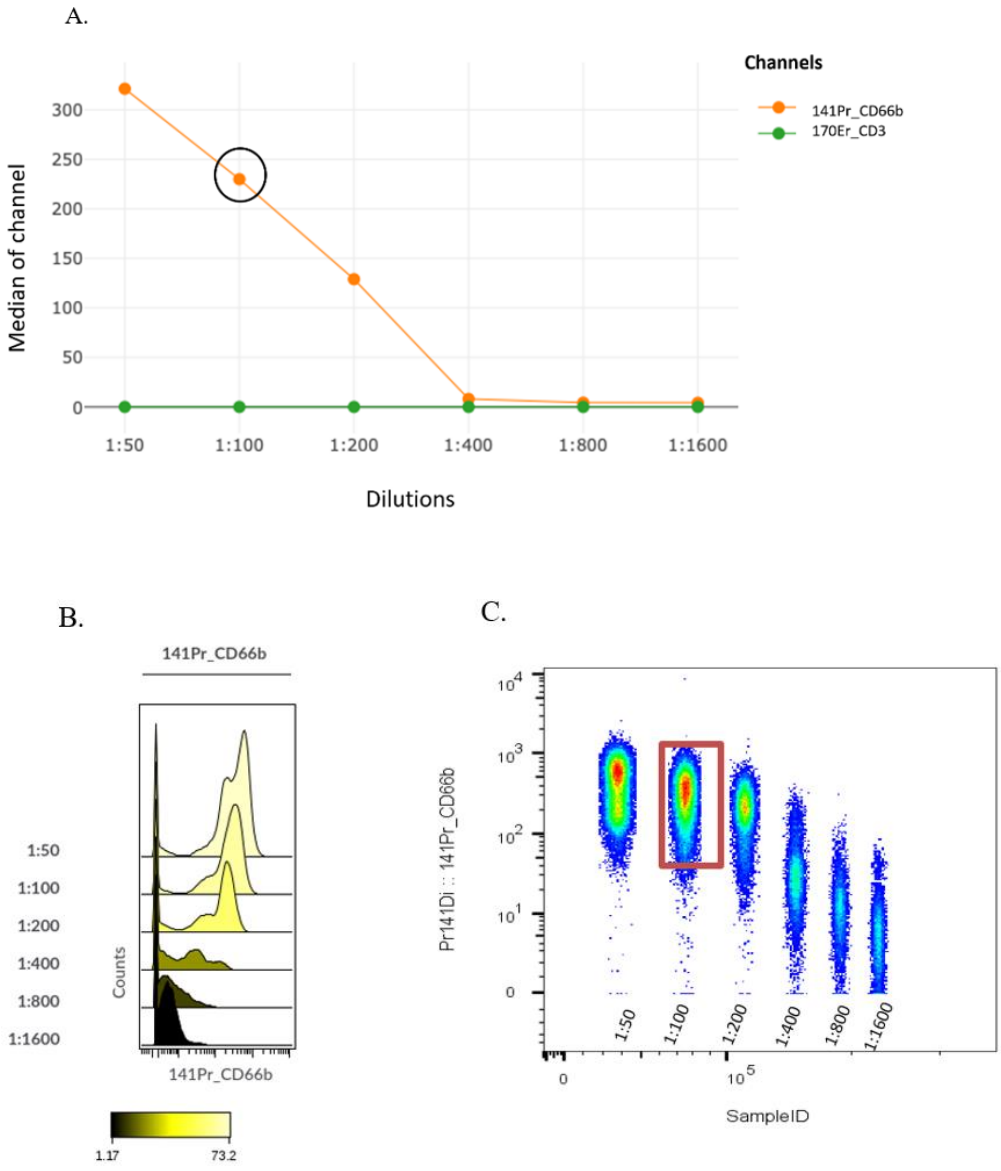

Figure 4.2: Titration analysis of CD66b-Pr141 antibody.

Fixed blood cell is aliquoted and stained with a backbone panel containing serially diluted CD66b-Pr141 antibody. ***A)*** *The optimal titer of 1:00 was chosen by evaluating the maximum separation between the positive from negative population. The circle gate indicates the ideal optimal titer.* ***B)*** *Histogram of signal generated from each concentration is represented with a color scale indicating signal intensity varying from minimum to maximum respectively.* ***C)*** *Visual representation of the concatenated fcs file showing decreasing concentration of antibodies which allows efficient gating of positive cells. The optimal concentration is highlighted in red.*

4.1.3 Panel Validation for CD66b-Pr141

To validate the conjugation of CD66b to Pr141 for mass cytometry, an efficient antibody titration approach was utilized to stain samples from a healthy donor for cell surface markers, CD45, CD14, CD66b, CD3, CD4, CD56, and CD8. The viSNE dimensionality reduction algorithm in Cytobank was applied to identify cells based on expression level densities of cell surface markers from low to high intensity. An illustration of our approach presented in Figure 4.3 revealed well defined, converged maps that separates immune subtypes with minimal overlap or spill over. CD3+ cells are the most abundant cell type within CD45+ cells in this representative healthy control sample.

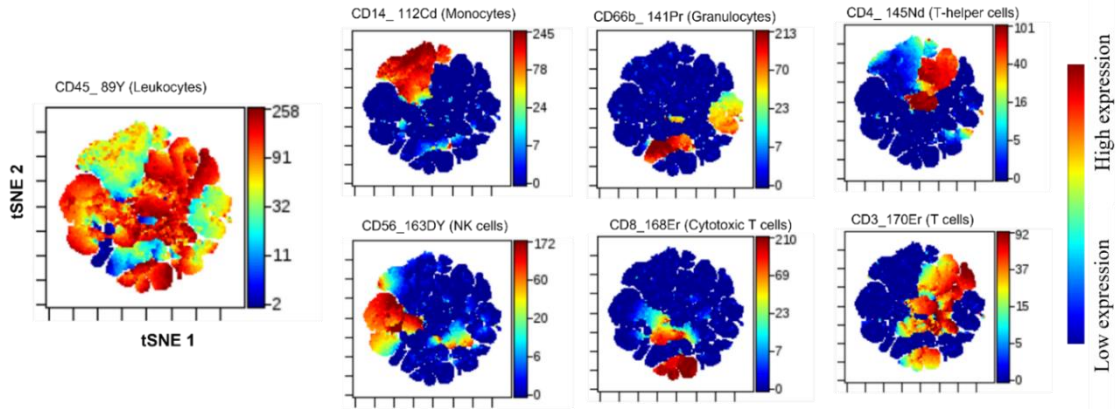

Figure 4.3: viSNE representation of cell population.

The population distribution with color over lay represents the cell density in each region in the map. Each event (cell) is represented as a dot in high dimensional space. CD45, a common surface leukocyte marker for all hematopoietic cells is observed to be densely expressed, reflecting the intensity of antigen expression of six different markers, CD14, CD66b, CD4, CD3, CD8 and CD56. These cell populations are colored based on the expression of their respective channel.

4.1.4 Analysis of major immune cell subsets in CyTOF reveals lower frequencies of NKT cells in APS-1 patients compared to healthy controls.

To visualize immune cell populations of APS-1 patients and healthy controls, FlowSOM algorithm was explored to identify clusters of lineage markers within the vSNE plot. Single cells of common immune subsets from 6 patients and 6 controls were clustered to provide the best predictive signaling pattern between groups. High dimensional plot on viSNE were performed using equal sampling of 67,796 events per sample. Figure 4.5 is an illustration of distinct expression of phenotyping markers presented in a heat map using calculated raw values of percentages of varying subgroups of CD45+ cells.

Our results show the presence of granulocytes, even though they were not depleted. This indicates that they were not completed isolated; but only reduced in count. However, this probably served

its purpose in making the lymphocyte population relatively larger and hence we could analyze more of the cells we wanted in Cytof. Based on the expression of surface markers, eleven subgroups of the CD45+ leukocyte population identified in the viSNE plots , are CD3+, CD4+, CD8+ T cells, CD14+ monocytes, CD66b+ granulocytes, CD3-CD56+ NK cells, CD3+CD56+ NKT cells, CD19+ B cells, Tregs and TCR γδ cells (Figure 4.4). Otherwise, the most abundant cell types other than granulocytes were T cells and monocytes, as is expected.

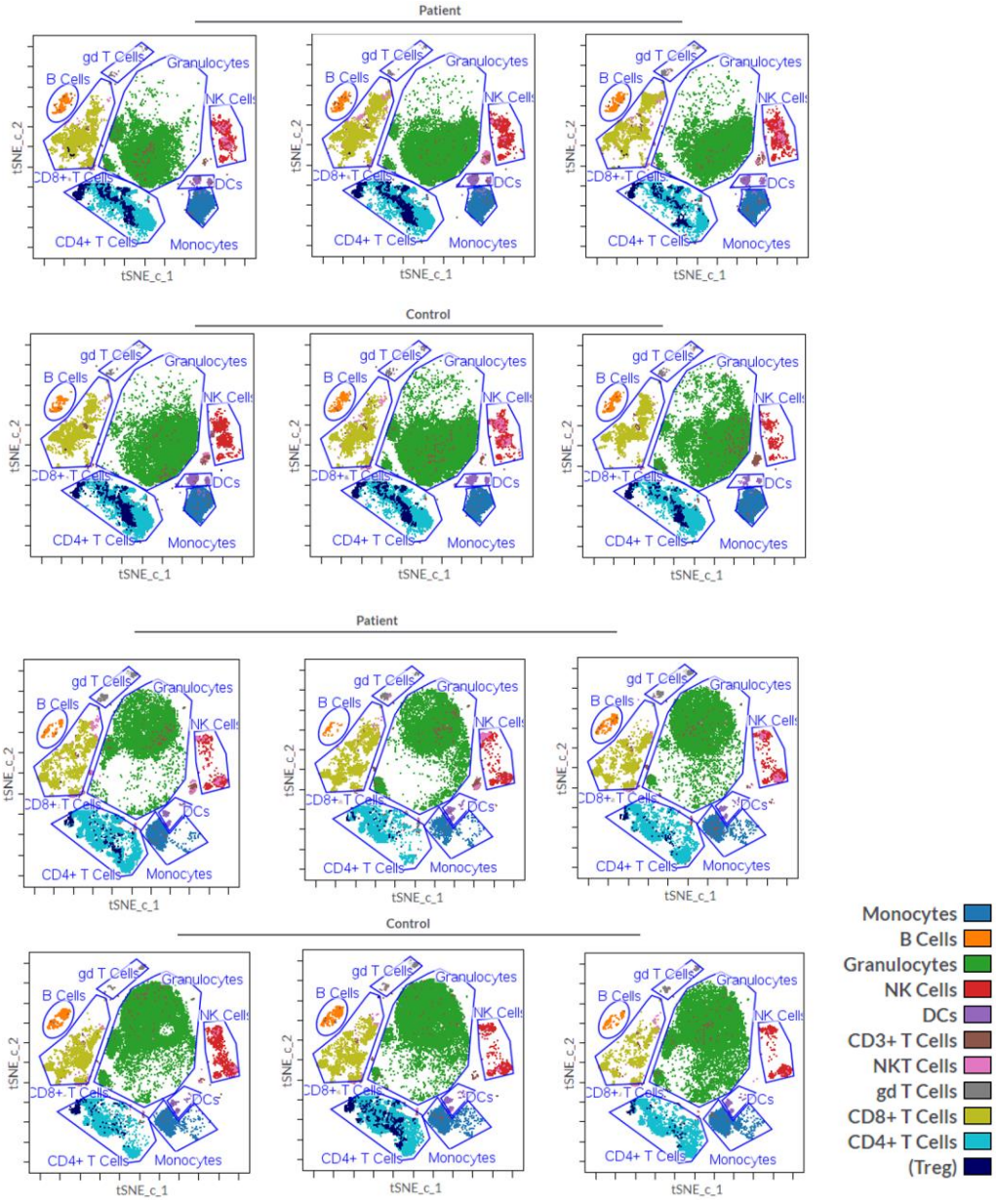

Figure 4.4: Illustration of overlaid FlowSOM clustering data on dimension reduction map categorized into populations by manual gating.

Samples from six APS-1 patients and six healthy donors were mapped using FlowSOM based on the expression of eleven markers. The major cell population are shown using color profile. Each dot represents a single cell color-coded by subtype.

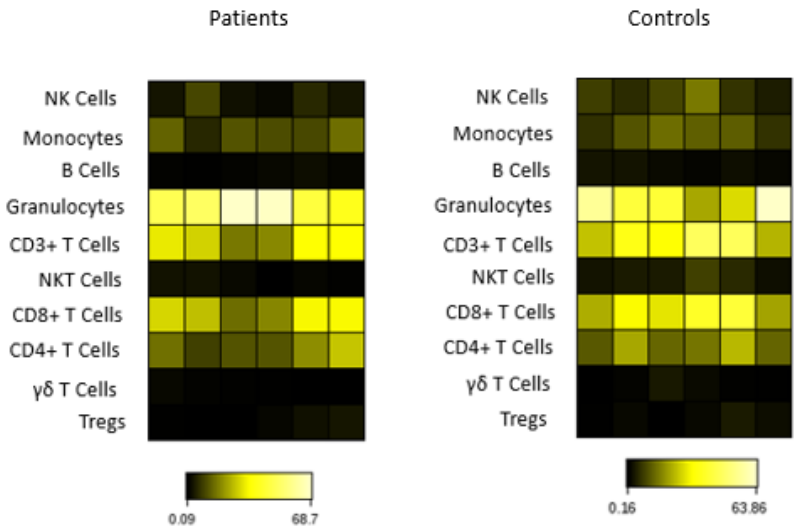

Figure 4.5: Heatmap visualisation to marker expression by FlowSOM metacluster:

Expression fingerprint of gated population plotted on heatmap plot against patients and controls to quantitatively compare the phenotype abundance of each cluster. Level of expression marker is displayed by a black to yellow scale. CD3+ cells, granulocytes and CD8+ cells reveals high number of cells in both groups while T helper cells and monocytes are observed to be moderately expressed. NK cells are observed to fairly expressed in the control group compared to patients, while Tregs, NKT cells and B cells seems to be lowly present across subjects.

Statistical analysis of each lineage cluster was further explored to define the significant differences in the frequency of each cell population between patients and healthy controls (Astrolabe service). Overall, there were no major differences between groups, except for NKT cells which were lower in frequencies in patients compared to controls (mean APS-1=4.901; mean healthy controls=11.35, p=0.00433) and NK cells which were also lower in APS-1 patients with an almost significant P value (mean APS-1=3.637; mean healthy controls=7.374, p=0.0649). However, different expression levels were observed in various subsets between individual persons.

A.

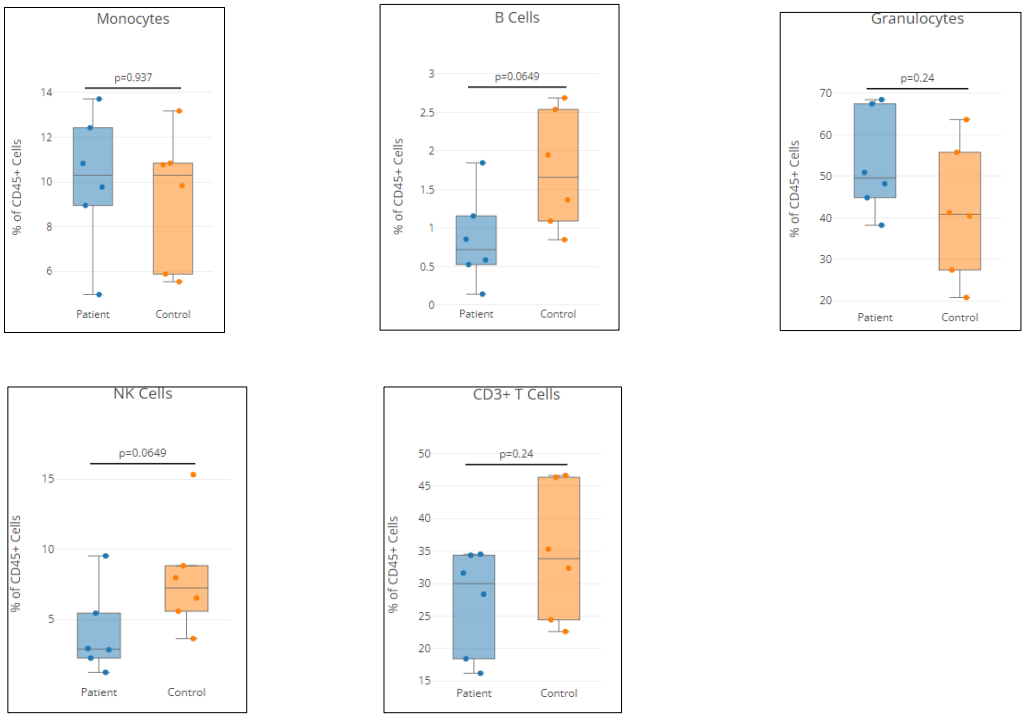

B. Frequency of T cell populations.

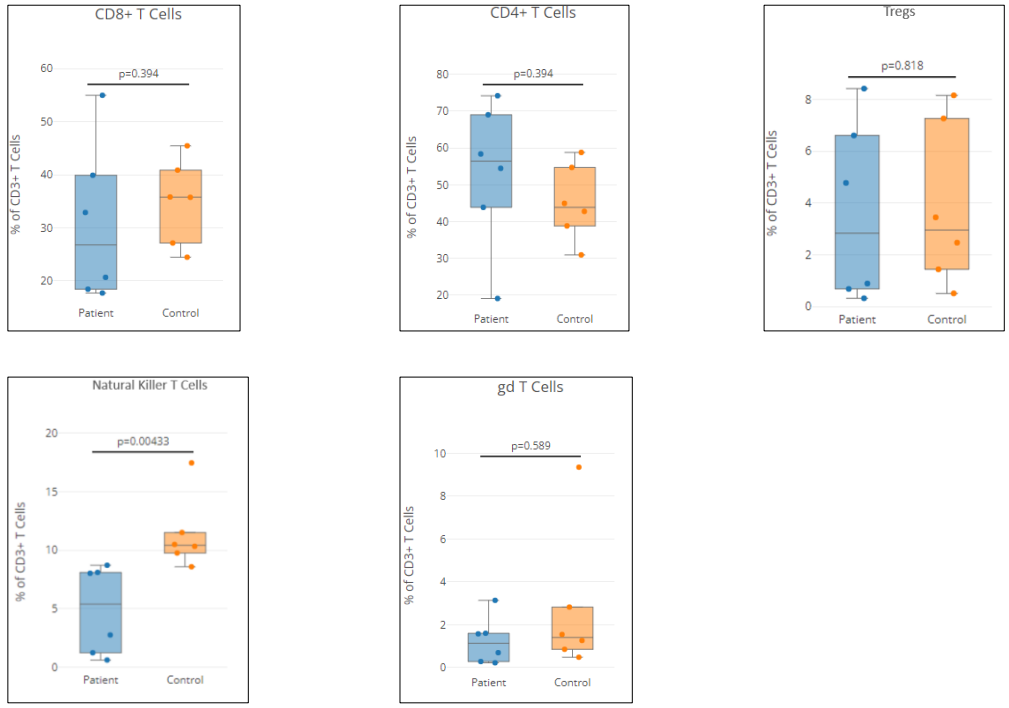

Figure 4.6: Mass cytometry statistical analysis of Six APS-1 patients and six healthy controls.

Frequencies of immune cell subsets in APS-1 patients versus healthy controls. ***A)*** *Box plots showing the frequency of immune subpopulations. Mann Whitney Unpaired non-parametric test revealed no significant differences ($p<0.05$) between groups.* ***B)*** *The frequency of the varying subgroups of CD3+ T cells. A significant alteration of $p= 0.00433$ between groups was revealed in NKT cells. Dots represents individual samples and bars indicate median.*

4.2 FLOW CYTOMETRY

To optimize the procedure for characterization of immune cell subset using flow cytometry, all panels were first titrated (Figure *3.4***:** Titration analysis of FOXP3.). For each functional marker, compensation, and fluorescent minus one controls were performed to check for fluorescent spread as well as to set the threshold for positivity. At the analysis stage, it was observed that some of the FMOs negative gates were far more negative in comparison with the following cell staining. FMO controls were therefore used whenever possible; otherwise, unstained cells in the same run were deemed as negative controls for setting the threshold for positivity.

4.2.1 Comparison of Flowcytometry Staining Buffer

A comparative study was also performed using two different reagent buffers, BD Cytofix/Cytoperm™ Fixation/Permeabilization Solution Kit and eBioscience™ FOXP3 / Transcription Factor Staining Buffer Set according to the manufacturer's instruction. All different cell conditions from the study subjects were stained using these different buffer conditions. The two buffers separated most populations to the same extent and in the same way, but the eBioScience buffer was superior regarding FOXP3. This buffer was therefore chosen. A representative plot and comparisons of FOXP3 results from the two buffers in FlowJo is shown (*Figure 4.7*).

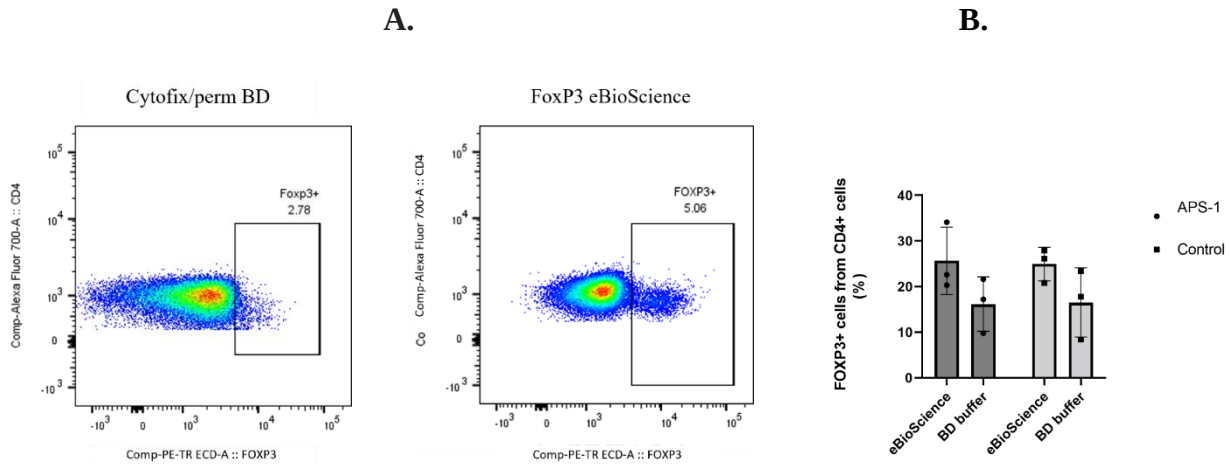

Figure 4.7: Illustration of change in FOXP3 signaling in Th17 cells using the two different buffer conditions.

A) *FOXP3 eBioScience buffer showed a high population of FOXP3+ cells, while a decreased population of FOXP3+ cells were identified using Cytofix / perm BD buffer after manual gating.* ***B)*** *Box plot comparative analysis of the frequency of FOXP3 staining from all subjects using eBioscience™ FOXP3 / Transcription Factor Staining Buffer Set generated statistically higher number of cells with a mean percentage of 26 compared to 16% mean in BD Cytofix/Cytoperm™ Fixation/Permeabilization Solution Kit.*

4.2.2 Phenotyping of T cells in unstimulated PBMCs from APS-1 patients and controls and Gating strategy.

Unstimulated PBMCs isolated from five healthy donors and five APS-1 patients were analyzed for the extracellular expression of CD3, CD4, CD8 and CXCR3. The intracellular expression of Eomes, T.bet, RORgt, FOXP3 and Gata3 was also analyzed. Lymphocytes were identified and gated by their forward and side scatter parameters (Figure 4.8).

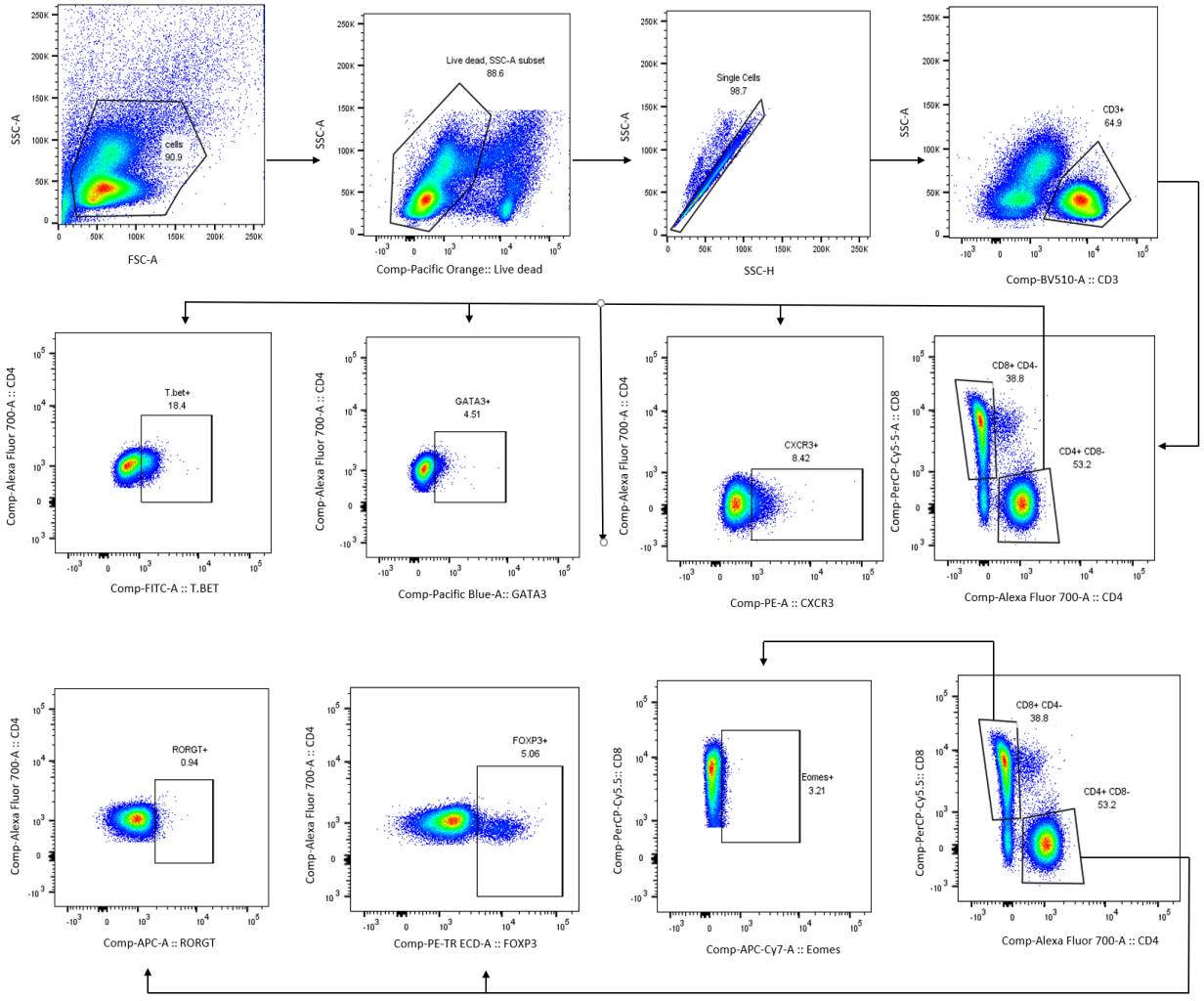

Figure 4.8: Gating strategy for identification of functional markers of undifferentiated cells.

Dead cells were excluded using viability dye, Pacific orange Live/Dead plotted against SSC-A. Further gating g out of singlets are based on SSC-A and SSC-H. Identification of T cells is based on CD3 positivity, while CD8+ and CD4+ T cells expressing CD3+ T cells are gated according to their expression level. CD4+ T cells were further split into T.bet+, RORgt+, CXCR3+, FOXP3+ and Gata3+ cells, while Eomes+ cells were discriminated from CD8+ T cells. Each dot represents a single cell that has passed through a laser. The same gating strategy was applied to Th2 and Th17 differentiated cells (4.2.5 and 4.2.6).

4.2.3 Altered Eomes expression within effector CD8+ T cells from naïve PBMCs of patients with APS-1

Eomes is defined by it cytolytic functional role in immune cell development. The gating strategy for Eomes from CD8+ population is represented in (Figure *4.8*). CD8+ T cell population from the CD3+ T cells was an average of 38% in APS-1 patients and approximately 40% in healthy controls.

Further analysis revealed an increased frequency of Eomes+ cells in APS-1 patients with a mean value of 4.96% compared to 1.21 mean percentage in healthy controls. This analysis revealed a significant alteration of <0.0079.

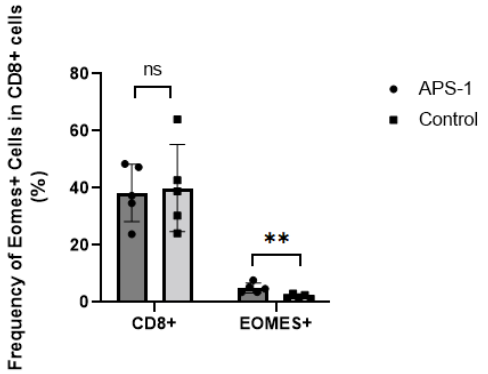

Figure 4.9: Eomes expression in CD8+ T cells.

*Box plot showing the frequency of Eomes expression within CD8+ T cells with a significant value of <0.0079. Statistical testing performed using Mann Whitney Unpaired non-parametric test (p value: * <0.05; ** <0.005). Dot represents individual samples and bar indicates the median*.

4.2.4 There were no differences between CD4+ T cells subsets in undifferentiated PBMCs between APS-1 patients and healthy controls

As shown in Figure 4.10, there were no significant differences between T cell subsets between APS-I patients and controls (P=ns for all comparisons). The trancription factor T.bet and the chemokine receptor CXCR3 were expressed in considerable large proportions of cells in both APS-I patients and in healthy controls. FOXP3 was also expressed in a level that represents the knowledge on how many Tregs there are in peripheral blood. GATA3 and RORgt were however very lowly expressed (less than 5%). It was therefore decided that we would try to differentiate Th2 and Th17 cells, respectively, to test the flow cytometry conditions and panel.

A. Live cells. **B. CD3+ T cells.** **C.**

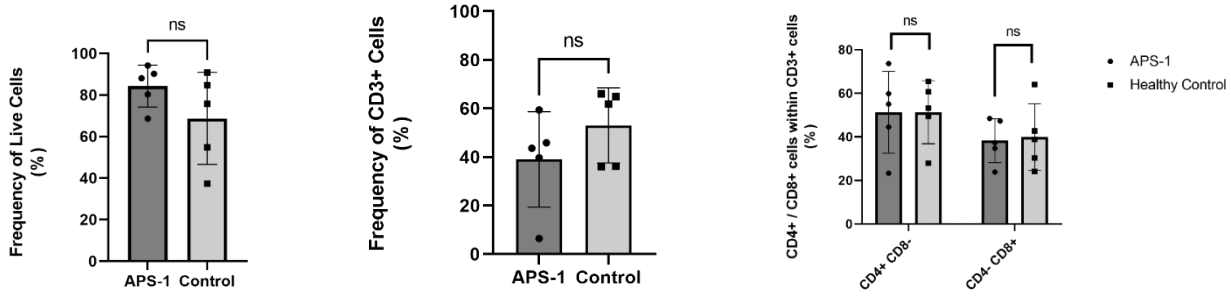

D. Distribution of candidate markers in Naïve CD4+ T cells.

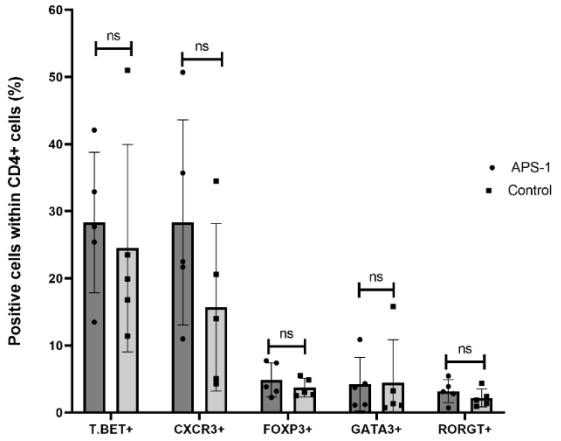

Figure 4.10: Expression of lineage subsets of CD4+ and CD8+ T cells.

A) *Frequency of live cells with CD45+ leukocyte population.* ***B)*** *The frequency of CD3+ cells.* ***C)*** *Graphical representation of mean frequency of CD4+ and CD8+ T cells within CD3+ T cells.* ***D)*** *Comparison of the mean percentage of all positive cell populations within the CD4+ T cells. Statistical testing performed using Mann Whitney Unpaired non-parametric test (p value: * <0.05; ** <0.005). Dot represents individual samples and bar indicates the median.*

4.2.5 TGF-β Mediates Th17 Differentiation and Induces FOXP3 Expression

To validate the differential expression of freshly isolated CD4+ T cells in response to signaling, PBMCs from three APS-1 patients and three healthy controls were stimulated with Dynabeads anti CD3/ anti CD28 monoclonal antibodies and induced with polarising cytokines. The cells were analysed by flowcytometry on day 7. The phenotypes of CD4+ T cells were characterized by the expression of Rorgt, Gata3 and FOXP3. These populations were gated from CD4+ cells using the same gating strategy as for unstimulated PBMC (Figure 4.8 and Figure 4.11).

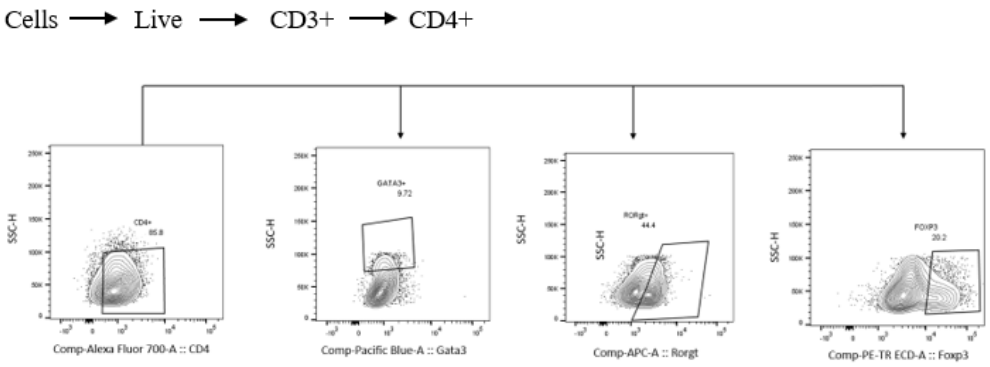

Figure 4.11: Gating Strategy for Th17 differentiated dells for T cell subsets.

CD3+ cells were gated out from the single live population. Further gating was performed to target CD4+ cells for identifying the gene expression of Gata3, Rorgt and FOXP3. Each dot represents a single cell that has passed through a laser.

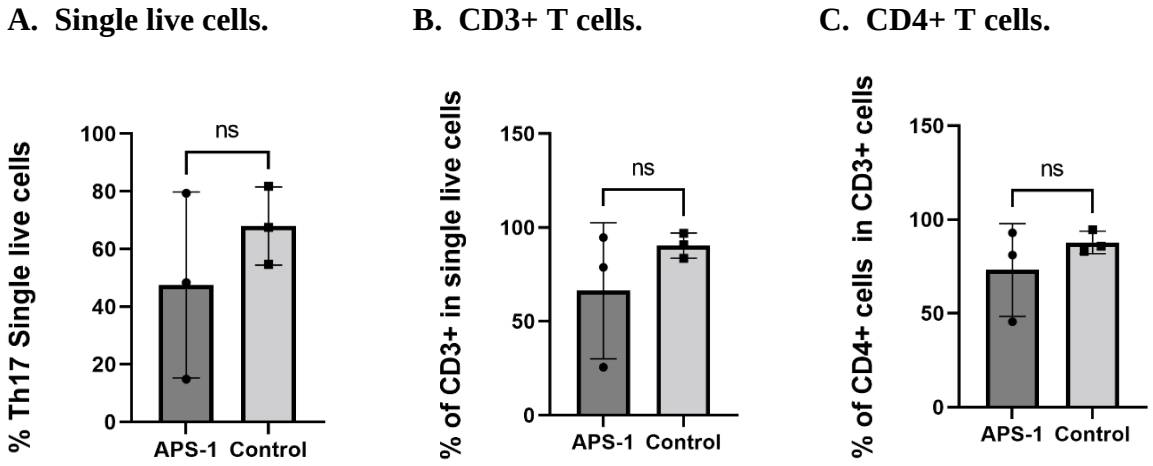

D. Comparison of Percentage of CD4+ positive cell poulation.

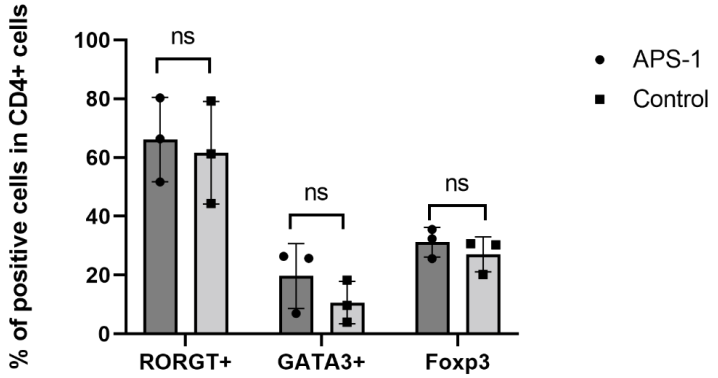

Figure 4.12: Frequency of T cell subsets expressed by Th17 polarized cells.

Naïve CD4+ T cells were Cultured for 7 days under Th17 polarizing conditions. No significant variations ($p<0.05$) were detected in all positive cells expressed by CD4+ cells between patients and controls. Statistical testing performed using Mann Whitney Unpaired non-parametric test ($p<0.05$). Dot represents individual samples and bar indicates the median.

Total number of the major T cell marker CD3 and CD4 were comparably lower in patients than in healthy controls, (CD3+ mean: APS-I= 66.3; mean HC= 90.4 P= 0.4) and (CD4+ mean: APS-I= 73.1; mean HC= 87.8 P= 0.4) but the results were not significant. There were furthermore trends of a slightly increased expression of Rorgt and Gata3 analyzed from CD4+ population in patients (Rorgt mean: APS-I=66.13; mean HC= 61.63, P= 0.7) and (Gata3+ mean: APS-I= 19.68; mean HC= 10.66, P= 0.4). Notably, the stimulation of naïve CD4+ cells to Th17+ cells resulted in a proliferation of over 60% Rorgt+ cells in both groups compared to <5% in unstimulated cells, a fold increase of ≥10 Figure 4.12d). In contrast, low levels of Gata3 (<10-20%) were revealed across patients and healthy controls.

It is generally accepted that Th17 cells are defined by the expression of Rorgt. Interestingly, an upregulation of FOXP3 was also revealed here in both APS-1 and healthy controls (Figure 4.12D). An explanation of this might be the presence of TGF-β, a critical signaling cytokine in Th17 differentiation which also plays a role in the lineage diversion to FOXP3 [129].

4.2.6 Th2 Cell Expansion Promotes Proliferation of Gata3

Purified CD4+ cells from PBMCs of APS-1 patients (n=3) and healthy donors (n=3) were examined after stimulation with IL-4 in combination with anti-human CD3, IL-2 in Th2 differentiation media using flowcytometry. Gates where manually performed using same strategy as for unstimulated PBMCs (Figure 4.8 and Figure 4.13). To separate the CD4+ populations of interest, each subset was gated against SSC-H versus the CD4+ cells.

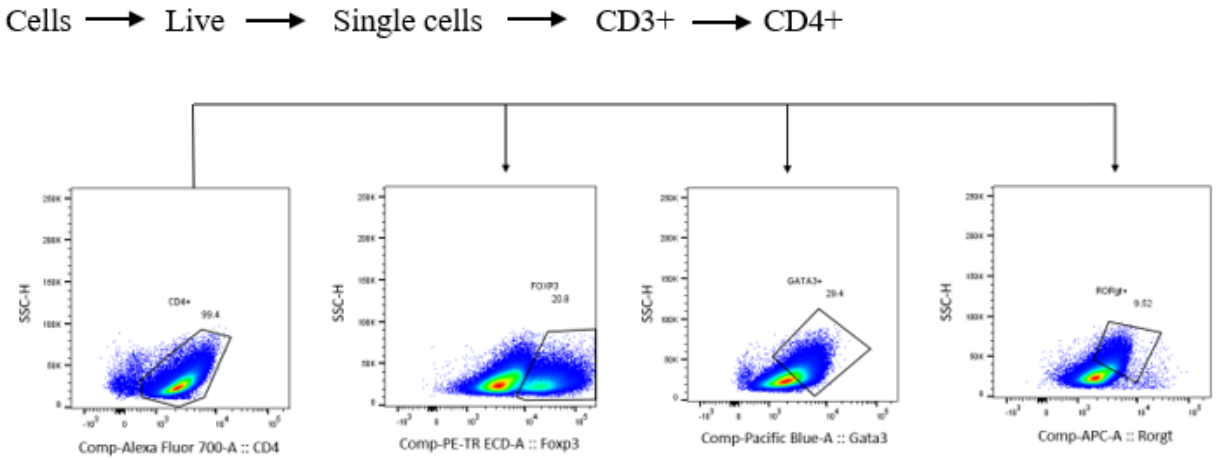

Figure 4.13: Gating strategy for Th2 differentiation.

A representation of the expression profile of FOXP3+, Gata3+ and Rorgt+ cells. Each dot represents a single cell that has passed through a laser.

Data from the analysis showed an increased proliferation of all functional markers in response to Th2 cytokines compared to naïve undifferentiated cells. The analysis demonstrated a predominance of Gata3+ cells representing an average of 26.8% in APS-1 patients and 35.2% in healthy controls (fold change of about 6 compared to undifferentiated PBMCs). Furthermore, Th2 differentiated cells showed about 25% moderate expression of about FOXP3 and a slight upregulation of expression of Rorgt at about 10%. The frequency of these subsets was similar between patients and healthy controls.

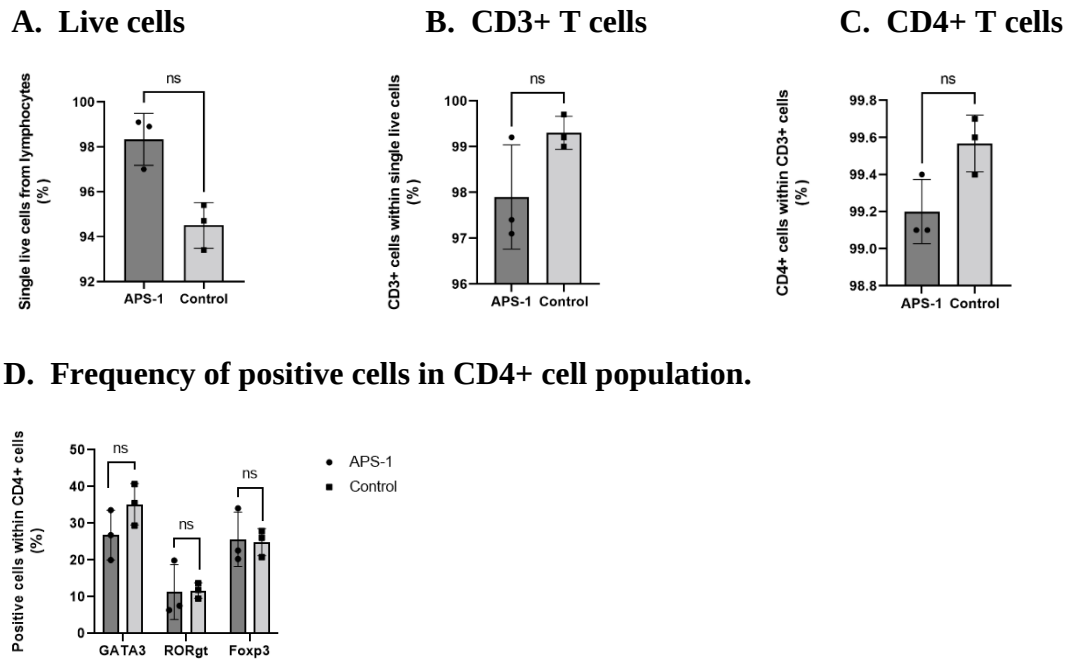

Figure 4.14: Comparative analysis of cells expressed in stimulated CD4+ cells.

Unpaired non-parametric analysis showed no statistical variations ($p<0.05$) in APS-1 patients and controls. Dot represents individual samples and bar indicates the median.

4.2.7 Cytokine Production by Th2 and Th17 Differentiated Cells

To extend this study, the cytokine profile of CD4+ differentiated cells were analyzed after stimulation as a confirmation that polarized Th2 and Th17 cells secrete the right cytokines, and that we indeed had generated Th2 and Th17 cells, respectively. Th17 differentiated cells revealed lower detectable values of IL-5, (mean: APS-I= 0pg/mL; mean HC= 3.52pg/mL). However, slightly elevated levels of IL-17 were detected in patients (mean=408.2pg/mL) compared to healthy controls with a mean value of 247.5pg/mL, although with no significance reached (P=0.7) (Figure *4.15*), Notably, these secretions were highly variable among the patients. Th2 cells from patients and healthy controls secreted an average of 747 pg/mL and 1045.35pg/mL of the IL-5 cytokine, respectively, with a p value of 0.7, and a very minor production of IL-17 (mean= 184.64

pg/mL) in patients, comparably lower than the control group (mean= 286.55pg/mL, p=0.7). No significant differences were observed in the cytokine production of Th2 and Th17 polarized cells.

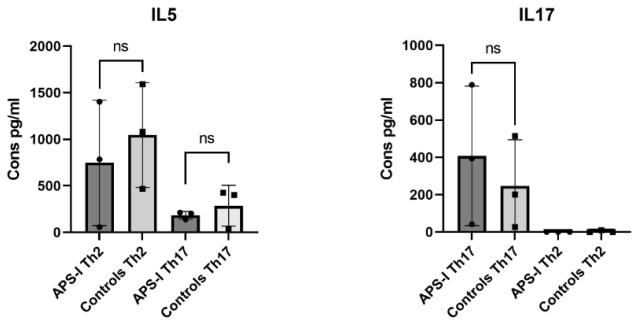

Figure 4.15: Box plot representation of Th2 and Th17 cytokine profile.

No notable variation was observed between patients and controls. Statistical analysis was performed using Mann Whitney unpaired test. Dot represents individual samples and bar indicates the median.

4.2.8 Comparison of T cell population in CyTOF and Flow Cytometry

The material source of CyTOF analysis (n=6) was fixed whole blood while PBMCs were used for flow cytometry analysis (n=5) on the same patients alongside age and sex matched healthy controls. These blood products were processed with different conditions for optimal detection of target populations. Here, we evaluate the frequency of some T cell subsets, CD3+, CD4+, CD8+ and FOXP3+ and Tregs + cells to enable comparison between both methods.

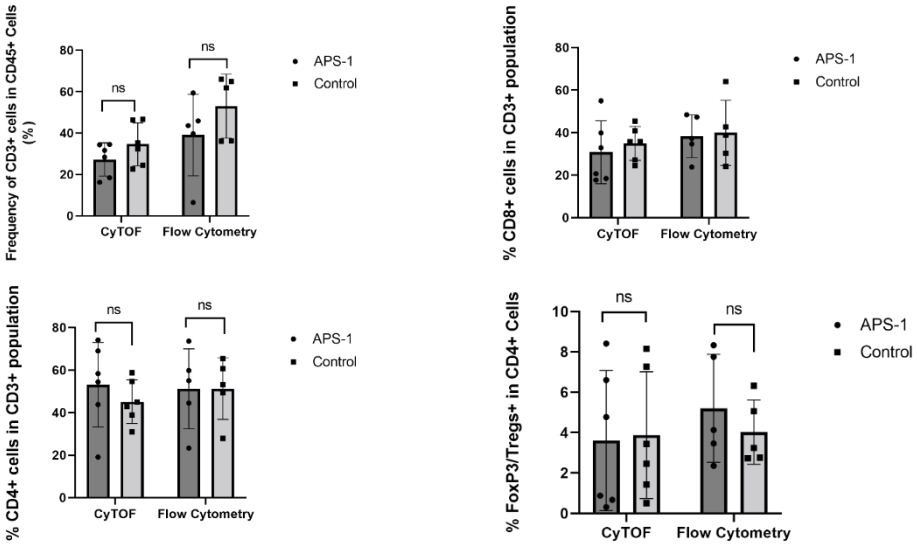

Figure 4.16: Expression of T cell subsets analysed by CyTOF and flowcytometry.

For all subsets evaluated, no significant interference was observed. CD3+ T cells (CyTOF mean: APS-I=27.2; mean HC= 34.6, P= 0.24); (FC mean: APS-I= 39; mean HC= 53, P= 0.42). CD8+ cells (CyTOF mean: APS-I=30.8; mean HC= 34.9, P= 0.39); (FC mean: APS-I= 38.3; mean HC= 38.98, P= >0.999). CD4+ cells (CyTOF mean: APS-I=53.16; mean HC= 51.2, P= 0.39); (FC mean: APS-I= 51.2; mean HC= 51.2, P= 0.42). Tregs cells (CyTOF mean: APS-1=3.6; mean HC= 3.87, P= 0.8); FOXP3 (FC mean: APS-I= 5.2; mean HC= 4, P= 0.55). Unpaired non-parametric analysis showed no statistical variations (p<0.05) in APS-1 patients and controls. Dot represents individual samples and bar indicates the median.

5 DISCUSSION

Immune phenotyping of cell subsets could help unravel mechanisms that are involved in autoimmune processes. Single cell proteomic techniques like mass and flow cytometry have revolutionised current immunophenotyping methodology and revealed ground-breaking knowledge of basic immunology mechanisms, and pathological pathways. To understand autoimmune disease initiation and progression, we must reveal how immune cells work together both in health and disease, and how the immune machinery fails causing break of self-tolerance.

Here, we have utilized an established in-house mass cytometry protocol to study a selected part of the main immune subsets in blood, and especially looked into T cell subsets. We have complimented the study by generating and optimising an immune panel for flow cytometry utilizing T cell transcription factors as targets. These techniques have been applied to undifferentiated and Th17- and Th2-polarised cells in a small cohort of APS-I patients, a model disorder for endocrine autoimmunity. Our results show minor divergences compared to healthy controls, with only a decreased comparable level of NKT-cells in APS-I patients compared to control subjects as main finding.

Fixed whole blood was here the choice of material to characterize a wide specter of immune cell subsets of APS-1 patients compared to healthy controls using mass cytometry. Purified leukocytes represented by PBMCs were however the choice for flow cytometry T cell profiling. Whole blood and PBMCs are the conventional choice materials for immune profiling which provides an insight of leukocyte populations in the bloodstream to identify gene expression that may be associated with disease pathogenesis [130]. Each of these biological products have distinctive attributes and gene expression profiles since they contain different kinds of cell subsets and are processed differently. However, they are not without limitations, ranging from sample collection, processing, and storage. Whole blood provides a wholesome assessment of immune cell populations. It is readily accessible and requires minimal processing, whereas the actual process of isolating PBMCs from whole blood is generally daunting and requires special laboratory facilities [131]. However, whole blood needs instant fixation post-sampling while PBMCs can be fixed after sampling to minimise intracellular damage. We used both presented blood preservations in this thesis mainly because the mass cytometry panel has been optimised for whole blood in our lab, and PBMC for flow cytometry characterization of T cells because we wanted to differentiate the Th2 and Th17 lineages using live cells.

5.1.1 Mass Cytometry allows identification of immune cell population

Mass cytometry has emerged as a high throughput method for immune characterization based on the fact that it is possible to assess the level of over 40 markers simultaneously, and to identify over 100 cell subsets. Choosing markers that are essential in defining the cell population to be studied is an important step in an experimental design. A CyTOF panel of 37 antibodies has been established successfully in the lab previously (*Shahinul et al; manuscript in progress*). Importantly, some compromises needed to be done on the lineage and functional antibody markers in the protocol because the method chosen for blood preparation.

Whole blood from patients and healthy controls must be processed to generate single cell suspension which requires a multistep workflow involving stabilisation, fixation, and erythrocyte lysis. Whole blood stabilisation is optimal for rapid leukocyte storage and preserves the integrity of surface and intracellular epitopes for downstream analysis [132]. At the same time, it reduces sample manipulation which may affect essential features of different immune cell subsets and allows analysis of samples in small volumes with less resources [133]. Stabilization of whole blood also provides the convenience to be able to assemble and freeze samples in an extensive immune profiling of large groups and later process them at the same time reducing batch effects or technical variations. Fixation of stabilised whole blood is instantly required for cell stability and long term storage, even though it is known to destroy epitopes which may hamper cell permeability and antibody recognition [134]. Fixation may also cause modification of epitopes which is responsible for loss of signal, despite this limitation, cell populations in this study showed clear separation. For these reasons, the choice of using Cytodelics-fixated cells for mass cytometry resulted in the exclusion of most of the chemokines and chemokine receptors in our panel, for instance CCR7, CCR6 and CXCRs, as these do not work well with Cytodelics. These chemokine and their receptors lack compatibility with some fix/lyse agents and have been implicated in a study where they exhibited non-specific signalling [135]. Intracellular markers including transcription factors were also excluded because these need extensive optimalisation and also requires additional cumbersome steps in the mass cytometry protocol.

Considering that neutrophils make up almost 50-70% of all circulating leukocytes [136], also given that agranulocytes are the main population of interest in this study, granulocytes depletion by positive selection of neutrophils was incorporated using CD66abce depletion by magnetic separation. The human CD66 antigen phenotype is a member of the carcinoembryonic antigen–related cell adhesion molecules (CEACAM) family involved in a variety of cellular processes. Even though the granulocyte depletion was established in our protocol, we still observed a

relatively large population of granulocytes in samples. This could be due to sample handling, technical variations and because the Cytodelic treatment could potentially interfere with the CD66b-molecule. All samples did nevertheless reveal that a large proportion of the granulocytes where indeed removed. The presence of these unwanted cells did not disturb the rest of the analyses.

The CD66b conjugation in this project was achieved based on learning purpose. Validation and titration after conjugation are critical steps that was taken to avoid unspecific binding and false positive signaling due to excessive antibody concentration. The recovery rate post conjugation from our result was 56.7%, this is acceptable but less than recommended expected recovery of ≥60%. The ability to multiplex all patient and healthy control samples into one barcode, stain them with antibody cocktails to assess immune phenotypes of T cells, DCs, monocytes, granulocytes, Treg, B cells, NK and NKT cells in their desired concentration reduced data collection variability and enabled direct comparison of signal across samples. To facilitate subset identification, FlowSOM compartmentalized cell into groups and enabled individual identification of variable frequencies of distinct immunophenotypes using marker expression within each individual cell.

5.1.2 Altered expression of NKT cells in APS-1 patients

Immune phenotyping studies of APS-1 patients is very limited in the literature; Therefore, the first goal in this project was to identify lineage markers in major cell populations of our study groups. Analysis from our high dimensional CyTOF data showed no large variations in the selected positive target populations but revealed alterations in NKT cells; these were lower in samples from APS-1 patients than from healthy controls. This result corresponds with a study that recorded a severe loss of NKT cells in nuclear factor-kappa B (NF-κB) deficient mice study [137]. Signaling response from NF-κB is crucial for AIRE expression, Treg maintenance and in general, immune tolerance maintenance [138]. Low intensity of NKT cells have further been implicated in different autoimmune conditions in both humans and mice [139]. Several mice studies have reported similar trends of significant reduced numbers of NKT cells in AIRE deficiency [140-142]. Separate studies on mice lacking lymphotoxin also revealed loss of expression in NKT cells in the absence of functional AIRE [143, 144]. NKT cells are phenotypically diverse, and their role in autoimmunity has been extensively studied; However, still the mechanisms of NKT cell responses in autoimmunity are vague and poorly understood [139].

Our data also showed a slight variation of monocytes between patients and control, even though no obvious difference was detected. Monocytes are known to have inflammatory and tissue

repairing effects and have been involved in some autoimmune diseases through secretion of cytokines and chemokines [145]. Previously, monocytes were found to vary to a large extent between APS-1 patients and controls using flowcytometry [146]. Hong and colleagues further demonstrated a significant high percentage of peripheral blood monocytes in APS-1 patients with CMC compared with healthy controls. Increased level of monocytes in in CMC patients may be attributable to the presence of *Candida* inflammatory response [147]. Studies by Perniola et al 2008 and Wolff et al 2010 also observed large number of monocytes in APS-1 patients with no alteration by flowcytometry [148, 149].

Increased frequencies of CD66b+ cells have previously been observed in patients with biallelic loss of function variants of AIRE. Neutrophils, also carrying CD66b are the most abundant leukocytes contributing to autoimmune processes through their dysregulated and phagocytic function. A study on a large cohort of APS-1 patients with autoimmune pneumonitis revealed high numbers of activated neutrophils in the airways [150]. Since we attempted to remove the neutrophils prior to analysis, it is not possible to give an estimate on the frequency of these cells in this project.

Despite that patients and mice deficient of AIRE have been shown to have circulating autoantibodies driven by B cells [151], APS-1 patients in comparison with healthy controls were characterized by lower numbers of B cells. This agrees with Sng et al that reported signal loss in B cell activity of AIRE defective patients [152]. Our study did not reveal any disturbance in B cell activity.

NK cells are characterized by the cytotoxic activity in virally infected cells and have been shown to secrete IFN-γ when primed with pro-inflammatory cytokines [153]. Emma Lindh et al demonstrated normal activity of NK cells in mice and two APS-1 patients, and concluded the independent development and role of NK cells in AIRE deficiency [154]. Results from this study showed no discrepancies in CD56+ NK cells between groups which is consistent with a previous study addressing unaltered NK cell frequency in APS-1 patients [149].

In addition, we found varying frequencies in T cell subset expression, without revealing any statistical differences between patients and controls. Comparably to healthy controls, a slight reduction was observed in γδ T cells in patients, while the Treg population did not differ between groups. Tregs have indeed been found with lower frequencies and impaired in APS-1 in previous studies [110, 111, 149, 155]. We presume that the number of subjects included in this study make us unable to reveal the same results.

5.1.3 Optimization of transcription factor panel for flow cytometry

For in depth T cell analysis, a transcription factor panel for flowcytometry was optimised to evaluate the responsiveness of our target cells to stimulation, as well as cytokine production capacity of different T cell subsets of APS-1 patients. Stimulation and intracellular staining is a major way to evaluate immune cell responses at single cell level. One vital step in intracellular staining is to validate staining for each surface marker or transcription factor through titrations, compensation and FMO controls. This allows detection of positive signal and determines specificity of the antibody [156]. Although, our FMO controls were not representative of the negative cell population, they were used whenever possible. Another important step is choosing the best buffer condition for fixation and permeabilization to ensure stability of cell membrane and to able to access the intracellular epitopes. Since these can also have the tendency to affect cell integrity and decrease fluorescence signal, it is highly recommended to test different buffers to determine the best that offers optimal staining signal for target cells.

To address this, a comparative study between BD Cytofix/Cytoperm Fixation/Permeabilization Solution Kit and eBioscience FOXP3/Transcription Factor Staining Buffer Set was conducted on our cohort simultaneously to determine the optimal buffer condition for our target cells. FOXP3 staining buffer from eBioscience showed high expression and a better separation between the positive and negative population especially FOXP3, and also showed consistency in other cell population. This result corresponds to findings from Law et al 2009, that showed clarity of separation of FOXP3 population using FOXP3 eBioscience buffer when compared to four other different buffers while highlighting the importance of using the same staining condition for the entire study [157]. Time constraints did not permit the testing of other buffers, e.g., a methanol-based buffer.

Cell mediating responses can be characterized based on cytokine secretion profiles in blood or PBMCs which can be assessed at single cell level in optimal conditions [158]. Transcription factors are master regulators in Th cell subsets and accomplish their regulatory functions through secretion of specific cytokines driven by stimulatory responses from APCs. Th cell differentiation is an important player in immune responses and peripheral tolerance maintenance and is responsible for complications and disruptions in the immune system. APCs express AIRE which may alter Th cells via expression of signaling molecules and cytokine production. Therefore, defining cells by their transcription factors in this study might help elucidate the complex role of AIRE as a transcription regulator which mutations in its gene is the culprit in development of APS-1 disease [81]. We have differentiated naïve PBMCs under polarising conditions to generate Th17 cells and

Th2 cells. Th17 cells mediate inflammations which triggers autoimmune diseases and its impairment is associated with CMC which is one of the components of APS-1 disorder [108], while Th2 cells are characterized by the modulatory function in immune response to parasitic infections. Overall, this study revealed that we managed to skew compositions of CD4+ T cell populations. However, assessment with flowcytometry and ELISA did not show any difference between patients and controls.

Previous studies have demonstrated the mediating role of AIRE in cytokine production of Th17 including TGF-β and IL-6 which have been detected to be increased in situations of AIRE over-expression. In a similar trend, TGF-β and IL-6 are involved in RORgt expression which is indeed a vital transcription factor for Th17 differentiation [159].

5.1.4 Expression of Cells within CD4+ and CD8+ T Cells

In this study, the immune phenotypes of APS-1 patients and healthy controls were characterized using PBMCs in its naïve state and subsequent identification of cell populations of Rorgt, T.bet, CXCR3, GATA3 and FOXP3 cells detected no significant difference. However, Eomes was expressed in high numbers in CD8+ T cells with alterations. Eomes have been implicated in differentiation of effector memory cells. Knox et al characterised Eomes expression in human CD8+ T cell memory populations and observed high frequencies of Eomes in effector cells [160].

Results from CD4+ T cell expressing cells raised doubts on the effectiveness of the flowcytometry protocol for all markers. As a next step, the naïve PBMCs were stimulated, skewed towards Th2 and Th17 phenotypes and profiled. It was observed that expression in stimulated PBMCs under polarised conditions differed in comparison with naïve PBMCs. Differential T cell responses to stimulation in the presence of Th2 and Th17 polarising cytokines was confirmed by identification of RORgt+ and GATA3+ expression and secretion of their distinct cytokines, IL-17, and IL-5. We concluded that the stimulations were successful, although we recognize that even further optimizations depending on the ultimate goal could be beneficial.

Based on the result of this analysis and as expected, naïve CD4+ T cells differentiated towards Th17 cells with high proliferation of Rorgt in response to anti CD3/anti CD28 coated plates, and IL-1β, IL-6, IL-23, TGF-β1 with an addition of anti IFN-γ and anti-IL4 to block lineage diversion to Th1 and Th2 cells respectively. Further analysis revealed low level of GATA3+ cells expression, while increased number of FOXP3+ cells were seen in both groups. It can be speculated that the presence of TGF-β1 elicited proliferations of FOXP3 [129]. Surprisingly, IL-6 to some extent could not repress the induction of FOXP3 in this study considering its crucial role

in the balance between Th17 and Tregs proliferation. It is widely known that Rorgt expression promoted by STAT3 orchestrates Th17 polarisation promoting IL-17 expression [161]. However, high expressions of Rorgt and FOXP3 were observed in Th17 cells deficient of STAT3 in this study. Yang Xuexian et al demonstrated the regulatory function of STAT in lineage specific gene expression speculating that the absence of STAT3 in RORgt expression can trigger vigorous expression of FOXP3+ cells, indicating that IL-6 in combination with STAT3 is critical for blockade of FOXP3 expression and increased proliferations of RORgt in Th17 cells [162].

Going further, naïve PBMCs primed with Th2 cytokines IL4, in combination with IL-2, anti-Human CD3, penicillin and Streptomycin to drive differentiation of Th2 cells. The human Th2 differentiation media used contained factors important for Th2 cytokines. We show that GATA3 is present in both naïve and stimulated PBMCs but is more upregulated during Th2 differentiation. GATA3 is plays an important role in the development of thymocytes [163]. RORgt+ cells were shown to be lowly expressed. We also find that Th2 cells skewed towards FOXP3+ cells.

For more evaluations, supernatants from Th17 differentiated cells were further defined on the basis of cytokine production and high production of the IL-17 cytokine was observed, while IL-5 was barely detectable. This result is consistent with the known fact that RORgt regulates IL-17 secretion in CD4+ T cell population and might be involved in modulating signaling in Th17 inflammatory responses [161]. We also observed the induction of IL-5 mediated b1y GATA3+ expression. Surprisingly, low levels of IL-17 cytokine were also secreted in Th2 differentiated cells.

5.1.5 Comparison of CyTOF and Flow Cytometry Staining on T cell response

We have evaluated the distribution of specific T cell sub populations in blood samples processed for CyTOF and flowcytometry. For CyTOF, whole blood was fixed based on Cytodelics, while naïve PBMCs for flowcytometry were separated by density centrifugation. study. CyTOF workflow have used a fix, freeze, stain protocol, whereas PBMCs were frozen and thawed before use. This freezing and thawing step which, to some extent could have a negative impact in cell morphology and detectability as well as introduce some technical bias that may cause from loss of cell concentration and thawing process [164]. However, these were not taken into consideration in this comparison as we are interested in whether the different cytometric methods affects cell frequency.

Manual gating for T cell populations was performed based on two methodologies. Flowcytometry gates out populations on the basis of size and complexity/granularity using the FCS and SSC

parameters while CyTOF utilises the DNA intercalator (191Ir and 193Ir) to gate events. The expression of our target cells were identified by using the bivariate dot plots.

Based on our findings, the frequency of T cell responses from fixed blood and naïve PBMCs did not show any profound alterations. The frequency of positive T Cells were similar by CyTOF and Flowcytometry indicating the effectiveness of both techniques in identifying T cells subsets. The proportion of CD3+ cells was slightly increased in PBMCs compared to fixed blood. Among CD3+ cells, CD4+ and CD8+ cells had nearly the same frequency between patients and controls for both techniques. The analysis of Tregs (CD4+ FoxP3+) in peripheral blood by flow cytometry showed no differences between patients and controls. The same was observed in Tregs (CD3+ CD14- CD19- CD56- CD4+ CD8- TCRγδ- CD25+ CD127-) analysed by CyTOF using fixed blood in this study. Some studies have compared PBMCs and fixed blood using flow cytometry, mass cytometry or both and got nearly similar results [133, 165]. These findings show that T cell populations were not influenced by sample type. We were able to detect cell populations in similar distribution irrespective of technique or sample material.

6 CONCLUSION

In summary, we have used the two proposed methodological strategies to demonstrate the identification of distinct immune subsets in APS-1 patients using fixed blood and peripheral blood. Although whole blood is considered the suitable material source for gene expression analysis; with good optimalization, PBMCs and fixed blood can effectively detect immune cells in patients.

Here, we saw few immune subsets deviations in APS-I patients compared to healthy controls, but the reason behind this and consequence for immune balance is still obscure. Therefore, the effects of AIRE deficiency in the development and function of NKT cells pertaining to immune responses need to be investigated further. On the other hand, T helper cells through the secretion of cytokines are considered a valuable tool for understanding the pathogenesis of autoimmune disease and can serve as potential therapeutic targets for treatment. A thorough investigation of NKT cells and cytokine secreting Th cells, or in general, distinct immune subsets using different sample types and methods could have potentials to further enhance a broader understanding of gene expression and elucidate disease pathogenesis in APS-1 patients. To our knowledge, there are limited studies of immune profiling of APS-1 patients using CyTOF. This findings in the present study may facilitate an improved comprehension of distinctive features of immune cells in endocrine autoimmunity.

6.1 LIMITATIONS

This study was burdened with several constraints: the size of the study group, restricted number of cell types, and limited time frame. APS-1 is incredibly rare; hence, access to samples is very limited. With only few participants included, it is difficult to conclude the prospects of the results since immune profiles vary greatly between individuals. It would be interesting to study a bigger cohort of APS-1 patients for in-depth interrogation so as to gain more insight into the mechanism of this rare disease.

Limited time was another challenge that hampered this study, due to technical problems like breakdown of the CyTOF instrument, and delays in blood collection from sex- and age- matched healthy donors for the control group which was collected over time and thereafter analyzed in parrel with patient’s sample.

An additional potential limitation is low cell concentration. Cell storage, freezing and thawing steps, as well as lots of washing steps in both techniques may have consequences that could lead to bias in sample size and cell viability.

Compared to flowcytometry, CyTOF has a lower acquisition rate, despite the fact that it is considered an improved version of flowcytometry, and because cells are vaporized during acquisition, there is no possibility of downstream analysis for further investigations. Furthermore, data interpretation in CyTOF is complex and challenging. Hence, it requires advanced statistical and programming knowledge [113]. Despite these limitations, we were able to identify distinct immune subsets using both techniques.

6.2 FUTURE PERSPECTIVES

An elaborated experimental panel design and a greater understanding of limitations and complications are among the leading success factors in cytometric studies. These will further enhance the capability to harness the beneficial role of CyTOF and flow cytometry methodologies to phenotypically characterize diverse cell lineages at single cell resolution, which may unveil novel alterations that influence diagnosis and reveal new treatment options to limit the self-destruction of the endocrine glands.

APS-1 is characterized by multiple endocrine dysfunction and its phenotypic expression is highly variable. Therefore, a better characterization will facilitate the identification of signaling phenotype that could be important in exposing the implication of dysregulated immune response in APS-1 and on the function of AIRE. Proteomic, transcriptomic, and functional assays on isolated subsets from APS-1 patients, and by utilizing different activation agents to study the immune subset outcome. For instance, single cell transcriptomics (10x technology) and flow or mass cytometry with phosphor-specific markers to study signaling pathways. These could certainly aid in a better prognostic assessment and management of APS-1.

REFERENCES

1. Chaplin, D.D., *Overview of the immune response.* The Journal of allergy and clinical immunology, 2010. **125**(2 Suppl 2): p. S3-S23.
2. Marshall, J.S., et al., *An introduction to immunology and immunopathology.* Allergy, Asthma & Clinical Immunology, 2018. **14**(2): p. 49.
3. Sakaguchi, S., *Regulatory T Cells: Key Controllers of Immunologic Self-Tolerance.* Cell Press, 2000. **101**(5): p. 455-458.
4. Nicholson, L.B., *The immune system.* Essays in biochemistry, 2016. **60**(3): p. 275-301.
5. Hoffmann, J.A. and J.-M. Reichhart, *Drosophila innate immunity: an evolutionary perspective.* Nature Immunology, 2002. **3**(2): p. 121-126.
6. InformedHealth.org, *The innate and adaptive immune systems* 2006, Institute for Quality and Efficiency in Health Care (IQWiG).
7. Smith, N.C., M.L. Rise, and S.L. Christian, *A Comparison of the Innate and Adaptive Immune Systems in Cartilaginous Fish, Ray-Finned Fish, and Lobe-Finned Fish.* Frontiers in Immunology, 2019. **10**(2292).
8. Goodnow, C.C., et al., *Cellular and genetic mechanisms of self tolerance and autoimmunity.* Nature, 2005. **435**(7042): p. 590-7.
9. Clark, R. and T. Kupper, *Old Meets New: The Interaction Between Innate and Adaptive Immunity.* Journal of Investigative Dermatology, 2005. **125**(4): p. 629-637.
10. Bonilla, F.A. and H.C. Oettgen, *Adaptive immunity.* Journal of Allergy and Clinical Immunology, 2010. **125**(2): p. S33-S40.
11. Delves, P.J. and I.M. Roitt, *The Immune System.* New England Journal of Medicine, 2000. **343**(1): p. 37-49.
12. Hardy, R.R. and K. Hayakawa, *B cell development pathways.* Annu Rev Immunol, 2001. **19**: p. 595-621.
13. Oliveira, C., et al., *Recent advances in characterization of nonviral vectors for delivery of nucleic acids: Impact on their biological performance.* Expert Opinion on Drug Delivery, 2014. **12**.
14. Govers, C., et al., *T cell receptor gene therapy: strategies for optimizing transgenic TCR pairing.* Trends in Molecular Medicine, 2010. **16**(2): p. 77-87.
15. Gustafsson, K., T. Herrmann, and F. Dieli, *Editorial: Understanding Gamma Delta T Cell Multifunctionality - Towards Immunotherapeutic Applications.* Frontiers in Immunology, 2020. **11**.
16. Kumar, B.V., T.J. Connors, and D.L. Farber, *Human T Cell Development, Localization, and Function throughout Life.* Immunity, 2018. **48**(2): p. 202-213.

17. Janeway CA Jr, T.P., Walport M, et al *Immunobiology: The Immune System in Health and Disease*. 2001, Garland Science: New York.
18. Kaech, S.M., E.J. Wherry, and R. Ahmed, *Effector and memory T-cell differentiation: implications for vaccine development.* Nature Reviews Immunology, 2002. **2**(4): p. 251-262.
19. Gutcher, I. and B. Becher, *APC-derived cytokines and T cell polarization in autoimmune inflammation.* The Journal of Clinical Investigation, 2007. **117**(5): p. 1119-1127.
20. Nakayama, T. and M. Yamashita, *The TCR-mediated signaling pathways that control the direction of helper T cell differentiation.* Semin Immunol, 2010. **22**(5): p. 303-9.
21. Luckheeram, R.V., et al., *CD4$^+$T cells: differentiation and functions.* Clinical & developmental immunology, 2012. **2012**: p. 925135-925135.
22. Youngblood, B., et al., *Effector CD8 T cells dedifferentiate into long-lived memory cells.* Nature, 2017. **552**(7685): p. 404-409.
23. Cox, M.A., S.M. Kahan, and A.J. Zajac, *Anti-viral CD8 T cells and the cytokines that they love.* Virology, 2013. **435**(1): p. 157-69.
24. Andersen, M.H., et al., *Cytotoxic T Cells.* Journal of Investigative Dermatology, 2006. **126**(1): p. 32-41.
25. Stiehm, E.R., *Joseph A. Bellanti (ed) Immunology IV: Clinical Applications in Health and Disease.* Journal of Clinical Immunology, 2012. **32**(3): p. 647-647.
26. Ouyang, W., et al., *Regulation and functions of the IL-10 family of cytokines in inflammation and disease.* Annu Rev Immunol, 2011. **29**: p. 71-109.
27. Asseman, C., et al., *An essential role for interleukin 10 in the function of regulatory T cells that inhibit intestinal inflammation.* J Exp Med, 1999. **190**(7): p. 995-1004.
28. Lee, J., et al., *The Multifaceted Role of Th1, Th9, and Th17 Cells in Immune Checkpoint Inhibition Therapy.* Frontiers in Immunology, 2021. **12**.
29. Cousens, L.P., et al., *Two roads diverged: interferon alpha/beta- and interleukin 12-mediated pathways in promoting T cell interferon gamma responses during viral infection.* J Exp Med, 1999. **189**(8): p. 1315-28.
30. Szabo, S.J., et al., *A novel transcription factor, T-bet, directs Th1 lineage commitment.* Cell, 2000. **100**(6): p. 655-69.
31. Stark, J.M., C.A. Tibbitt, and J.M. Coquet, *The Metabolic Requirements of Th2 Cell Differentiation.* Frontiers in Immunology, 2019. **10**.
32. Cano RLE, L.H., *Introduction to T and B lymphocytes*, in *Autoimmunity: From Bench to Bedside*, S.Y. Anaya JM, Rojas-Villarraga A, et al, Editor. 2013, El Rosario University Press: Bogota (Colombia).

33. Liao, W., J.-X. Lin, and W.J. Leonard, *IL-2 family cytokines: new insights into the complex roles of IL-2 as a broad regulator of T helper cell differentiation.* Current Opinion in Immunology, 2011. **23**(5): p. 598-604.
34. Paul, W.E. and J. Zhu, *How are T(H)2-type immune responses initiated and amplified?* Nat Rev Immunol, 2010. **10**(4): p. 225-35.
35. Usui, T., et al., *GATA-3 suppresses Th1 development by downregulation of Stat4 and not through effects on IL-12Rbeta2 chain or T-bet.* Immunity, 2003. **18**(3): p. 415-28.
36. Hundorfean, G., M.F. Neurath, and J. Mudter, *Functional relevance of T helper 17 (Th17) cells and the IL-17 cytokine family in inflammatory bowel disease.* Inflamm Bowel Dis, 2012. **18**(1): p. 180-6.
37. Ivanov, I.I., et al., *The Orphan Nuclear Receptor RORγt Directs the Differentiation Program of Proinflammatory IL-17⁺ T Helper Cells.* Cell, 2006. **126**(6): p. 1121-1133.
38. Miossec, P., T. Korn, and V.K. Kuchroo, *Interleukin-17 and type 17 helper T cells.* N Engl J Med, 2009. **361**(9): p. 888-98.
39. Hirota, K., et al., *Preferential recruitment of CCR6-expressing Th17 cells to inflamed joints via CCL20 in rheumatoid arthritis and its animal model.* The Journal of experimental medicine, 2007. **204**(12): p. 2803-2812.
40. Steinmetz, O.M., et al., *CXCR3 mediates renal Th1 and Th17 immune response in murine lupus nephritis.* J Immunol, 2009. **183**(7): p. 4693-704.
41. Dardalhon, V., et al., *IL-4 inhibits TGF-beta-induced Foxp3+ T cells and, together with TGF-beta, generates IL-9+ IL-10+ Foxp3(-) effector T cells.* Nat Immunol, 2008. **9**(12): p. 1347-55.
42. Veldhoen, M., et al., *Transforming growth factor-beta 'reprograms' the differentiation of T helper 2 cells and promotes an interleukin 9-producing subset.* Nat Immunol, 2008. **9**(12): p. 1341-6.
43. Wong, M.T., et al., *Regulation of human Th9 differentiation by type I interferons and IL-21.* Immunol Cell Biol, 2010. **88**(6): p. 624-31.
44. Trifari, S., et al., *Identification of a human helper T cell population that has abundant production of interleukin 22 and is distinct from T(H)-17, T(H)1 and T(H)2 cells.* Nat Immunol, 2009. **10**(8): p. 864-71.
45. Nomura, T. and S. Sakaguchi, *Foxp3 and Aire in thymus-generated Treg cells: a link in self-tolerance.* Nature Immunology, 2007. **8**(4): p. 333-334.
46. Vignali, D.A.A., L.W. Collison, and C.J. Workman, *How regulatory T cells work.* Nature reviews. Immunology, 2008. **8**(7): p. 523-532.
47. Chen, C., et al., *Transcriptional regulation by Foxp3 is associated with direct promoter occupancy and modulation of histone acetylation.* J Biol Chem, 2006. **281**(48): p. 36828-34.

48. Anderson, M.S. and M.A. Su, *AIRE expands: new roles in immune tolerance and beyond.* Nature Reviews Immunology, 2016. **16**(4): p. 247-258.
49. Setoguchi, R., et al., *Homeostatic maintenance of natural Foxp3(+) CD25(+) CD4(+) regulatory T cells by interleukin (IL)-2 and induction of autoimmune disease by IL-2 neutralization.* The Journal of experimental medicine, 2005. **201**(5): p. 723-735.
50. Noval Rivas, M. and T. Chatila, *Regulatory T cells in allergic diseases.* Journal of Allergy and Clinical Immunology, 2016. **138**: p. 639-652.
51. Bennett, C.L., et al., *The immune dysregulation, polyendocrinopathy, enteropathy, X-linked syndrome (IPEX) is caused by mutations of FOXP3.* Nature Genetics, 2001. **27**(1): p. 20-21.
52. Kekäläinen, E., et al., *A Defect of Regulatory T Cells in Patients with Autoimmune Polyendocrinopathy-Candidiasis-Ectodermal Dystrophy.* The Journal of Immunology, 2007. **178**(2): p. 1208.
53. Laakso, S., et al., *Regulatory T cell defect in APECED patients is associated with loss of naive FOXP3(+) precursors and impaired activated population.* Journal of autoimmunity, 2010. **35**: p. 351-7.
54. Farhangnia, P. and M. Akbarpour, *Immunological Tolerance*, in *Reference Module in Biomedical Sciences*. 2021, Elsevier.
55. Husebye, E.S., M.S. Anderson, and O. Kämpe, *Autoimmune Polyendocrine Syndromes.* New England Journal of Medicine, 2018. **378**(12): p. 1132-1141.
56. Snyder, P.W., *Chapter 5 - Diseases of Immunity1*, in *Pathologic Basis of Veterinary Disease (Sixth Edition)*, J.F. Zachary, Editor. 2017, Mosby. p. 242-285.e5.
57. Klein, L., et al., *Positive and negative selection of the T cell repertoire: what thymocytes see (and don't see).* Nature reviews. Immunology, 2014. **14**(6): p. 377-391.
58. Starr, T.K., S.C. Jameson, and K.A. Hogquist, *Positive and negative selection of T cells.* Annu Rev Immunol, 2003. **21**: p. 139-76.
59. Palmer, E., *Negative selection - Clearing out the bad apples from the T-cell repertoire.* Nature reviews. Immunology, 2003. **3**: p. 383-91.
60. Xing, Y. and K.A. Hogquist, *T-cell tolerance: central and peripheral.* Cold Spring Harbor perspectives in biology, 2012. **4**(6): p. a006957.
61. Ardavi´n, C., *Thymic dendritic cells.* Immunology Today, 1997. **18**(7): p. 350-361.
62. Žumer, K., K. Saksela, and B.M. Peterlin, *The Mechanism of Tissue-Restricted Antigen Gene Expression by AIRE.* The Journal of Immunology, 2013. **190**(6): p. 2479.
63. Gallegos , A.M. and M.J. Bevan *Central Tolerance to Tissue-specific Antigens Mediated by Direct and Indirect Antigen Presentation.* Journal of Experimental Medicine, 2004. **200**(8): p. 1039-1049.

64. Mackay, I.R., *Tolerance and autoimmunity.* Western Journal of Medicine, 2001. **174**(2): p. 118-123.
65. Keir, M.E., et al., *PD-1 and its ligands in tolerance and immunity.* Annu Rev Immunol, 2008. **26**: p. 677-704.
66. Mueller, D.L., *Mechanisms maintaining peripheral tolerance.* Nature Immunology, 2010. **11**(1): p. 21-27.
67. Getahun, A., M. Smith, and J. Cambier, *Mechanisms of Peripheral B Cell Tolerance.* Encyclopedia of Immunobiology, 2016.
68. Russell, D.M., et al., *Peripheral deletion of self-reactive B cells.* Nature, 1991. **354**(6351): p. 308-311.
69. Valdes, A.Z., *Chapter 17 - Immunological tolerance and autoimmunity*, in *Translational Autoimmunity*, N. Rezaei, Editor. 2022, Academic Press. p. 325-345.
70. Kono, D.H. and A.N. Theofilopoulos, *Chapter 19 - Autoimmunity*, in *Kelley and Firestein's Textbook of Rheumatology (Tenth Edition)*, G.S. Firestein, et al., Editors. 2017, Elsevier. p. 301-317.e5.
71. Takahashi, H., et al., *Autoimmunity and immunological tolerance in autoimmune bullous diseases.* Int Immunol, 2019. **31**(7): p. 431-437.
72. Romagnani, S., *Immunological tolerance and autoimmunity.* Internal and Emergency Medicine, 2006. **1**(3): p. 187-196.
73. Lam-Tse, W.K., A. Lernmark, and H.A. Drexhage, *Animal models of endocrine/organ-specific autoimmune diseases: do they really help us to understand human autoimmunity?* Springer Seminars in Immunopathology, 2002. **24**(3): p. 297-321.
74. Lee, G.R., *The Balance of Th17 versus Treg Cells in Autoimmunity.* International journal of molecular sciences, 2018. **19**(3): p. 730.
75. Manel, N., D. Unutmaz, and D.R. Littman, *The differentiation of human T(H)-17 cells requires transforming growth factor-beta and induction of the nuclear receptor RORgammat.* Nat Immunol, 2008. **9**(6): p. 641-9.
76. Liao, W., J.-X. Lin, and W.J. Leonard, *Interleukin-2 at the crossroads of effector responses, tolerance, and immunotherapy.* Immunity, 2013. **38**(1): p. 13-25.
77. Zhang, F., G. Meng, and W. Strober, *Interactions among the transcription factors Runx1, RORgammat and Foxp3 regulate the differentiation of interleukin 17-producing T cells.* Nature immunology, 2008. **9**(11): p. 1297-1306.
78. Rudra, D., et al., *Transcription factor Foxp3 and its protein partners form a complex regulatory network.* Nat Immunol, 2012. **13**(10): p. 1010-9.
79. Mousset, C.M., et al., *Comprehensive Phenotyping of T Cells Using Flow Cytometry.* Cytometry A, 2019. **95**(6): p. 647-654.

80. Aaltonen, J., et al., *An autoimmune disease, APECED, caused by mutations in a novel gene featuring two PHD-type zinc-finger domains.* Nature Genetics, 1997. **17**(4): p. 399-403.
81. Nagamine, K., et al., *Positional cloning of the APECED gene.* Nat Genet, 1997. **17**(4): p. 393-8.
82. Oftedal, Bergithe E., et al., *Dominant Mutations in the Autoimmune Regulator AIRE Are Associated with Common Organ-Specific Autoimmune Diseases.* Immunity, 2015. **42**(6): p. 1185-1196.
83. Abbott, J.K., et al., *Dominant-negative loss of function arises from a second, more frequent variant within the SAND domain of autoimmune regulator (AIRE).* J Autoimmun, 2018. **88**: p. 114-120.
84. Betterle, C., N.A. Greggio, and M. Volpato, *Autoimmune Polyglandular Syndrome Type 1.* The Journal of Clinical Endocrinology & Metabolism, 1998. **83**(4): p. 1049-1055.
85. Wolff, A.S.B., et al., *Autoimmune Polyendocrine Syndrome Type 1 in Norway: Phenotypic Variation, Autoantibodies, and Novel Mutations in the Autoimmune Regulator Gene.* The Journal of Clinical Endocrinology & Metabolism, 2007. **92**(2): p. 595-603.
86. Zhan, F. and L. Cao, *Late-onset autoimmune polyendocrine syndrome type 1: a case report and literature review.* Immunologic research, 2021. **69**(2): p. 139-144.
87. Myhre, A.G., et al., *Autoimmune polyendocrine syndrome type 1 (APS I) in Norway.* Clinical Endocrinology, 2001. **54**(2): p. 211-217.
88. Perheentupa, J., *Autoimmune polyendocrinopathy-candidiasis-ectodermal dystrophy.* J Clin Endocrinol Metab, 2006. **91**(8): p. 2843-50.
89. Ahonen, P., et al., *Clinical variation of autoimmune polyendocrinopathy-candidiasis-ectodermal dystrophy (APECED) in a series of 68 patients.* N Engl J Med, 1990. **322**(26): p. 1829-36.
90. Husebye, E.S. and M.S. Anderson, *Autoimmune polyendocrine syndromes: clues to type 1 diabetes pathogenesis.* Immunity, 2010. **32**(4): p. 479-487.
91. Mazza, C., et al., *Clinical heterogeneity and diagnostic delay of autoimmune polyendocrinopathy-candidiasis-ectodermal dystrophy syndrome.* Clin Immunol, 2011. **139**(1): p. 6-11.
92. Constantine, G.M. and M.S. Lionakis, *Lessons from primary immunodeficiencies: Autoimmune regulator and autoimmune polyendocrinopathy-candidiasis-ectodermal dystrophy.* Immunological reviews, 2019. **287**(1): p. 103-120.
93. Husebye, E.S., et al., *Clinical manifestations and management of patients with autoimmune polyendocrine syndrome type I.* Journal of Internal Medicine, 2009. **265**(5): p. 514-529.

94. Orlova, E.M., et al., *Expanding the Phenotypic and Genotypic Landscape of Autoimmune Polyendocrine Syndrome Type 1.* The Journal of Clinical Endocrinology & Metabolism, 2017. **102**(9): p. 3546-3556.
95. Gylling, M., et al., *The hypoparathyroidism of autoimmune polyendocrinopathy-candidiasis-ectodermal dystrophy protective effect of male sex.* J Clin Endocrinol Metab, 2003. **88**(10): p. 4602-8.
96. Erichsen, M.M., et al., *Clinical, Immunological, and Genetic Features of Autoimmune Primary Adrenal Insufficiency: Observations from a Norwegian Registry*. The Journal of Clinical Endocrinology & Metabolism, 2009. **94**(12): p. 4882-4890.
97. Winqvist, O., F.A. Karlsson, and O. Kämpe, *21-Hydroxylase, a major autoantigen in idiopathic Addison's disease.* Lancet, 1992. **339**(8809): p. 1559-62.
98. Gardner, J.M., et al., *Deletional tolerance mediated by extrathymic Aire-expressing cells.* Science, 2008. **321**(5890): p. 843-7.
99. Heino, M., et al., *Autoimmune Regulator Is Expressed in the Cells Regulating Immune Tolerance in Thymus Medulla*. Biochemical and Biophysical Research Communications, 1999. **257**(3): p. 821-825.
100. Anderson, M.S., et al., *Projection of an immunological self shadow within the thymus by the aire protein.* Science, 2002. **298**(5597): p. 1395-401.
101. Guo, C.J., et al., *The immunobiology and clinical features of type 1 autoimmune polyglandular syndrome (APS-1).* Autoimmun Rev, 2018. **17**(1): p. 78-85.
102. Peterson, P., T. Org, and A. Rebane, *Transcriptional regulation by AIRE: molecular mechanisms of central tolerance.* Nature Reviews Immunology, 2008. **8**(12): p. 948-957.
103. Meager, A., et al., *Anti-interferon autoantibodies in autoimmune polyendocrinopathy syndrome type 1.* PLoS medicine, 2006. **3**(7): p. e289-e289.
104. Liston, A., et al., *Genetic lesions in T-cell tolerance and thresholds for autoimmunity.* Immunol Rev, 2005. **204**: p. 87-101.
105. Wolff, A.S., et al., *Anti-cytokine autoantibodies preceding onset of autoimmune polyendocrine syndrome type I features in early childhood.* J Clin Immunol, 2013. **33**(8): p. 1341-8.
106. Meloni, A., et al., *Autoantibodies against Type I Interferons as an Additional Diagnostic Criterion for Autoimmune Polyendocrine Syndrome Type I.* The Journal of Clinical Endocrinology & Metabolism, 2008. **93**(11): p. 4389-4397.
107. Söderbergh, A., et al., *Prevalence and Clinical Associations of 10 Defined Autoantibodies in Autoimmune Polyendocrine Syndrome Type I.* The Journal of clinical endocrinology and metabolism, 2004. **89**: p. 557-62.
108. Humbert, L., et al., *Chronic Mucocutaneous Candidiasis in Autoimmune Polyendocrine Syndrome Type 1*. Frontiers in Immunology, 2018. **9**.

109. Levin, M., *Anti-interferon auto-antibodies in autoimmune polyendocrinopathy syndrome type 1.* PLoS medicine, 2006. **3**(7): p. e292-e292.
110. Kekäläinen, E., et al., *A defect of regulatory T cells in patients with autoimmune polyendocrinopathy-candidiasis-ectodermal dystrophy.* J Immunol, 2007. **178**(2): p. 1208-15.
111. Laakso, S.M., et al., *Regulatory T cell defect in APECED patients is associated with loss of naive FOXP3(+) precursors and impaired activated population.* J Autoimmun, 2010. **35**(4): p. 351-7.
112. Laakso, S.M., et al., *IL-7 dysregulation and loss of CD8+ T cell homeostasis in the monogenic human disease autoimmune polyendocrinopathy-candidiasis-ectodermal dystrophy.* J Immunol, 2011. **187**(4): p. 2023-30.
113. Ornatsky, O., et al., *Highly multiparametric analysis by mass cytometry.* Journal of Immunological Methods, 2010. **361**(1): p. 1-20.
114. Spitzer, Matthew H. and Garry P. Nolan, *Mass Cytometry: Single Cells, Many Features.* Cell, 2016. **165**(4): p. 780-791.
115. Nowicka, M., et al., *CyTOF workflow: differential discovery in high-throughput high-dimensional cytometry datasets [version 4; peer review: 2 approved].* F1000Research, 2019. **6**(748).
116. Olsen, L.R., et al., *The anatomy of single cell mass cytometry data.* Cytometry Part A, 2019. **95**(2): p. 156-172.
117. Bendall, S.C., et al., *A deep profiler's guide to cytometry.* Trends in immunology, 2012. **33**(7): p. 323-332.
118. Bandura, D.R., et al., *Mass Cytometry: Technique for Real Time Single Cell Multitarget Immunoassay Based on Inductively Coupled Plasma Time-of-Flight Mass Spectrometry.* Analytical Chemistry, 2009. **81**(16): p. 6813-6822.
119. McKinnon, K.M., *Flow Cytometry: An Overview.* Current protocols in immunology, 2018. **120**: p. 5.1.1-5.1.11.
120. Maecker, H.T., J.P. McCoy, and R. Nussenblatt, *Standardizing immunophenotyping for the Human Immunology Project.* Nature reviews. Immunology, 2012. **12**(3): p. 191-200.
121. Gadalla, R., et al., *Validation of CyTOF Against Flow Cytometry for Immunological Studies and Monitoring of Human Cancer Clinical Trials.* Front Oncol, 2019. **9**: p. 415.
122. Leng, S.X., et al., *ELISA and multiplex technologies for cytokine measurement in inflammation and aging research.* The journals of gerontology. Series A, Biological sciences and medical sciences, 2008. **63**(8): p. 879-884.
123. Chiswick, E.L., et al., *Detection and quantification of cytokines and other biomarkers.* Methods in molecular biology (Clifton, N.J.), 2012. **844**: p. 15-30.

124. Mazur, P., *Cryobiology: The Freezing of Biological Systems.* Science, 1970. **168**(3934): p. 939-949.
125. Yokoyama, T., M. L., & Ehrhardt, R. O, *Cryopreservation and Thawing of Cells.* Current Protocols in Immunology, 2012. **99**(1): p. A.3G.1–A.3G.5.
126. Strober, W., *Trypan blue exclusion test of cell viability.* Curr Protoc Immunol, 2001. **Appendix 3**: p. Appendix 3B.
127. Bagwell, C.B., et al., *Automated Data Cleanup for Mass Cytometry.* Cytometry A, 2020. **97**(2): p. 184-198.
128. Gurtovenko, A.A. and J. Anwar, *Modulating the Structure and Properties of Cell Membranes: The Molecular Mechanism of Action of Dimethyl Sulfoxide.* The Journal of Physical Chemistry B, 2007. **111**(35): p. 10453-10460.
129. Chen, W., et al., *Conversion of peripheral CD4+CD25- naive T cells to CD4+CD25+ regulatory T cells by TGF-beta induction of transcription factor Foxp3.* The Journal of experimental medicine, 2003. **198**(12): p. 1875-1886.
130. Bushel, P.R., et al., *Blood gene expression signatures predict exposure levels.* Proc Natl Acad Sci U S A, 2007. **104**(46): p. 18211-6.
131. Moris, P., et al., *Whole blood can be used as an alternative to isolated peripheral blood mononuclear cells to measure in vitro specific T-cell responses in human samples.* Journal of Immunological Methods, 2021. **492**: p. 112940.
132. Brodin, P., D. Duffy, and L. Quintana-Murci, *A Call for Blood—In Human Immunology.* Immunity, 2019. **50**(6): p. 1335-1336.
133. Silva, M.H., et al., *Stabilization of blood for long-term storage can affect antibody-based recognition of cell surface markers.* Journal of Immunological Methods, 2020. **481-482**: p. 112792.
134. de Ruiter, K., et al., *A field-applicable method for flow cytometric analysis of granulocyte activation: Cryopreservation of fixed granulocytes.* Cytometry Part A, 2018. **93**(5): p. 540-547.
135. Sakkestad, S.T., J. Skavland, and K. Hanevik, *Whole blood preservation methods alter chemokine receptor detection in mass cytometry experiments.* Journal of Immunological Methods, 2020. **476**: p. 112673.
136. Rosales, C., *Neutrophil: A Cell with Many Roles in Inflammation or Several Cell Types?* Front Physiol, 2018. **9**: p. 113.
137. Sivakumar, V., et al., *Differential requirement for Rel/nuclear factor kappa B family members in natural killer T cell development.* The Journal of experimental medicine, 2003. **197**(12): p. 1613-1621.
138. Miraghazadeh, B. and M.C. Cook, *Nuclear Factor-kappaB in Autoimmunity: Man and Mouse.* Frontiers in Immunology, 2018. **9**.

139. Godfrey, D.I. and M. Kronenberg, *Going both ways: Immune regulation via CD1d-dependent NKT cells.* The Journal of Clinical Investigation, 2004. **114**(10): p. 1379-1388.
140. Mi, Q.-S., et al., *The autoimmune regulator (Aire) controls iNKT cell development and maturation.* Nature Medicine, 2006. **12**(6): p. 624-626.
141. Heino, M., et al., *RNA and protein expression of the murine autoimmune regulator gene (Aire) in normal, RelB-deficient and in NOD mouse.* European journal of immunology, 2000. **30**(7): p. 1884-1893.
142. Elewaut , D., et al., *NIK-dependent RelB Activation Defines a Unique Signaling Pathway for the Development of Vα14i NKT Cells.* Journal of Experimental Medicine, 2003. **197**(12): p. 1623-1633.
143. Elewaut, D., et al., *Membrane Lymphotoxin Is Required for the Development of Different Subpopulations of NK T Cells.* The Journal of Immunology, 2000. **165**(2): p. 671-679.
144. Chin, R.K., et al., *Lymphotoxin pathway directs thymic Aire expression.* Nature Immunology, 2003. **4**(11): p. 1121-1127.
145. Navegantes, K.C., et al., *Immune modulation of some autoimmune diseases: the critical role of macrophages and neutrophils in the innate and adaptive immunity.* Journal of Translational Medicine, 2017. **15**(1): p. 36.
146. Bruserud, Ø., et al., *Altered Immune Activation and IL-23 Signaling in Response to Candida albicans in Autoimmune Polyendocrine Syndrome Type 1.* Frontiers in Immunology, 2017. **8**.
147. Hong, M., et al., *Pattern recognition receptor expression is not impaired in patients with chronic mucocutanous candidiasis with or without autoimmune polyendocrinopathy candidiasis ectodermal dystrophy.* Clinical and Experimental Immunology, 2009. **156**(1): p. 40-51.
148. Perniola, R., et al., *Innate and adaptive immunity in patients with autoimmune polyendocrinopathy–candidiasis–ectodermal dystrophy.* Mycoses, 2008. **51**(3): p. 228-235.
149. Wolff, A.S.B., et al., *Flow Cytometry Study of Blood Cell Subtypes Reflects Autoimmune and Inflammatory Processes in Autoimmune Polyendocrine Syndrome Type I.* Scandinavian Journal of Immunology, 2010. **71**(6): p. 459-467.
150. Ferré, E.M.N., et al., *Lymphocyte-driven regional immunopathology in pneumonitis caused by impaired central immune tolerance.* Science Translational Medicine, 2019. **11**(495): p. eaav5597.
151. Meager, A., et al., *Anti-Interferon Autoantibodies in Autoimmune Polyendocrinopathy Syndrome Type 1.* PLOS Medicine, 2006. **3**(7): p. e289.
152. Sng, J., et al., *AIRE expression controls the peripheral selection of autoreactive B cells.* Science immunology, 2019. **4**(34): p. eaav6778.

153. Yokoyama, W.M., S. Kim, and A.R. French, *The Dynamic Life of Natural Killer Cells.* Annual Review of Immunology, 2004. **22**(1): p. 405-429.
154. Lindh, E., et al., *AIRE deficiency leads to impaired iNKT cell development.* Journal of Autoimmunity, 2010. **34**(1): p. 66-72.
155. Berger, A.H., et al., *Transcriptional Changes in Regulatory T Cells From Patients With Autoimmune Polyendocrine Syndrome Type 1 Suggest Functional Impairment of Lipid Metabolism and Gut Homing.* Frontiers in Immunology, 2021. **12**.
156. Roederer, M., *Compensation in flow cytometry.* Current protocols in cytometry, 2002. **22**(1): p. 1.14. 1-1.14. 20.
157. Law, J.P., et al., *The importance of Foxp3 antibody and fixation/permeabilization buffer combinations in identifying CD4+CD25+Foxp3+ regulatory T cells.* Cytometry. Part A : the journal of the International Society for Analytical Cytology, 2009. **75**(12): p. 1040-1050.
158. Maecker, H.T., et al., *Use of overlapping peptide mixtures as antigens for cytokine flow cytometry.* Journal of immunological methods, 2001. **255**(1-2): p. 27-40.
159. Li, H., et al., *Autoimmune regulator-overexpressing dendritic cells induce T helper 1 and T helper 17 cells by upregulating cytokine expression.* Mol Med Rep, 2016. **13**(1): p. 565-571.
160. Knox, J.J., et al., *Characterization of T-bet and eomes in peripheral human immune cells.* Frontiers in immunology, 2014. **5**: p. 217-217.
161. Crome, S.Q., et al., *The role of retinoic acid-related orphan receptor variant 2 and IL-17 in the development and function of human CD4+ T cells.* European Journal of Immunology, 2009. **39**(6): p. 1480-1493.
162. Yang, X.O., et al., *STAT3 Regulates Cytokine-mediated Generation of Inflammatory Helper T Cells**. Journal of Biological Chemistry, 2007. **282**(13): p. 9358-9363.
163. Ting, C.N., et al., *Transcription factor GATA-3 is required for development of the T-cell lineage.* Nature, 1996. **384**(6608): p. 474-8.
164. Costantini, A., et al., *Effects of cryopreservation on lymphocyte immunophenotype and function.* Journal of Immunological Methods, 2003. **278**(1): p. 145-155.
165. Gadalla, R., et al., *Validation of CyTOF Against Flow Cytometry for Immunological Studies and Monitoring of Human Cancer Clinical Trials.* Frontiers in Oncology, 2019. **9**.
166. Bruserud, Ø., et al., *A Longitudinal Follow-up of Autoimmune Polyendocrine Syndrome Type 1.* The Journal of Clinical Endocrinology & Metabolism, 2016. **101**(8): p. 2975-2983.
167. Oftedal, B., et al., *Dominant Mutations in the Autoimmune Regulator AIRE Are Associated with Common Organ-Specific Autoimmune Diseases.* Immunity, 2015. **42**: p. 1185-96.

APPENDIX

1. List of APS-1 patients

	APS-1 PATIENTS		CONTROL	
NO.	Sex	Age	Sex	Age
1	F	51	F	51
2	M	59	M	58
3	M	32	M	31
4	M	37	M	40
5	M	52	M	54
6	M	64	F	66

All the patients included in the Cytof study had a confirmed APS-I diagnosis with mutations in both alleles of the *AIRE* gene, except for one patient who had only the disease-causing dominant mutation c.932G>A in the *AIRE* gene. All these six had autoantibodies against the signature autoantigen IFN-omega and in addition a variety of other autoantibodies; all of them have been reported on previously in Norwegian APS-I cohort studies [166, 167]. For flow cytometry, one male was excluded and five of the same patients were included but with different time-points of sampling.

2. Raw Percentage of population for varying subgroups of CD45+ Cells

Monocytes

Patient	Control
12.43	5.534
4.96	9.832
10.831	13.181
9.775	10.841
8.95	10.775
13.718	5.876

Population	Condition A	Condition B	Mean A	Mean B	SD A	SD B	n A	n B	p-value	Significance p-value
Monocytes	Patient	Control	10.11	9.34	2.796	2.762	6	6	0.9372	ns

B Cells

Patient	Control
0.525	2.687
0.142	2.538
0.584	1.366
1.156	0.848
1.845	1.95
0.854	1.09

Population	Condition A	Condition B	Mean A	Mean B	SD A	SD B	n A	n B	p-value	Significance p-value
B Cells	Patient	Control	0.8511	1.747	0.542	0.6996	6	6	0.06494	ns

Granulocytes

Patient	Control
48.217	55.786
50.925	41.256
68.47	40.451
67.467	20.802
44.855	27.421
38.219	63.672

Population	Condition A	Condition B	Mean A	Mean B	SD A	SD B	n A	n B	p-value	Significance p-value
Granulocytes	Patient	Control	53.03	41.56	11.26	14.85	6	6	0.2403	ns

NK Cells

Patient	Control
2.254	7.666
9.397	5.126
1.64	7.775
0.993	14.34
4.872	6.015
2.667	3.325

Population	Condition A	Condition B	Mean A	Mean B	SD A	SD B	n A	n B	p-value	Significance p-value
NK Cells	Patient	Control	3.637	7.374	2.844	3.466	6	6	0.06494	ns

DCs

Patient	Control
0.823	0.662
1.159	0.743
0.32	0.64
0.181	1.922
1.446	2.176
1.81	0.733

Population	Condition A	Condition B	Mean A	Mean B	SD A	SD B	n A	n B	p-value	Significance p-value
DCs	Patient	Control	0.9565	1.146	0.582	0.6435	6	6	0.8182	ns

CD3+ T Cells

Patient	Control
31.614	24.422
28.357	35.288
16.203	32.362
18.427	46.616
34.514	46.343
34.357	22.612

Population	Condition A	Condition B	Mean A	Mean B	SD A	SD B	n A	n B	p-value	Significance p-value
CD3+ T Cells	Patient	Control	27.25	34.61	7.342	9.444	6	6	0.2403	ns

3. Raw Percentage of population for varying subgroups of CD3+ T Cells

NKT Cells

Patient	Control
8.095	10.328
8.707	9.752
8.02	10.488
0.608	17.457
2.748	11.506
1.228	8.578

Population	Condition A	Condition B	Mean A	Mean B	SD A	SD B	n A	n B	p-value	Significance p-value
CD3+CD14-CD19-CD56+ NKT Cells	Patient	Control	4.901	11.35	3.439	2.868	6	6	0.004329	**

gd T Cells

Patient	Control
3.14	0.483
1.602	1.547
1.575	9.357
0.696	2.826
0.282	0.853
0.223	1.265

Population	Condition A	Condition B	Mean A	Mean B	SD A	SD B	n A	n B	p-value	Significance p-value
gd T Cells	Patient	Control	1.253	2.722	1.008	3.056	6	6	0.5887	ns

CD8+ T Cells

Patient	Control
20.678	40.865
54,96	24.469
17.724	35.747
32.89	45.447
39.899	35.81
18.448	27.143

Population	Condition A	Condition B	Mean A	Mean B	SD A	SD B	n A	n B	p-value	Significance p-value
CD8+ T Cells	Patient	Control	30.77	34.91	13.52	7.272	6	6	0.3939	ns

CD4+ T Cells

Patient	Control
43.858	44.942
19.095	58.782
69.012	38.815
58.369	30.939
54.46	42.764
74.185	54.703

Population	Condition A	Condition B	Mean A	Mean B	SD A	SD B	n A	n B	p-value	Significance p-value
CD4+ T Cells	Patient	Control	53.16	45.16	18.12	9.353	6	6	0.3939	ns

CD25+ CD127- (Treg)

Patient	Control
0.882	1.431
0.312	3.44
0.674	0.501
4.771	2.462
6.603	7.26
8.415	8.154

Condition A	Condition B	Mean A	Mean B	SD A	SD B	n A	n B	p-value	Significance p-value
CD25+ CD127- (Treg)	Patient	Control	3.609	3.875	3.171	2.867	6	6	0.8182	ns

4. **Median comparison of live cells with each cell population in patients and control**

Markers	**Median difference between patients (n= 5) and control (n= 5)**	**P-value***
LIVE CELLS	-12.20 (75.80 – 88.0)	0.3095
CD3+	18.20 (61.80 – 43.60)	0.4206
CD4+	-1.8 (53.20 - 55.0)	>0.9999
CD8+	1.5 (38.80 - 37.30)	>0.9999
EOMES+	-3 (1.72 - 4.72)	0.0079**
CXCR3+	-11.50 (21.6 – 33.10)	0.222
T.BET+	-7.8 (19.90 - 27.70)	0.4206
FOXP3+	-0.89 (3.24 - 4.13)	0.548
GATA3+	-7.93 (5.57 - 13.5)	0.69
RORgt+	-1.24 (1.87-3.11)	0.4206

Median comparison of live cells with each cell population in patients and control

Markers	Median difference between patients (n= 5) and control (n= 5)	P-value*
LIVE CELLS	-12.20 (75.80 – 88.0)	0.3095
CD3+	18.20 (61.80 – 43.60)	0.4206
CD4+	-1.8 (53.20 - 55.0)	>0.9999
CD8+	1.5 (38.80 - 37.30)	>0.9999
EOMES+	-3 (1.72 - 4.72)	0.0079**
CXCR3+	-11.50 (21.6 – 33.10)	0.222
T.BET+	-7.8 (19.90 - 27.70)	0.4206
FOXP3+	-0.89 (3.24 - 4.13)	0.548
GATA3+	-7.93 (5.57 - 13.5)	0.69
RORgt+	-1.24 (1.87-3.11)	0.4206

Comparison of Th2 expressing cells in patients and healthy controls

Markers	Median difference between patients (n= 3) and control (n= 3)	P-value*
LIVE CELLS	-4.2 (94.7-98.9)	0.1000
CD3+	1.8 (99.20 - 97.40)	0.3000
CD4+	0.5 (99.6 – 99.10)	0.2000
GATA3+	8.7 (35.5- 26.8)	0.2000
RORgt+	4.33 (11.9 – 7.57)	0.7000
FOXP3+	3.5 (26.1 – 22.6)	>0.9999

Comparison of Th17 expressing cells in patients and controls

Markers	Median difference between patients (n= 3) and control (n= 3)	P-value*
LIVE CELLS	19.10 (67.7 – 48.4)	0.4000
CD3+	12 (90.8 – 78.8)	0.4000
CD4+	4.8 (85.8 – 81.0)	0.4000
GATA3+	-15.98 (9.72 – 25.7)	0.4000
RORgt+	-5.1 (61.3 – 66.4)	0.7000
FOXP3+	-2.1 (30.3 - 32.4)	0.4000